UNICAMP

UNIVERSIDADE ESTADUAL DE CAMPINAS
INSTITUTO DE BIOLOGIA

VERÔNICA MUNIZ COUTO

ASSOCIATION OF CAPSAICIN WITH LOCAL ANESTHETICS TO INCREASE ANALGESIA

ASSOCIAÇÃO DE CAPSAICINA COM ANESTÉSICOS LOCAIS PARA AUMENTO DA ANALGESIA

CAMPINAS

2019

VERÔNICA MUNIZ COUTO

ASSOCIATION OF CAPSAICIN WITH LOCAL ANESTHETICS TO INCREASE ANALGESIA

ASSOCIAÇÃO DE CAPSAICINA COM ANESTÉSICOS LOCAIS PARA AUMENTO DA ANALGESIA

Thesis presented to the Institute of Biology of the University of Campinas in partial fulfillment of the requirements for the degree of Doctor of Science, in the area of Drugs, Medicines, and Supplies for Health.

Tese apresentada ao Instituto de Biologia da Universidade Estadual de Campinas como parte dos requisitos exigidos para obtenção do título de Doutora em Ciências, na Área de Fármacos, Medicamentos e Insumos para Saúde.

ESTE ARQUIVO DIGITAL CORRESPONDE À VERSÃO FINAL DA TESE DEFENDIDA PELA ALUNA VERÔNICA MUNIZ COUTO E ORIENTADA PELA ENEIDA DE PAULA.

Orientador: Profa. Dra. ENEIDA DE PAULA

Co-Orientador: Profa. Dra. LAURA DE OLIVEIRA NASCIMENTO

CAMPINAS

2019

Campinas, 5 de junho de 2019

COMISSÃO EXAMINADORA

Profa. Dra. Eneida de Paula

Prof. Dr. Jorge Fernando Brandão Pereira

Profa. Dra. Cíntia Maria Saia Cereda

Prof. Dr. Francisco Benedito Teixeira Pessine

Profa. Dra. Renata Fonseca Vianna Lopez

Os membros da Comissão Examinadora acima assinaram a Ata de Defesa, que se encontra no processo de vida acadêmica do aluno.

.

Resumo

Os anestésicos locais (AL) são imprescindíveis na prática médica, porém eles não permitem bloqueio seletivo das fibras nociceptivas e falham em anestesiar tecidos inflamados. A capsaicina (CAP) é um composto pouco hidrossolúvel utilizado como analgésico. Há relatos na literatura de que a injeção de AL seguida de CAP leva a diminuição do bloqueio motor, em animais. Os AL e CAP são também utilizados individualmente, em formulações tópicas, para tratamento da dor crônica. Esta tese relata pela primeira vez o efeito analgésico de uma associação medicamentosa entre AL e CAP em tecido inflamado e, também, descreve o desenvolvimento de uma formulação tópica dos mesmos. Na parte 1 da tese, a CAP foi complexada com HP-β-ciclodextrina, aumentando sua solubilidade aquosa em 20 vezes. Esse complexo foi liofilizado com ciclo otimizado e caracterizado por Calorimetria Diferencial de varredura, Difração de Raios-X e microscopia eletrônica de varredura. Essas técnicas forneceram evidências da complexação entre a ciclodextrina e CAP, enquanto a Ressonância Magnética Nuclear (RMN) comprovou a formação de complexo de inclusão. O liofilizado (ressuspenso em solução contendo o AL mepivacaina) foi administrado em camundongos, resultando em diminuição do bloqueio motor do nervo ciático e, em outro teste, aumento significativo da anestesia em tecido inflamado. A parte 2 da tese relata o desenvolvimento de uma nova formulação contendo exclusivamente CAP e o AL lidocaína (LDC). A mistura equimolar dos fármacos produziu um sistema líquido à temperatura ambiente, com padrão amorfo relatado por Difração de Raios-X. A espectroscopia de infra-vermelho indicou interação intermolecular entre os compostos, confirmada por medidas de RMN. Esta técnica indicou formação de ponte de hidrogênio intermolecular, entre os grupos carbonila (CAP) e amida (LDC), o que explica a redução da temperatura de fusão dos componentes, para abaixo de 25 °C, caracterizando uma mistura eutética profunda. A mistura $[LDC]_1[CAP]_1$ revelou-se altamente estável e aumentou a lipofilicidade dos fármacos, característica que pode ser útil para maior permeação dos mesmos na pele. Ambas partes desta tese geraram resultados promissores para futura aplicação clínica da associação medicamentosa entre AL e CAP. Na Parte 1, foi obtida uma formulação parenteral que possibilitou atingir efeito desejável de anestesia, apesar da condição de inflamação. Na Parte 2, o estudo de pré-formulação revelou uma nova alternativa de medicação tópica para o tratamento da dor neuropática.

Abstract

Local anesthetics (LA) are crucial in medical practice to numb parts of the body. However, LA do not allow selective blocking of nociceptive fibers and fail to anesthetize inflamed tissues. Capsaicin (CAP) is a poorly hydrosoluble compound used as an analgesic. There are reports in the literature that the injection of LA followed by CAP leads to a decrease in motor blockade in animals. LA and CAP are also used individually in topical formulations for the treatment of chronic pain. This thesis reports for the first time the analgesic effect of a drug combination (LA and CAP) on inflamed tissue and also describes the development of a topical formulation of them. In part 1 CAP was complexed with HP-β-cyclodextrin, which increases its water solubility by 20 times. The complex was lyophilized under an optimized cycle and characterized by Differential Scanning Calorimetry, X-ray Diffraction and Scanning Electron Microscopy. These techniques provided evidence on the complexation between cyclodextrin and CAP, while Nuclear Magnetic Resonance (NMR) proved the inclusion complex formation. The lyophilized complex (resuspended in a solution with mepivacaine) was injected in mice, resulting in: i) decreased motor blockade of the sciatic nerve; ii) significant increase of anesthesia in a mechanical test, in inflamed tissue. In part 2 of this thesis, a new formulation containing exclusively the lidocaine (LA) and capsaicin was reported. The equimolar mixture of these drugs produced a liquid system at room temperature, with an amorphous pattern reported by X-ray diffraction. Infrared spectroscopy indicated intermolecular interaction between the compounds, as confirmed by NMR. This technique indicated a strong intermolecular hydrogen bond between the carbonyl (CAP) and amide (LDC) groups, which explains the reduction of the melting temperature of the components to below 25 ° C, characterizing a deep eutectic mixture. The $[LDC]_1[CAP]_1$ mixture proved to be highly stable and it increased the lipophilicity of the drugs, which may lead to improve their permeation into the skin. Both parts of this thesis have generated promises for future clinical application of the combination of drugs (LA and CAP). In Part 1, a parenteral formulation was developed that achieved desirable anesthesia effect, despite the inflammatory condition. In Part 2, the pre-formulation study provided a new topical formulation suitable for the treatment of neuropathic pain.

Figure list

Table list

Abbreviation list

API	active pharmaceutical ingredient
ANVISA	Agência Nacional de Vigilância Sanitária
BVC	bupivacaine
CAP	capsaicin
CD	cyclodextrin
CE	complexation efficiency
CS	chemical shift
D	drug
D_c	diffusion coefficient
DDS	drug delivery systems
DEM	deep eutectic mixture
DL	detection limit
DOSY	diffusion ordered spectroscopy
DSC	differential scanning calorimetry
DVS	dynamic vapor sorption
FDA	United States Food and Drug Administration
FT-IR	Fourier transform infrared
HPLC	high pressure liquid chromatography
HP-β-CD	hydroxypropyl-beta-cyclodextrin
IL	ionic liquid
ITC	isothermal titration calorimetry
LA	local anesthetic
LDC	lidocaine base
LDC-HCl	lidocaine hydrochloride
MVC	mepivacaine
MPE	maximum possible effect
NMR	nuclear magnetic resonance
NOE	nuclear overhauser effect
n.o.	not observed
PBS	phosphate buffered saline
PXRD	powder x-ray diffraction
QL	quantification limit
QX-314	lidocaine N-ethyl bromide
RH	relative humidity
RSD	relative standard deviation
ROESY	rotating-frame overhauser spectroscopy
SD	standard deviation
SEM	scanning electron microscopy
Tm	melting temperature
Tg	glass transition temperature
TRPV1	transient receptor potential vanilloid 1

USP	United State Pharmacopeia
UV/Vis	ultraviolet-visible spectroscopy
^{1}H NMR	proton nuclear magnetic resonance
^{13}C NMR	carbon nuclear magnetic resonance

Summary

1. INTRODUCTION

1.1. Pain management

Pain is a protection mechanism of the organism against tissue injury resulting from harmful stimuli such as thermal, mechanical, and chemical (Schulman and Strichartz, 2011). Injury information and pain stimuli are transmitted to the central nervous system by specific sensory nervous, the nociceptors (Mense, 1983).

Acute pain usually comes on suddenly caused by a specific disease or injury, and it disappears when there is no longer an underlying cause for the pain (Grichnik and Ferrante, 1991). To avoid acute pain during minor surgeries and dental procedures the first-line therapy is local anesthesia. Nowadays, there are many local anesthetics agents with distinct physicochemical properties and specific applications (Suzuki et al., 2019).

On the other hand, chronic pain continues even after the injury or illness that caused it has healed. One type of chronic pain is neurophatic pain which is caused by a lesion or disease affecting the somatosensory nervous system (Treede et al., 2008). The treatment for neuropathic pain is still a great challenge and involves the use of antidepressants, anticonvulsants, opioids, and N-methyl-D-aspartic acid antagonists (Jensen et al., 2009; Murnion, 2018). However, all of those are systemic therapy agents with multiple side effects, therefore topical agents might be preferable when safety and tolerability are a concern (Sommer and Cruccu, 2017). Currently, there are only two topical product available for the treatment of peripheral neuropathic pain: high-dose of capsaicin patch (8% w/v) or lidocaine patch (4% w/v) (Murnion, 2018; Sommer and Cruccu, 2017).

1.2. Local anesthetic

Local anesthetics (LA) reversible disrupts the generation of action potential by binding to voltage-dependent sodium channels in excitable membranes. Consequently, it prevents the transmission of nociceptive information reaching the central nervous system (Hung, 2011).

LA are administrated to anesthetize skin, subcutaneous tissue, and peripheral nerves for a variety of medical procedures. The clinically available injectable concentrations vary in a range from 0.2 to 4%, and should not affect the patient's consciousness (Malamed, 2014). During injection, LA is placed directly into the tissue around the nerve and duration of anesthesia is related to the time the anesthetic molecule remains adjacent to the neural fibers (Becker and Reed, 2012). In addition, topical LA must cross skin barriers in order to exert their effect. This may be achieved by either using a LA with a low pKa value, ensuring acceptable amounts of the neutral form (permeable to skin), or with higher dose (McLure and Rubin, 2005).

1.2.1. Chemical structure

Most of the commercially available local anesthetic agents have a structure characterized by a hydrophilic and a hydrophobic part, separated by a polar intermediate chain, containing an ester or amide bond (**Figure 1**) (Covino and Giddon, 1981). The hydrophilic moiety (usually with an amine group) is the ionizable part of the molecule, responsible for the aqueous solubility of the LA. The intermediate chain (ester/amide) determines the activity and biotransformation (serum, hepatic) of the anesthetic agent. The lipophilic portion (usually an aromatic ring) of LA is responsible for their ability to diffuse through the nerve cell membrane and, consequently, for their potency and toxicity. Currently LAs of the amino-esters and amino-amides classes are the most used in the medical clinic (Suzuki et al., 2019).

In the majority of LAs the amine group has a pKa between 7.6-8.9, which explains the coexistence of a fraction in the neutral form (of greater partition in membranes) and ionized fraction (which is responsible for the speed of action) in physiological pH (de Araújo et al., 2008). For most LA, the amine group is mostly protonated at pH 7.4, with a small but significant fraction in the neutral form. Both the neutral and protonated forms of LA interact with the sodium channel and are responsible for the sensory block (de Paula et al., 2010, 2012; Lagan and McLure, 2004). Although both forms of LA are pharmacologically relevant, it is first necessary for the LA (in the neutral form) to permeate the nerve membrane to find the binding sites in the voltage-dependent sodium channel (de Araújo et al., 2008; Ueno et al., 2008).
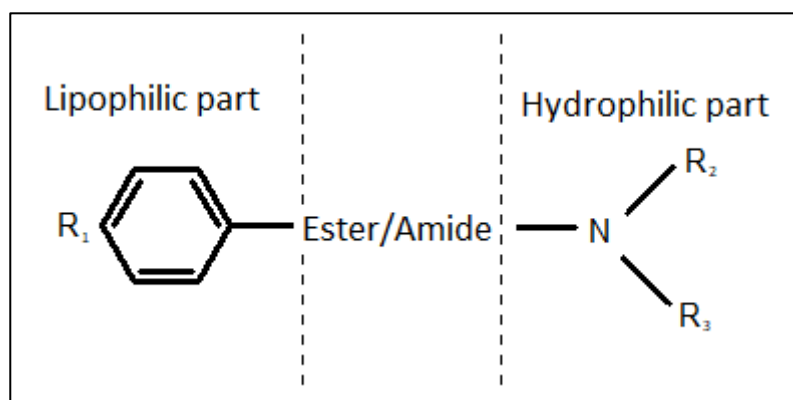
Figure 1- Representative diagram of the basic structure of local anesthetics.

1.2.2. Mechanism of action

As mentioned before, local anesthetics block the impulse propagation in the nerve fibers by preventing the conductance of the Na^+ ions through the voltage-dependent sodium channel, necessary for membrane depolarization (Covino and Vassallo, 1976).

The voltage-dependent mammalian sodium channel is composed of a large α subunit (with 4 domains of 6 transmembrane alpha-helices - S1-S6 - each) and β subunits. The neutral form of LA is known to bind to the hydrophobic amino acid side chain in the sixth helix of domain IV of the α-subunit of the channel (Ragsdale et al., 1996; Bagnéris et al., 2014), while the protonated form of LA binds to the channel through the cytoplasmic side (Narahashi et al., 1970), in the inactivating gate particle, a cytoplasmic loop between domains III (S6) and domain IV (S1) of the channel (de Araújo et al., 2008).

In addition, LAs partition to lipids bilayer of neural cells causing lateral phase expansion, increased dynamics and decreased molecular order of lipids. They may cause some conformational modification in the sodium channels, which would lead to temporary inactivation of it (de Paula and Schreier, 1996; de Araújo et al., 2008; de Paula et al., 2008).

1.2.3. Non-ideal anesthetic effect

Although modern local anesthetic agents are safer than their predecessors, they still provoke undesirable effects and fail to curb pain in inflammatory conditions. LA block the voltage-dependent sodium channels not only in sensory fibers (specific sensory block), but also in adjacent fibers. When reaching the peripheral nerve, the LAs find fibers Aδ and C (leading to pain and temperature stimulus), Aα and Aβ fibers (with motor and proprioception functions such as pressure, touch and position), as well as fibers with autonomous function (Barash et al., 2013). Therefore, LA produce not only numb but also paralysis, low blood pressure, and motor blockage.

Additionally, LA fail to anesthetize inflamed tissues. The presence of inflammation considerably decreases the potency of LA agents in anesthetic procedures. Pharmacokinetic factors (increased blood flow and pH change - favoring the presence of the protonated LA species over the neutral one) and pharmacodynamics (increased nerve sensitization) are indicated as the reasons for such failure in anesthesia (Miller, 2010; Tsesis, 2014). The presence of inflammation decreases local anesthetic efficacy, especially in dental anesthesia demanding the injection of higher volume of LA solution than in an ordinary procedure. For instance, the anesthetic effect of injections of lidocaine and mepivacaine are extremely affected in teeth with irreversible pulpitis (Dunbar et al., 1996; Reisman et al., 1997). Larger doses of LA can be administered to achieve anesthesia, but the risk of systemic toxicity limits the total administered dose (Grant et al., 1997).

1.2.4. Mepivacaine

Mepivacaine hydrochloride (MVC) was introduced in dentistry in 1960, and started to be used in dentistry without need of association with vasoconstrictors, due to its intrinsic vasoactive properties (Luduena et al., 1960; Moore and Hersh, 2010; Su et al., 2014). MVC plays an important role in dental anesthesia, with intermediate duration of anesthesia in comparison to other anesthetic agents, but with a rapid onset (de Araújo et al., 2004; Malamed, 2014). Because of its low systemic toxicity, MVC is also used in a series of regional anesthetic procedures, at doses between 0.5 and 2 % (w/v) (McLure and Rubin, 2005).

The molecular structure of mepivacaine hydrochloride (molar mass = 282.81 g/L) is similar to that of other LA used in dentistry: prilocaine and lidocaine. But MVC is a cyclic local amino-amide LA, since its amine group (pKa = 7.9) is part of a piperidine ring (**Figure 2**) methyl substituted (Malamed, 2014). Other cyclic amino-amide LA are ropivacaine and bupivacaine, with propyl and butyl substituents, respectively, on carbon 1 of the piperidine ring.
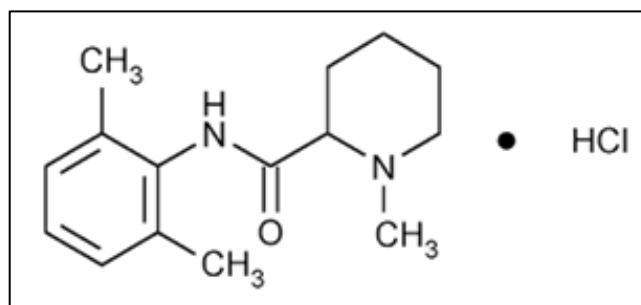
Figure 2- Chemical structure of mepivacaine hydrochloride.

1.2.5. Lidocaine

Lidocaine (LDC) an a linear amino-amide LA (**Figure 3**), clinically introduced in 1947 (Lagan and McLure, 2004). LDC (molar mass = 234.34 g/L) is used in concentrations of 0.5 – 2% (w/v) for infiltration anesthesia as well as peripheral, spinal, and epidural blocks (Suzuki et al., 2019). LDC evokes a profound block with a rapid speed of onset due to its lower pKa (7.9), and short duration of action, compared to long-acting LA such as bupivacaine (Lagan and McLure, 2004).
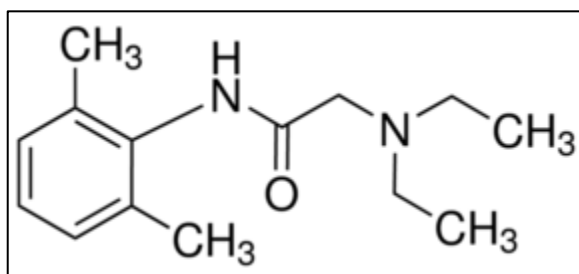
Figure 3- Chemical structure of lidocaine

In 1999, the LDC topical patch (5% w/v) was approved by the FDA (United States Food and Drug Administration) for the treatment of pain associated with postherpetic neuralgia, a severe chronic neuropathic pain condition (Suzuki et al.,

2019). Another interesting LDC topical formulation is the EMLA cream (AstraZeneca PLC, London, U.K.), a eutectic mixture of LDC and prilocaine (each at 2.5% w/v concentration). EMLA provides dermal analgesia due to it easy skin penetration (McLure and Rubin, 2005) and its use in dentistry as well. (Daneshkazemi et al., 2016)

1.3. Capsaicin

Capsaicin (CAP) is the active ingredient in *Capsicum* peppers (Caterina et al., 1997). CAP molecule (molar mass= 305.41 g/L) has a substituted methyl ether phenolic ring linked by a polar (amide) group to a long hydrocarbon chain (**Figure 4**). It is highly volatile and hydrophobic, therefore, surfactant, and organic solvents are used to solubilize it (O'Neill et al., 2012). New drug delivery strategies have been developed to improve the low aqueous solubility (0.006% w/v) of capsaicin (Turgut et al., 2004), such as: inclusion complexation with hydroxypropyl-β-cyclodextrin (Zi et al., 2008), encapsulation in niosomes (Tavano et al., 2011), encapsulation in polymeric nanocapsules (Rollyson et al., 2014) and in nanostructured lipid carriers (Agrawal et al., 2015).
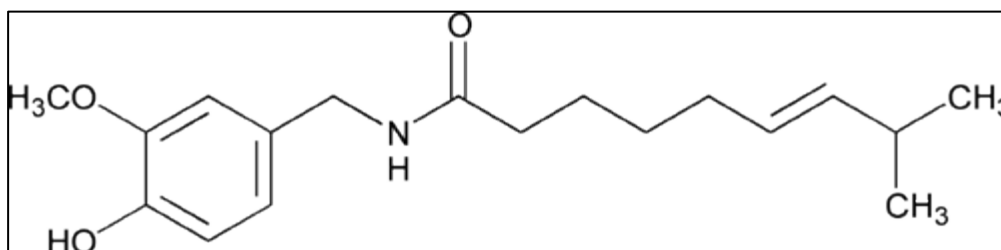
Figure 4- Chemical structure of capsaicin.

The pharmacological activity of CAP depends on factors such as dose (from 0.025 - 8% w/v), and route of administration (O'Neill et al., 2012; Rollyson et al., 2014). So far, the major pharmacological application of CAP is as an analgesic (for the treatment of pain) given its binding to the transient receptor potential vanilloid (TRPV1), or transient receptor potential cation channel subfamily V member 1, or capsaicin receptor, is a heat and pain receptor (Rollyson et al., 2014). Treatment with capsaicin is effective in different conditions such as neuropathic pain (e.g. Qutenza, 8% patch, Averitas Pharma, Inc), postsurgical neuropathic pain and post-herpetic neuralgia (e.g. injectable

capsaicin Adlea; Anesiva Inc.) and painful diabetic peripheral neuropathy (Fattori et al., 2016).

1.3.1. Mechanism of action

The TRP (transient receptor potential) ion channels constitute a large family of channels with permeability to monovalent cations plus calcium ions (Clapham et al., 2001). Among these channels, the type 1 transient potential vanilloid receptor (TRPV1) is activated by pain stimulus, including noxious heating, low pH and vanilloid binders such as capsaicin (Puopolo et al., 2013).

TRPV1 are channels expressed in neurons involved in nociception, in the peripheral and central nervous systems (Palazzo et al., 2012). When activated by noxious stimuli or capsaicin, TRPV1 temporarily opens initiating depolarization mediated by the influx of sodium and calcium ions. This results in action potential that is delivered to the brain and creates a heat and burning/stinging skin sensation.

Capsaicin binds to the TRPV1 receptor generating an initial excitation of the nociceptive neurons. Then, when TRPV1 is repeatedly activated by capsaicin, a refractory effect is observed by desensitization of the receptor (Anand and Bley, 2011; Knotkova et al., 2008). As a result, the TRPV1 channel becomes nonresponsive not only to capsaicin but also to various nociceptive stimuli (Szallasi and Blumberg, 1999).

1.4. Combination of local anesthetic and capsaicin

1.4.1. Parental formulation

Peripherally, TRPV1 channels are located exclusively in the cellular bodies and axons of nociceptive fibers Aδ and C, which drive the pain stimulus (Kissin, 2008). According to Binshtok and coworkers, when CAP binds to TRVP1 the ionic channel opens, being it large enough to allow the passage of compounds such as QX-314 (molecular mass = 343 g/mol), a quaternary (always protonated) analog of the LA lidocaine. The facilitated entry of QX-314 results in greater anesthetic effect, without concomitant increase of motor block, since TRPV1 channels are not expressed in motor fibers (Binshtok et al., 2007). Thus, the selective expression of TRPV1 channels by nociceptive neurons aroused the interest of some researchers in associating CAP

and LAs (Gerner et al., 2008). Kim et al. (2010) reported selective pain block with the application of QX-314 followed by capsaicin for anesthesia in the periphery of the trigeminal nerve of rats (Kim et al., 2010). In 2014, Wang end coworkers combined LA and CAP for the intrathecal anesthesia of rats and reported a significant decrease of motor blockade induced by bupivacaine, lidocaine, and articaine, compared to single administration of these LA agents (C. H. Wang et al., 2014).

In addition, the TRPV1 channels are highly selective for cations, and allow the entrance of LA in the protonated form into the nerve fibers (Puopolo et al., 2013). This fact may be useful in (acidic) inflamed tissues, in which the occurrence of anesthesia failure is mainly attributed to increased fraction of protonated LA species that is poorly permeable to the neuron membrane (Tsesis, 2014). Therefore, the association of LA and CAP in a single parenteral formulation is an interesting approach to selectively increase the anesthetic potency.

1.4.2. Topical formulations in pain relief

Currently, LAs and CAP are individually used as topical medication for neuropathic pain relief (Casale et al., 2017). Lidocaine patch (5% w/v) is a topical delivery system that should be applied 12 hours a day (Suzuki et al., 2019). Capsaicin is an active ingredient in many topical medications aimed to treat peripheral neuropathic pain, especially when it is associated with post herpetic neuralgia (McCormack, 2010). The combined (LDC and CAP) therapy in a topical application should produce pharmacological effect only at the site of application, without significant systemic levels of the drugs.

Several application of CAP, as a cream at a low concentrations (< 0.1 % w/v), or single exposure to a high concentration of capsaicin in a dermal patch (8 % w/v), desensitizes TRPV1 nociceptors, inhibiting the initiation of pain transmission (McCormack, 2010). CAP is poorly absorbed transdermally in humans, and therefore it is unlikely to produce systemic adverse effects (Anand and Bley, 2011). However, CAP application causes initial local skin reactions such as burning and stinging, reducing the patient compliance (Anand and Bley, 2011).

In some clinical trials, 4% w/v lidocaine or 2.5% lidocaine/2.5% w/v prilocaine (EMLA) cream were used as a pretreatment to reduce the initial discomfort

caused by CAP (Webster et al., 2011; Jensen et al., 2014). A topical formulation that simultaneous delivery high doses of CAP and LDC could reduce the discomfort associated to capsaicin application, and potentially improve pain management in neuropathic and inflammatory conditions.

1.5. Drug delivery systems

Drug delivery systems (DDS) designate the approaches, formulations and technologies for the distribution of pharmaceutical compounds in the body to safely achieve desired therapeutic effects (Allen and Alsen, 2013). In order to do that, drug delivery technologies modify the solubility, permeation, absorption, release, as well as the type of administration of bioactive molecules.

Most drugs have a hydrophobic nature what makes it difficult for them to reach the site of action and stay there long enough to exert their therapeutic effect (Aulton and Taylor, 2013; Tamjidi et al., 2013). Many strategies are used to increase drug solubility: micronization; use of surfactants; salt formation; adsorption; complexation in cyclodextrins; and dispersion in polymers. Cyclodextrins are interesting DDS carriers, capable of altering the solubility of drugs by forming macromolecular inclusion complexes. On the other hand, ionic liquids or deep eutectic mixtures are new approaches, used to modulate the solubility and permeation of active pharmaceutical ingredients (APIs) (Caparica, 2017).

1.5.1. Cyclodextrins

Cyclodextrins (CD) are cyclic oligosaccharides (**Figure 5**) formed from the enzymatic degradation of starch by bacteria (Loftsson, 2012; Crini, 2014). They are composed of glucopyranose units linked by alpha 1,4 linkages (Del Valle, 2004; Loftsson and Duchene, 2007). The CDs are able to non-covalently interact with a wide variety of molecules: lipophilic - forming molecular inclusion complexes in their inner (apolar) cavity - or hydrophilic – trough hydrogen bonds of the OH groups on their outer (polar) surface (Challa et al., 2005; Davis and Brewster, 2004).

The most common natural CDs are alpha (α-CD), beta (β-CD) and gamma (γ-CD) with 6, 7 and 8 glucopyranose units, respectively. The CD's macrocyclic ring incorporate the lipophilic part of poorly soluble drugs to form inclusion complexes that

are more hydrophilic than the free guest molecule (Messner et al., 2010). This inclusion-complex capacity of CDs is well exploited to increase drug solubility, improving its bioavailability and stability (Tiwari et al., 2010).

Since 1970, it is possible to purify and produce cyclodextrins as pharmaceutical excipients (Duchêne, 1987). Additionally, cyclodextrins have undergone chemical modifications and their derivatives are even more soluble as: hydroxypropyl-beta-cyclodextrin (HP-β-CD), sulfobutylether-beta-cyclodextrin and methyl-beta-cyclodextrin. Currently, over 35 different pharmaceutical products are marketed as cyclodextrin complexes around the world (Kurkov and Loftsson, 2013). HP-β-CD (**Figure 5**) in particular exhibits a 50-fold greater solubility than β-CD, and its use is approved for parenteral drug administration by the FDA (Gould and Scott, 2005).
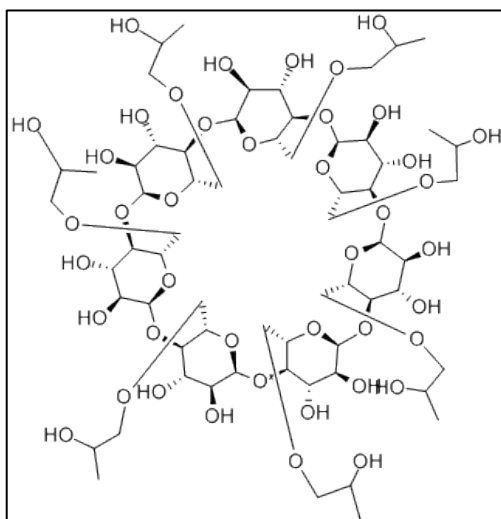
Figure 5- Chemical structure of hydroxypropyl-beta-cyclodextrin.

Several methods are described in the literature for the preparation of cyclodextrin complexes. Most of them use organic solvents for the solubilization of lipophilic actives, being the solvents removed, subsequently, by evaporation. However, the evaporation step is not suitable for volatile active principles, such as CAP. On the other hand, solubilization of host (CD) and guest molecules followed by water sublimation through lyophilization, produces a solid product with fast resuspension (Duchêne, 2011). Therefore, solubilization plus lyophilization should be the best method to produce an injectable HP-β-CD-CAP formulation.

In 2008, Zi and coworkers evaluated the percutaneous absorption of HP-β-CD-CAP inclusion complex (in hydrogel) through mouse skin. It was reported that HP-

β-CD enhanced CAP cutaneous penetration while increasing its solubility (Zi et al., 2008). Shen and col. (2012) used two CAP complexes, in β-CD and HP-β-CD, for the development of pesticide formulations, aiming to increase the solubility of CAP and to reduce the residues of its adsorption in soil (Shen et al., 2012). These authors demonstrated that the solubility of CAP was increased up to fifty-fold in the form of HP-β-CD inclusion complexes, as compared to free CAP. Currently, there is no study that developed a freeze-dried product containing capsaicin-in-cyclodextrin complexes for resuspension with LAs in order to increase anesthesia.

1.5.2. Ionic liquids

Ionic liquids (ILs) are chemical compounds with broad applications in the field of chemistry, biology, and medical science (Egorova et al., 2017). But only in 2007 ionic liquids have also been recognized as a potential solution for poorly soluble active pharmaceutical ingredient (API) and polymorphism (Hough et al., 2007). Alike conventional pharmaceutical salts, ILs are comprised of cations and anions but their melting points usually lay below 100 °C (Balk et al., 2015). Many ILs are actually liquids at room temperature showing distinct physical and chemical properties due to ionicity of the molecules.

To transform two API (usually weak acid and bases) into an IL, they should react like Brønsted acids and bases, as in the case of prilocaine/diclofenac and lidocaine/docusate (Balk et al., 2015; Moreira et al., 2015). This dual active component system is able to combine both API biological activity while potentially modifying their physical properties (Kelley et al., 2013). Only systems with fully ionized molecules are considered IL (Balk et al., 2015; Moreira et al., 2015). It is worthy to mention that the degree of ionicity is not yet predictable before the physicochemical characterization, so that different (solid and liquid) multicomponents can be formed instead of IL (e.g. deep eutectic mixtures, co-crystals, molten salts).

1.5.3. Deep eutectic mixture

Eutectic mixtures can be formed between APIs and/or excipients resulting in a mixture of distinguish physicochemical properties (e.g. lower melting point) than the pure compounds (Avula et al., 2010). When the eutectic mixture is liquid at room

temperature the system is called a deep eutectic solvent or deep eutectic mixture (DEM) (Abbott et al., 2003).

ILs and DEMs show similarities and have been used interchangeably in the literature (Smith et al., 2014). However, they are chemically different, since ILs are ionic bonded and DEMs are formed by two neutral molecules attracted by hydrogen bonds (Cherukuvada and Nangia, 2014; Smith et al., 2014).

A well-known example of eutectic formulation is the mixture of the local anesthetic lidocaine and prilocaine (EMLA). These APIs are poorly water soluble and have slow skin permeation when administrated individually. Their eutectic mixture formulation has a melting point (22°C) below the body temperature, thus showing better skin permeation and anesthesia potency (Broberg and Evers, 1985; Brodin et al., 1984). Recent evidences suggest that other DEM formulations containing APIs would also increase the permeation of their components such ibuprofen with menthol, and LDC with ibuprofen and etodolac (Duarte et al., 2017; Miwa et al., 2016; H. Wang et al., 2014).

The transformation of APIs into a dual component liquid form, such as IL and DEM, is an inexpensive approach to optimize the delivery and pharmacological effect of actives (Kelley et al., 2013).

2. SIGNIFICANCE AND IMPACT OF THE PRESENT RESEARCH

The combination of LA with CAP may result in nociceptor-specificity which is useful in a variety of clinical settings as epidural anesthesia and postoperative analgesia. Besides, this combination could help to overcome of the most important limitation of LA, its failure in inflammation condition. This condition demands a high volume of the drug which can put the patient in risk of systemic toxicity. Therefore, any new strategy to decrease the anesthetic concentration needed to achieve the desired effect under inflammation is highly desirable.

Previous studies have only reported the co-administration of LA and CAP, being CAP solubilized in organic solvent (ethanol) and surfactant (polysorbate 80) (Binshtok et al., 2009, 2007; Gerner et al., 2008; Kim et al., 2010). In addition to the double injection discomfort, the solvents cause irritation and other adverse reactions when injected in humans (Strickley, 2004). CDs are then a suitable alternative to replace the use of organic solvents and surfactants, increasing the solubility and stability of pharmaceutical formulations (Loftsson and Duchene, 2007). Therefore, the first part of this thesis was devoted to produce a drug association between MVC (with low affinity for cyclodextrins) and capsaicin (complexed in HP-β-CD) in a single dose formulation.

In Part 2, the IL and DEM systems were explored as a low cost strategy to overcome delivery problems of LA and CAP. Although IL and DEM are similar, their chemical properties suggest different application for local anesthesia. An IL formulation, which contains mainly ions, is usually very soluble and suitable for parental delivery, while a DEM could be exploited to achieve better skin permeation, like EMLA (AstraZeneca PLC, London, U.K.).

The management of neuropathic pain remains a great challenge and many patients are not satisfied with the available treatments, due to undesirable systemic effects and limited efficacy (de León-Casasola and Mayoral, 2016.; Dworkin et al., 2010). Consequently, a therapy that combines the effects of LDC and CAP is very promising. Indeed, a topical medication could possibly have synergistic effects of the drugs, without undesirable systemic effects.

To our knowledge, up to now the effect of an injectable medication containing LA and CAP was never tested upon inflammation, neither as a topical formulation for pain treatment.

3. OBJECTIVES

PART 1

3.1. General objective

Part 1 of this project aimed to increase the solubility of CAP, by its complexation with HP-β-CD, in a freeze-dried parental formulation to be reconstituted in MVC solution, in order to optimize LA pharmacological properties.

3.2. Specific objectives

- To evaluate the effect of HP-β-CD on CAP solubility, finding the equilibrium time, the stoichiometry of complexation and HP-β-CD-CAP stability constant, in solution.
- To establish the best cycle process to freeze-dry the HP-β-CD-CAP complex.
- To characterize the solid HP-β-CD-CAP complex formation using different techniques.
- To evaluated if the inclusion complex, resuspended in MVC solution, would improve anesthesia compared to the free anesthetic solution, *in vivo.*

PART 2

3.3. General Objective

The goal of Part 2 was to study if a LA combined with CAP would form IL or DEM, changing the physicochemical characteristics of the actives, potentially their delivery and pharmacological effect.

3.4. Specific objectives

- To select, by thermal analysis, the most promising amino-amide anesthetic to form IL or DEM with CAP.

- To detect possible intermolecular interactions between LA and CAP by DSC, PXRD, IR and NMR.

- To analyze the stability of the LA-CAP product, and to determine if the solubility of the drugs were modified by the drug delivery system.

4. MATERIAL AND METHODS

PART 1

4.1.   Material

Capsaicin (Cayman Chemical Company), mepivacaine hydrochloride (donated by Cristália Produtos Químicos Farmacêuticos LTDA), hydroxypropyl-β-cyclodextrin (Sigma-Aldrich), acetonitrile HPLC-grade (Sigma-Aldrich), phosphoric acid (Ecibra), potassium phosphate monobasic and dibasic (Synth), sodium acetate (Sigma), acetic acid (Merck), ethanol HPLC-grade (Sigma-Aldrich), aluminum stubs, regenerated cellulose membrane (Spectrapore).

4.2.   Analytical method for capsaicin quantification

The raw material used in CAP pharmaceutical products is composed of no less than 55% pure capsaicin, 20% dihydrocapsaicin and no more than 15% of other capsainoids. Although the raw material was not pure, it was used in this study because there are reports in the literature that dihydrocapsaicin has similar pharmacological action to capsacin (Rollyson et al., 2014).

4.2.1. CAP quantification by UV-Vis spectroscopy

CAP quantification by UV/Vis absorption spectrophotometry (Varian Cary 50 Bio UV-Visible Spectrophotometer) was used in the phase solubility study and determination of complexation equilibrium time. First, the maximum absorption wavelength of CAP, diluted in water and pure ethanol, in the UV-VIS region was determined. Then, molar absorptivity coefficient (ε) and analytical curves were determined to quantify CAP in solution (50% v/v ethanol).

4.2.2. CAP quantification by High Performance Liquid Chromatography

In order to quantify CAP in small volumes (*in vitro* release test) High Performance Liquid Chromatography (HPLC) (Waters Breeze 2 System) was used. The analytical methodology for quantifying CAP followed the monograph of United States Pharmacopeia (USP, 32). Capsaicin samples were analyzed in 50% (v/v) ethanol solution. The mobile phase used was phosphoric acid (1:1000 v/v) and acetonitrile (7:3 v:v), at pH 2.4. The chromatographic column used was Luna® C18 (2) reverse phase, with 25 x 4.6 mm and particle size of 5 μm (Phenomenex, USA). The injected volume was 20 μL, with a flow rate of 1.0 mL/min and oven temperature of 30° C. The wavelength used for analysis was 280 nm. The parameters analyzed in the validation of the methodology were: specificity; precision; accuracy; limit of quantification; and detection.

Specificity

The specificity of a method should be demonstrated by the absence of significant interferences in the retention time of the drug. It was evaluated by the appearance of CAP and placebo (HP-β-CD) peaks.

Linearity

The linearity of a method is demonstrated by its ability to give analytical responses proportional to the concentration of the analyte in a sample. The calibration curve was prepared in the concentration range of 0.15 to 5.00 mM CAP, with at least 5 different concentrations. The correlation coefficient (r) should be above 0.990 according to ANVISA (Agência Nacional de Vigilância Sanitária) (RDC n°166, 2017).

Precision

Precision is the measure of how close the data values are to each other, in a number of measurements conducted at the same analytical conditions. The result can be expressed as the relative standard deviation (RSD) of a series of measures:

$$RSD = \frac{SD \times 100}{C}$$

(Equation 1)

where SD refers to the standard deviation, and C is the mean concentration. The precision parameter was considered in two levels:

- Intraday accuracy or repeatability: referring to the results obtained with the analytical procedure, in measures conducted within a short period of time (same day).

- Interday or intermediate precision: referring to the results obtained with the same analytical procedure performed on different days. According to ANVISA, the relative standard deviation should be no more than 5.0% (RDC n°166, 2017).

Quantification limit (QL) and detection limit (DL)

The quantification limit is the smallest amount of the substance in a sample that can be quantified. QL can be established by analyzing solutions of known and decreasing concentrations of the drug, to the lowest quantifiable level with acceptable accuracy and precision. QL is determined according to the equation:

$$QL = \frac{SDa \times 3}{S}$$

(Equation 2)

where SDa is the standard deviation of the (Y axys) intercept of at least 3 calibration curves, and S refers to the slope of the calibration curve.

The detection limit is the smallest amount of the substance in a sample that can be detected, but not necessarily quantified. DL can be established by analyzing solutions of known and decreasing concentrations of the analyte to the lowest detectable level. DL is determined by the equation:

$$DL = \frac{SDa \times 10}{S}$$

(Equation 3)

4.2.3. Solubility

In order to determine the solubility of CAP in water, three saturated solutions CAP of were prepared and sonicated (40 kHz) for 5 min. The solutions were stirred for additional 24 hours and then centrifuged for 20 minutes (4100 x *g*). The supernatant was diluted, and CAP concentration was determined by HPLC, according to item 4.2.2.

4.3.   Characterization of HP-β-CD-CAP in solution

4.3.1. Determination of the equilibrium time

The time to achieve the complexation equilibrium between HP-β-CD and CAP was determined to optimize the formulation preparation. The solution of 0.065 mM HP-β-CD-CAP was stirred at 350 rpm, at 25 °C or 45 °C. CAP was quantified by UV/Vis spectrophotometer (Agilent/HP 8453 UV-Visible Spectrophotometer) at 280 nm every hour, for 24 hours.

4.3.2. Phase solubility study

The effect of HP-β-CD on the solubility of capsaicin was investigated according to the phase solubility study established by Higuchi and Connors (Higuchi and Connors, 1965). In this experiment increasing concentrations of CD (from 0 to 10 mM) were added to saturated solutions of CAP (20 mg). The solutions were left under magnetic stirring for 48 hours (at 350 rpm and 25 °C). Aliquots of each vial were centrifuged for 10 min (4100 x g, Cientec microcentrifuge), filtered through 0.45 μm filter (Millex, Millipore) and properly diluted for capsaicin quantification by UV/VIS spectrophotometry, at 280 nm. Phase solubility diagrams were obtained by plotting the solubility of CAP, in mM, *versus* the concentration of HP-β-CD.
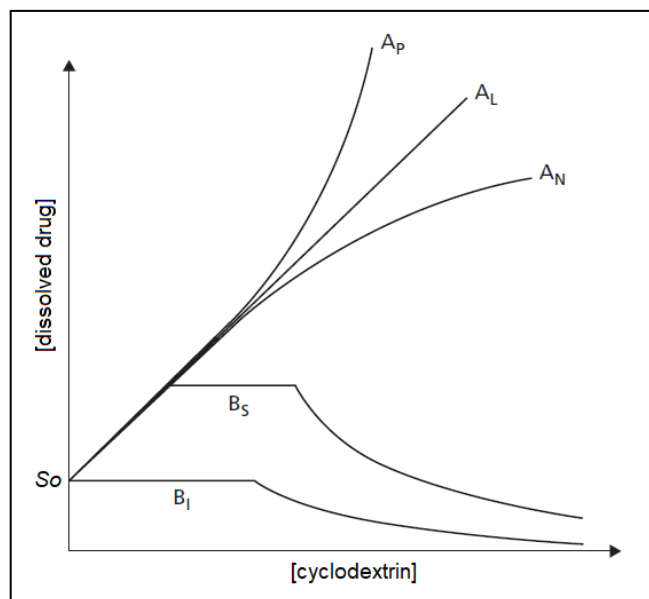
Figure 6– Representation of possible phase diagrams according to the solubility of the formed host-guest complex. Adapted from Loftsson and Brewster, 2010.

The affinity of the drug for the cyclodextrin is determined by the stability constant (equilibrium constant or affinity) of the complex, *Ks*. The assessment of a *Ks* value is based on the examination of the slope and intercept of a phase diagram (**Figure 6**). For a linear phase solubility diagram ("A$_L$" type) in a 1:1 stoichiometry (molar) complex, *Ks* can be calculated by equation 4, where S_0 is the aqueous molar solubility (intercept) of the drug (Loftsson and Brewster, 2010):

$$Ks\,(1{:}1) = \frac{\text{slope}}{S_0\,(1\text{-slope})}$$

(Equation 4)

4.3.3. Complexation efficiency

The complexation efficiency (CE) is an important parameter for the pharmaceutical development cyclodextrin-based formulations. It reveals the adequate drug/cyclodextrin ratio to ensure maximum solubility of the inclusion complex (Loftsson et al., 2005). From the results found in the phase solubility study (item 4.3.2.) it was possible to calculate CE and drug/cyclodextrin ratio (D:CD).

CE can be calculated in complexes of 1:1 stoichiometry (molar) through equation 5 (Brewster and Loftsson, 2007):

$$CE = \frac{slope}{1- slope} = S_0.\, Ks = \frac{[complexed\ CD]}{[free\ CD]}$$

<div align="right">(Equation 5)</div>

With the CE value it is still possible to calculate the drug/CD molar ratio in the formulation, according to equation 6:

$$D:CD = 1 : \frac{CE+1}{CE}$$

<div align="right">(Equation 6)</div>

4.3.4. Determination of the stoichiometry of complexation by isothermal titration calorimetry

Isothermal titration calorimetry (ITC) is the most sensitive method for determining the interaction stoichiometry (complexation) between cyclodextrins and drugs (Bouchemal and Mazzaferro, 2012). The equipment used at the Biomembranes lab of UNIFESP was the MicroCal VP-ITC, in collaboration with Dr. Karin do Amaral Riske. At 25 ° C, small volumes (10 µL) of HP-β-CD solution (10 mM) in CAP solution (0.4 mM) were injected, both solutions containing 10% ethanol. The heat released during the interaction was monitored at each injection and presented as a function of the HP-β-CD-CAP molar ratio, subtracting the heat of dilution (titration of HP-β-CD solution in 10% ethanol). The data were adjusted using the one-site model, according to equation 7:

$$Q = \frac{N M_t \varDelta H V_{cel}}{2}\left(1 + \frac{1}{NKcM_t} + \frac{X_t}{NM_t} - \sqrt{\left(1 + \frac{1}{NKcM_t}\right)^2 + \frac{4X_t}{NM_t}}\right)$$

<div align="right">(Equation 7)</div>

where Q is the amount of heat after each injection, V_{cel} is the cell volume and M_t and X_t are the molar concentrations of CAP and HP-β-CD, respectively. This model assumes that there is a single site of HP-β-CD-CAP interaction, and allows

determination of the molar enthalpy (ΔH), binding stoichiometry (N) and equilibrium constant (Kc).

4.4.   Preparation of the freeze-dried HP-β-CD-CAP

4.4.1. Preparation of the 1: 1 HP-β-CD-CAP

To prepare the 1:1 stoichiometry (molar) complex 119.5 mg HP-β-CD was solubilized in 10 mL deionized water (8.2 mM); and 25 mg of capsaicin was solubilized in 1.5 mL ethanol (99% v/v) (54 mM). Under stirring (350 rpm) at 45 °C, the capsaicin solution was added dropwise to the HP-β-CD solution. The system was agitated for 20 hours for the equilibrium of complexation. Then, the sample was frozen in liquid nitrogen and lyophilized (Freezone 4.5 liter Benchtop Freeze Dry System, Labconco).

4.4.2. Preparation of the 4:1 HP-β-CD-CAP (with excess cyclodextrin)

A 100 mL solution of HP-ß-CD (1g) and capsaicin (0.05 g) was prepared at 25 ºC. The solution was magnetic stirred (350 rpm) for 20 hours and filtered in 0.45 µm filter (Millex, MilliPore). Then, 4 mL of these samples were transferred to lyophilization vials. The parameters of freeze-drying were calculated with the Smart Freeze Dryer Technology software, based on the collapse temperature information (see item 4.4.3.), morphology of the sample, fill volume and vials diameter. The freeze-drying process was carried out (Lyostar 3, SP Scientific) by three process: freezing, primary drying and secondary drying. The freezing process started at the temperature of 25 °C and it was cooled to -40 °C, with a 1 °C/min ramp. The samples were then held in this low temperature for 2 hours. The primary drying had a heating ramp of 0.5 °C/min, until -15 ºC (pressure of 150 mTorr), remaining for 90 min at -15 °C. Then, the temperature was raised up to 5 °C until the end of the primary drying. In the secondary drying, the temperature was raised up to 40 °C with a ramp of 0.1 °C/min, remaining at 40 °C for 4 hours.

4.4.3. Collapse temperature

The collapse temperature is defined as the temperature at which the total loss of the structure occurs (between the dry product matrix and the sublimation interface) (Meister et al., 2009). The collapse temperature was determined to optimize the freeze-drying cycle of the 4:1 (molar ratio) stoichiometry complex, in a Nikon polarized light microscope, model Elipse E600 (Nikon, Japan) coupled to a lyophilization module (Lyostat 2, model FDCS 196, Linkam Instruments, Surrey, UK). The equipment was calibrated with aqueous NaCl solution (eutectic temperature of -21.1 °C). The process of freezing was carried out with ramps of 10 °C/min up to -60 °C, at 750.0 mTorr. Then, the heating was performed in a ramp of 5 °C/min, up to 0 °C, under 100 mTorr pressure.

4.4.4. Stability test

A lyophilized dosage form should be evaluated under storage conditions. Each vial of HP-β-CD-CAP was resuspended in 4 mL of deionized water, and the stability studies were performed in a long-term condition (25 ± 2 °C storage condition) with analysis every 3 months, for a 12 months, accordingly to the Q1A (R2) guideline of ICH (International Conference on Harmonization of Technical Requirements for Registration of Pharmaceuticals for Human Use). Stability testing of new drug substances and products states that no "significant change" for a drug product is defined as a 5% change in assay (UV-Vis spectroscopy) from its initial value. The samples should also meet the acceptance criteria for: appearance of the cake; pH value; and time for resuspension (ICH Q1A (R2), 2003).

4.5.   Characterization of the freeze-dried HP-β-CD-CAP complex

Characterization of the solid 1:1 HP-β-CD-CAP complex was performed using differential scanning calorimetry and powder x-ray diffraction techniques, to investigate the interaction between capsaicin and HP-β-CD in equimolar concentration. Characterization of the freeze-dried product (4:1 HP-β-CD-CAP) was carried out with the differential scanning calorimetry, powder x-ray diffraction, scanning

electron microscopy, and nuclear magnetic resonance to investigate the amorphization of the sample, and the HP-β-CD-CAP inclusion complex formation.

4.5.1. Differential scanning calorimetry

Differential Scanning Calorimetry (DSC) is a technique used to characterize cyclodextrins complexes, by comparing the thermal behavior of pure compounds, their physical mixtures and inclusion complexes (Cui et al., 2012). The samples (5 mg) were analyzed in a Differential Exploration Calorimeter (DSC1, Mettler Toledo) at Laboratório de Recursos Analíticos e de Calibração, Faculdade de Engenharia Química, Unicamp. The heating rate of the samples was 5 °C/min, between 20 °C and 200 °C. Samples were analyzed in 18 mL aluminum, non-hermetic crucibles.

4.5.2. Powder X-ray diffraction

Powder X-ray diffraction (PXRD) was used to investigate the crystallinity degree or amorphization of the inclusion complex in the solid state. The measurements of X-ray diffraction of pure capsaicin, HP-β-CD, 4:1 HP-β-CD-CAP, and their physical mixture were performed in a benchtop X-ray diffractometer (Rigaku Miniflex II, Japan) operating in the Bragg–Brentano reflection mode, equipped with a cooper tube (Cu), line *Kα* radiation X-ray source (Trinity College Dublin, School of Pharmacy/Ireland). The angular intervals used was 5 ° to 40 °, at a rate of 5 °/min in 2θ ° angle, and step size of 0.05. The measurement of X-ray diffraction of 1:1 HP-β-CD-CAP was carried out in collaboration Dr. Margareth Franco of IPEN (Instituto de Pesquisas Energéticas e Nucleares, Brazil). A copper tube (Cu), line Kα radiation X-ray source, at a rate of 1° /minute, between 5 ° and 40 ° in 2θ, in a θ-2θ configuration.

4.5.3. Scanning electron microscopy

Scanning electron microscopy (SEM) was used to observe the morphology resulting from the complexation process between cyclodextrin and CAP. Solid samples of pure capsaicin, pure HP-β-CD, their physical mixture and inclusion complex (4:1 HP-β-CD-CAP) were glued to an aluminum stub using double-sided carbon tapes. The

stubs were covered in gold under vacuum for 200 seconds (Sputter Coater SCD-050) to become electrically conductive. The samples were analyzed by secondary electron emission (Scanning Electron Microscope JSM 500, Laboratório de Microscopia, IB/Unicamp).

4.5.4. Proton Nuclear Magnetic Resonance

Nuclear magnetic resonance spectrometry (NMR) is one of the most powerful techniques to investigate the interaction between guest compounds and the cyclodextrin molecule (de Paula et al., 2010b; Pessine et al., 2012). Proton NMR (^{1}H-NMR) provides evidence of the complexation, for instance, by the change in the ^{1}H chemical shift between the free CD and compounds species and the presumed complex. Following, Rotating Frame Overhauser Effect Spectroscopy (ROESY-NMR) and diffusion ordered spectroscopy (DOSY) measurements were performed in collaboration with Dr. Luis Fernando Cabeça, from Universidade Federal Tecnológica do Paraná (Londrina) in a Bruker Avance III 400 MHz. The samples were placed in a 5 mm probe for direct and indirect detection, with a z-magnetic gradient and selective pulses. The deuterium signal of the solvent was used as field lock and adjustment of the homogeneity of the magnetic field.

4.5.4.1. Rotating Frame Nuclear Overhauser effect

Nuclear Overhauser effect (NOE) is a phenomenon observed in NMR spectroscopy due to the transfer of the nuclear spin polarization from one population of nuclear spins to another, via cross-relaxation. The inter-atomic distances derived from the observed NOE are particularly useful to clarify the three-dimensional structure of a molecule or of a complex (Mura, 2014).

The ROESY spectrum was obtained in 4:1 HP-β-CD-CAP sample solubilized in D_2O, allowing determination of intramolecular and intermolecular NOEs, indicating non-covalent (through-the-space) proximities between hydrogens from CAP and HP-β-CD. ROESY2D was carried out using spin-locked conditions and NOE in the transverse positive plane. Pulse sequence was employed, with a mixing time of 300 ms.

4.5.4.2. Diffusion coefficient and determination of affinity constant

Diffusion Ordered Spectroscopy (DOSY) is an experiment that separates the signals of a mixture of components according to the size and shape of the molecules, and their diffusion coefficients (Morris and Johnson, 1992).

The molecular diffusion coefficient consists of random (Brownian) motion of the molecules due to the thermal energy of the system and can be calculated by the Stokes-Einstein equation:

$$Dc = \frac{k.T}{6\pi.\eta.r}$$

(Equation 8)

where D_c is the diffusion coefficient (m^2s^{-1}), k is the Boltzmann constant (1.3806×10^{-23} m^2 kg s^{-2} K^{-1}), T is the absolute temperature (K), η is the dynamic viscosity (Pas) and r the radius of the molecule.

DOSY technique is a tool used to determine the association constant (*Ka*), which is particularly important to evidence the binding between guest molecules and cyclodextrins. In addition to *Ka*, it is possible to calculate the complexed fraction ($F_{complexed}$) of the guest molecule. Both values were calculated by the following equations (Gounarides et al., 1999):

$$F_{complexed} = \frac{[D_{drug} - D_{complex}]}{[D_{drug} - D_{ciclodextrin}]}$$

(Equation 9)

$$Ka = \frac{[D_{drug} - D_{complex}]}{[D_{drug} - D_{ciclodextrin}] \times R}$$

(Equation 10)

where D_{drug} is the diffusion coefficient of free drug, $D_{complex}$ is the diffusion coefficient of the complex, $D_{cyclodextrin}$ is the diffusion coefficient of free cyclodextrin and R is the molar concentration of non-complexed cyclodextrin.

All the experiments were performed with 16 different field gradient amplitudes and the diffusion time of 0.06 s. The data processing program used was DOSY Toobox. The calculated coefficients for each selected signal were listed along with the respective standard deviations. The coefficient of diffusion and standard deviation of each species involved in the analysis was given by the arithmetic mean of all coefficients of the same species. The average acquisition time of the experiment was 40 minutes. The results of the DOSY analysis method are a pseudo two-dimensional spectrum with ^{1}H NMR chemical shifts at one axis and the calculated diffusion coefficient (10^{-10} m^2s^{-1}) on the other axis.

4.6. *In vitro* release

A "Franz-type" vertical diffusion cell system was used to evaluate the *in vitro* release of CAP dissolved in (20% v/v) ethanolic solution and complexed with HP-β-CD (Franz, 1975). This system consists of two compartments: the donor containing 1 mL of the sample; and the acceptor compartment, containing 12 mL of buffer (10 mM PBS, pH 7.4) kept at 37 °C, under mild stirring to ensure sink condition (Aulton and Taylor, 2013). A cellulose membrane (Spectrapore, with molecular exclusion pores of 1000 Da) separated the two compartments. Aliquots (200 µL) were withdrawn from the acceptor compartment at fixed intervals (15, 30, 60, 45, 60 and 90 minutes and every hour for 6 hours) and the volume was replaced with fresh medium. CAP was quantified by HPLC and concentrations were converted to % of cumulative release.

4.7. *In vivo* evaluation of the effect of HP-β-CD-CAP complex with LA

The drug combination between MVC and complexed CAP (HP-β-CD-CAP) was evaluated *in vivo*. A sample of freeze-dried HP-β-CD-CAP was resuspended in 4 mL of mepivacaine hydrochloride solution (MVC) to final concentrations of 1.6 mM (0.05%) capsaicin and 2% MVC. MVC solution was sterilized before use by filtration through 0.22 µm filters (Millex, Millipore). Since the clinical doses of local anesthetics

are usually expressed in percentage (w/v), throughout this experiment, CAP dose will be expressed in % (w/v), as well.

The *in vivo* assays were divided into two experiments approved by Animal ethic committee UNICAMP/IB Protocol #4402-1. The first evaluated the anesthesia of the sciatic nerve and the second evaluated the anesthesia in the inflamed paw of mice (male Swiss, 6 weeks old) obtained from CEMIB-UNICAMP (Centro de Bioterismo - UNICAMP, Campinas, SP, Brazil).

Groups:
- Saline solution (analgesia in inflamed tissue);
- 0.05% HP-β-CD-CAP sample (analgesia in inflamed tissue);
- 2% MVC solution (sciatic nerve block and analgesia in inflamed tissue);
- 0.05% HP-β-CD-CAP suspended in 2% MVC (sciatic nerve block and analgesia in inflamed tissue).

4.7.1. Sciatic nerve block

The technique of blocking the sciatic nerve of mice was performed according to the method described by Leszczynska and Kau. Initially, it was observed the ability of each mouse to walk normally on a metallic screen (with a mesh of 5 mm diameter) in the regular and inverted position. Only animals that fulfilled this requirement were subjected to experimentation. The samples were administered by intramuscular infiltration (0.1 mL) around the sciatic nerve, in the right hind paw of the animals (Leszczynska and Kau, 1992).

4.7.1.1. Sensory block

The sensory block was measured by the paw removal threshold of the animals against a mechanical stimulus. The sensory block was measured by a analgesy-meter (model 37215, Ugo Basile, Italy) which generates a gradual increase in pressure (grams) on the dorsal surface of the animal paw (Fletcher et al., 1997). The paw of the animal was gently placed under the plastic tip of the apparatus until the animal withdraw the paw, as indicative of pain (threshold). The baseline test was measured before injecting vehicle or drugs (baseline). After injection, the test was

performed every 15 minutes for 3 hours. The maximum cut-off value was 150 g to avoid foot injury and excessive stimulation of nociceptors. Results were calculated in maximum possible effect = (threshold - baseline)/(cutoff - baseline).

4.7.1.2. Motor block

The intensity of the motor block was evaluated according to level values: 0 (normal use of the injected paw), 1 (inability to completely flex the injected limb) and 2 (inability to use the injected paw) (Gantenbein et al., 1997). The evaluation was performed every 15 minutes until the animals totally recovery their movements.

4.7.2. Evaluation of analgesia in inflamed tissue

The mechanical allodynia was analyzed in mice hind paw by a Dynamic Plantar Aesthesiometer (model 37450, Ugo Basile, Italy). The animals were placed in an elevated cage for 2 hours before the test started for setting and training. After that, 25 µL of carrageenan (2% w/v) was applied in the subplantar region of the right mice paw to induce inflammation (Fehrenbacher et al., 2012). After 4 hours of injection, the basal measurement was performed with a thin steel rod (0 - 5 g for 20 seconds, 0.5 g/second). Then, the anesthetic formulations were applied into the same subplantar region of the right paw of the mice, and the pain threshold was evaluated every 15 minutes. One group of animals was injected with sterile saline, as the control group. After the mechanical stimulus, the time elapsed until the paw withdrawal as well as the applied pressure value were automatically recorded. The measures of time(s) were relativized to the baseline time (latency/baseline x 100) and presented according to the duration of the test (minutes) (Fletcher et al., 1997).

PART 2

The Part 2 of this thesis was performed at Trinity College Dublin, Dublin, Ireland. The following equipment belongs to The School of Pharmacy and Pharmaceutical Sciences: Diamond DSC, Rigaku Miniflex II desktop X-ray diffractometer, PerkinElmer Spectrum One FT-IR Spectrometer, Advantage-1 automated gravimetric vapor sorption analyzer. And the NMR studies were performed at School of Chemistry using 600 MHz NMR Bruker Avance II spectrometer and 400 MHz NMR Bruker Avance III spectrometer.

4.8. Material

Mepivacaine (Fluorochem), bupivacaine (Fluorochem), lidocaine (Sigma-Aldrich), lidocaine hydrochloride (Sigma-Aldrich), capsaicin (Cayman Chemical Company), acetonitrile (Sigma-Aldrich, U.S.A.), phosphoric acid (Astech), chloroform-deuterated (Sigma-Aldrich, U.S.A.).

4.9. Screening of LA to combine with CAP

The preparation of the sample was conducted by mechanochemical synthesis which is a solvent-free blending, this technique being preferred over other due to its environmental benefit (Martins et al., 2017). Different quantities of CAP and one of the tested LA (Bupivacaine, Mepivacaine, Lidocaine Hydrochloride, and Lidocaine base) were added to a mortar/pestle and mixed in different molar ratios. DSC analysis was performed following the method below (item 4.10.1.) and the LA:CAP mixture that showed the lowest melting temperature was selected for further characterization.

4.10. Physicochemical characterization

4.10.1. Thermal analysis

The thermal analysis was conducted to optimize the proportion of compounds in the sample and to characterize the thermal properties of the mixture. DSC thermograms were performed via an initial heating, at 10 ºC/min, to 100 °C (Lidocaine Hydrochloride, and Lidocaine base mixtures), 110 °C (bupivacaine) or 150 °C (mepivacaine); after that the samples underwent super-cooling (at 300 °C/min) to -65 °C and were submitted to a second heating (at 10 ºC/min). The DSC measurements were carried out using a Diamond DSC (PerkinElmer, U.S.A). The unit was refrigerated using a ULSP B.V. 130 cooling system with nitrogen (40 mL/min) as the purge gas. Samples were analyzed in 18 mL aluminum, non-hermetic crucibles. The unit was calibrated with indium and zinc standards.

The Schröder–van Laar equation (Equation 11) was used to calculate the eutectic temperature (Schröder, 1893; Van Laar, 1903).

$$ln(x_i) = -\frac{\Delta fus\, H_i^{\circ}}{R} + \left(\frac{1}{T} - \frac{1}{T_{fus}}\right)$$

(Equation 11)

The eutectic temperature was determined from the intersection of the two liquidus lines obtained from the Schröder–van Laar equation, describing a simple eutectic mixture, where x_i is the mole fraction of the compound at a temperature T, $\Delta fus\, H_i^{\circ}$ is the latent heat of fusion of a pure component, R is the gas constant (8.3144598 J.K^{-1}.mol^{-1}) and T_{fus} refers to the onset of the melting temperature of pure component.

4.10.2. Powder X-ray diffraction

PXRD diffractograms of the pure capsaicin, lidocaine, and mixture of LDC (base) and CAP (at molar ratio 6:4, [LDC]$_6$[CAP]$_4$; 1:1, [LDC]$_1$[CAP]$_1$; 4:6, [LDC]$_4$[CAP]$_6$) were determined using a Rigaku Miniflex II, a desktop X-ray

diffractometer (Rigaku, Japan) operating in the Bragg–Brentano reflection mode, equipped with a Cu Kα radiation X-ray source. The angular interval used was 5 ° to 40 ° in 2θ°, with a step size of 0.05.

4.11. Investigation of intermolecular interactions

4.11.1. Fourier- transform infrared spectroscopy

Fourier transform Infrared (FT-IR) spectra analysis was recorded on a PerkinElmer Spectrum One FT-IR Spectrometer (PerkinElmer, U.S.A.) in the region 4000-650 cm^{-1}. The spectra of the LDC:CAP mixture samples were normalized and background corrected.

4.11.2. Nuclear Magnetic Resonance

The ^1H and ^{13}C NMR spectra of pure LDC, CAP, and $[LDC]_1[CAP]_1$ in chloroform were record at 25 °C for 5% solution on a 600 MHz NMR (Bruker Avance II, operating at 600.13 MHz for proton, 150.9 MHz for carbon-13) using the Bruker Topspin 3.2 software. The spectrometer was set up with a Chloroform-deuterated sample in each case, to provide an external reference.

The ^1H and ^{13}C NMR spectra of neat samples of LDC, CAP, and $[LDC]_1[CAP]_1$ were record at 25 °C, 40 °C, and 70 ° C on a 400 MHz NMR, Bruker Avance III spectrometer, operating at 400.23 MHz for proton, 100.6 MHz for carbon-13), under open lock condition and using the Bruker Topspin 3.5 software.

4.12. Stability studies

Moisture-induced instability of the systems produced was tested in an Advantage-1 automated gravimetric vapor sorption analyzer (DVS) (Surface Measurement Systems Ltd, UK). The temperature was kept at 25.0 ± 0.1 °C. Approximately 10 mg of $[LDC]_1[CAP]_1$ samples were added to the sample basket. The sample were equilibrated at 0% relative humidity (RH) until a constant mass was

determined (dm/dt <0.002 g/min). The reference mass was recorded, and sorption-desorption analysis was carried out between 0 and 90% RH, in steps of 10% RH. At each stage, the sample mass was equilibrated (for at least 10 minutes) before RH was changed. Following DVS analysis, the samples were analyzed by PXRD in order to detect any crystallization.

4.13. Solubility studies

Solubility studies were performed at 37 °C using a conventional magnetic stirring method. A quantity of pure LDC, CAP or $[LDC]_1[CAP]_1$ (in excess of the expected saturated solubility) was added to 40 mL stirred vials, containing water. Samples were drawn from the vials at specific time points over a 24 hour-period. These aliquots were filtered with 0.45 μm membrane filters and diluted with 0.1% phosphoric acid:acetonitrile. (50:50 v/v) and analyzed by HPLC. The wavelength used for analysis was 280 nm for capsaicin and 210 nm for lidocaine, following the method described at item 4.2.2.

5. RESULTS AND DISCUSSION

PART 1

5.1. Analytical method for capsaicin quantification

5.1.1. CAP quantification by UV-Vis spectroscopy

CAP quantification by UV/Vis absorption spectrophotometry was used in the Determination of complexation equilibrium time and Phase solubility study. A detailed description of CAP quantification by UV-VIS spectroscopy is found in APPENDIX 1.

First, it was investigated the maximum absorption wavelength of CAP, diluted in water and ethanol, in the UV region. The wavelength of maximum absorption of CAP in aqueous solution was 278 nm, in agreement with previous report in the literature (Shen et al., 2012). The maximum absorption wavelength of capsaicin when dissolved in ethanol was slightly shifted to the red (λ = 280 nm), with no evident changes in the absorption intensity.

From the analytical curves, the calculated coefficient of molar absorptivity (ε) for capsaicin was 2760 ± 345 and 3004 ± 257, in water and ethanol (50% v/v), respectively. The regression coefficients of all curves were above 0.99. This value demonstrate the linear relationship predicted by the Lambert-Beer law between UV absorption and CAP concentration. Overall, both solvents are suitable for CAP quantification by UV spectrophotometry but in a different range of concentration: at concentrations below 0.065 mM and 0.3 mM, for water and ethanol (50% v/v), respectively. This difference reflects the poor water solubility of CAP, curbing its determination at high concentrations, despite the similar ε values determined in both solvents. The equation obtained in the CAP curve diluted in ethanol (50% v/v) was used in the phase solubility study for CAP quantification.

5.1.2. CAP quantification by HPLC

The CAP analytical method of quantification by HPLC followed the monograph of the American Pharmacopoeia (USP, 32). The method demonstrated

suitable specificity, showing well-resolved capsaicin and dihydrocapsaicin peaks, with no interferences. The coefficients of determination of the curves obtained were higher than 0.99, in the three-day tests, confirming the linearity of the method. The reproducibility, expressed by the relative standard deviation of concentrations, was less than 5%. The quantification and detection limit values were 0.001 mM and 0.0003 mM, respectively. The parameters used to evaluate the methodology were in accordance with the recommendations of ANVISA (RDC n° 166, 2017). A detailed description of capsaicin quantification by HPLC is found in APPENDIX 1.

5.1.3. Solubility of capsaicin

Saturated water solutions of CAP were assayed by UV to determine the CAP aqueous solubility. The determined solubility of CAP was 0.12 ± 0.02 mM, a similar result to that (0.19 mM) observed by Turgut and coworkers (Turgut et al., 2004). Thus, according to the Brazilian Pharmacopoeia (Agência Nacional de Vigilância Sanitária (Brazil) and Fundação Oswaldo Cruz, 2010) this active principle can be classified as practically insoluble in water.

Previous studies, have only reported the co-administration of LA and CAP (1-3 mM), being CAP solubilized in organic solvent (ethanol 20% v/v) and surfactant (polysorbate 80 and 20) (Binshtok et al., 2007; C. H. Wang et al., 2014). The results of the solubility tests indicate that CAP aqueous solubility is below the concentration needed to achieve the expected effect of the combination drug (LA with CAP). Although CAP is soluble in alcohol (USP, 32) the use of organic solvents is not recommended for parenteral administration because can cause pain, inflammation, and hemolysis upon injection (Strickley, 2004). Therefore, complexation with HP-β-CD may be an interesting strategy to increase CAP's solubility since this modified cyclodextrin is approved by the FDA for infiltrative use (Loftsson and Brewster, 2012).

6.1. Characterization of HP-β-CD-CAP complex in solution

6.1.1. Equilibrium time

Initially, spectrophotometric experiments were performed to establish the optical properties of the HP-β-CD-CAP complex. If there was any interaction between CAP and HP-β-CD cyclodextrin, some optical changes would be observed in HP-β-CD-CAP sample, when compared to the CAP spectrum, at the same drug concentration. The spectra of CAP, HP-β-CD and equimolar HP-β-CD-CAP samples were shown in **Figure 7**. HP-β-CD in solution showed no absorption peaks in the UV region (between 200-350 nm). The HP-β-CD-CAP sample showed a significant increase in the absorption intensity, when compared to CAP solution, in the same concentration. The hyperchromic shift is a phenomenon that occurs due the disturbance of the chromophore electrons when CAP is included into the cyclodextrin cavity (Shen et al., 2012; Zhao et al., 2016). Therefore, here is first indication that HP-β-CD and CAP are able to form a complex.
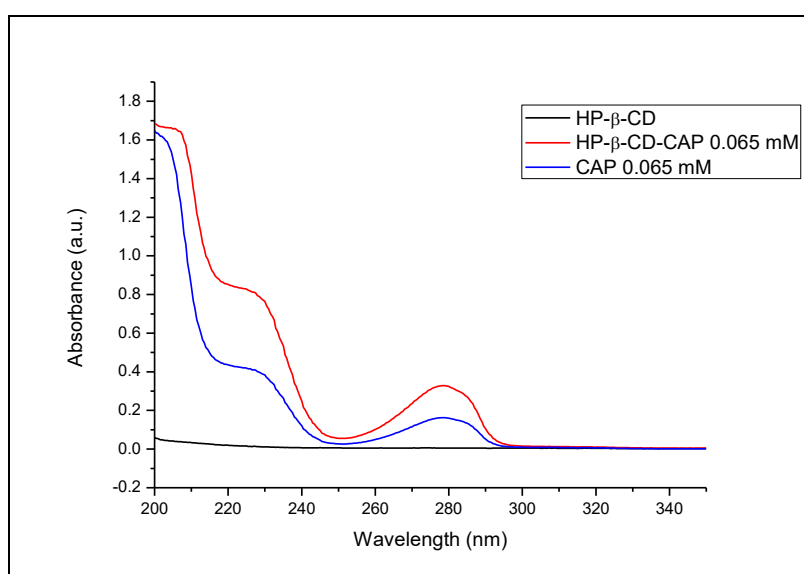
Figure 7- UV absorption spectra in water of capsaicin, free and complexed with HP-β-CD (1:1 molar ratio), after 1 hour of stirring at 25 ° C. The spectrum of HP-β-CD is also given, as a control.

The determination of the minimum time to reach the complexation equilibrium of HP-β-CD-CAP is an important parameter to optimize the preparation of the complex in solution. The study was performed at 25 °C and 45 °C and the equilibrium time was defined by the time when the absorbance becomes stable, for

over 2 hours. It can be observed that complexation at 45 °C is slightly faster than 25 °C at the initial time, but no notable differences between the both curves were found after 8 hours of stirring (**Figure 8**).
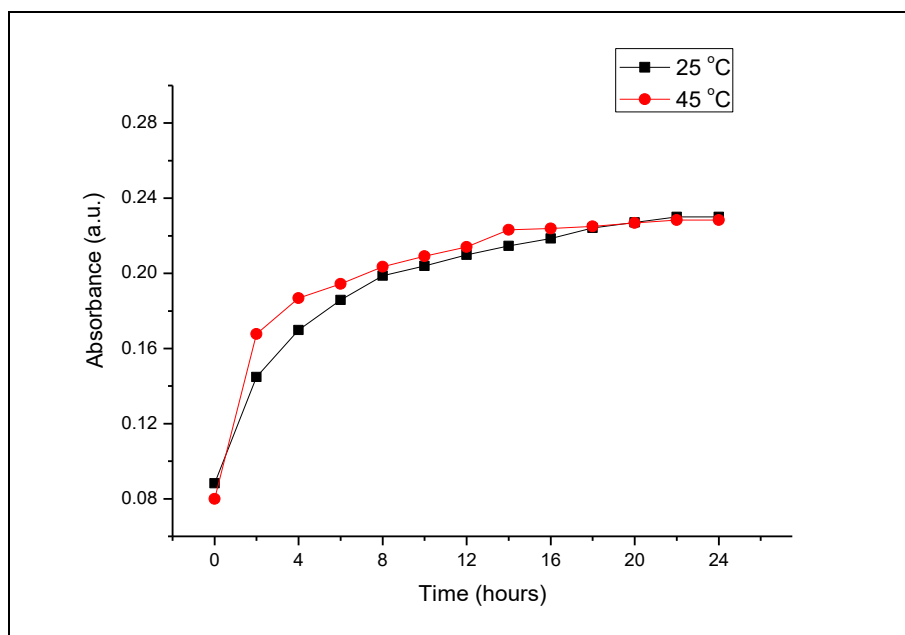
Figure 8 - HP-β-CD-CAP complexation kinetics, followed during 24 hours, at 25 and 45 °C.

The absorbance intensity became stable, for both temperatures, after *ca.* 20 hours of stirring. Some authors have described 3-7 days of stirring as method of complexation (Loftsson et al., 2005). However, CAP has stability issue in water and should be storage protected from light (Costanzo et al., 2014). Accordingly, a long time of preparation is not recommended and it was defined that HP-β-CD-CAP complex should be prepared under magnetic stirring (350 rpm) for 20 hours, at room temperature.

6.1.2. Phase solubility study

In order to evaluate the effect of HP-β-CD on CAP solubility, increasing concentrations of the CD were added to a saturated solution of CAP. According to

Higuchi and Connor, phase solubility diagrams can show two types of behavior (A and B), type A occurring when the formed complex is soluble and type B when the complex formed becomes insoluble, from a certain concentration of the binder (cyclodextrin), according to **Figure 6**. In the A_P and A_N formats, the binder significantly increase the solubility at higher and lower concentrations, respectively (Loftsson and Duchene, 2007). The A_L profile indicates a linear increase in solubility as a function of the binder (CD concentration). Chemically modified cyclodextrins, including HP-β-CD, usually produce soluble complexes (A_L-profile) (Del Valle, 2004). As expected, the system containing HP-β-CD and CAP showed an A_L type profile (**Figure 9**) in the range of 0 - 10 mM of HP-β-CD. The same phase diagram format was reported for HP-β-CD-CAP by other authors (Shen et al., 2012; Zhao et al., 2016; Zi et al., 2008). The apparent solubility of CAP improved up to 20 times considering the CD concentration studied here. Assuming that the complexation of HP-β-CD-CAP occurs in a 1:1 stoichiometry (as indicated by the A_L type diagram), the stability constant (*Ks*) was calculated according to Equation 4.
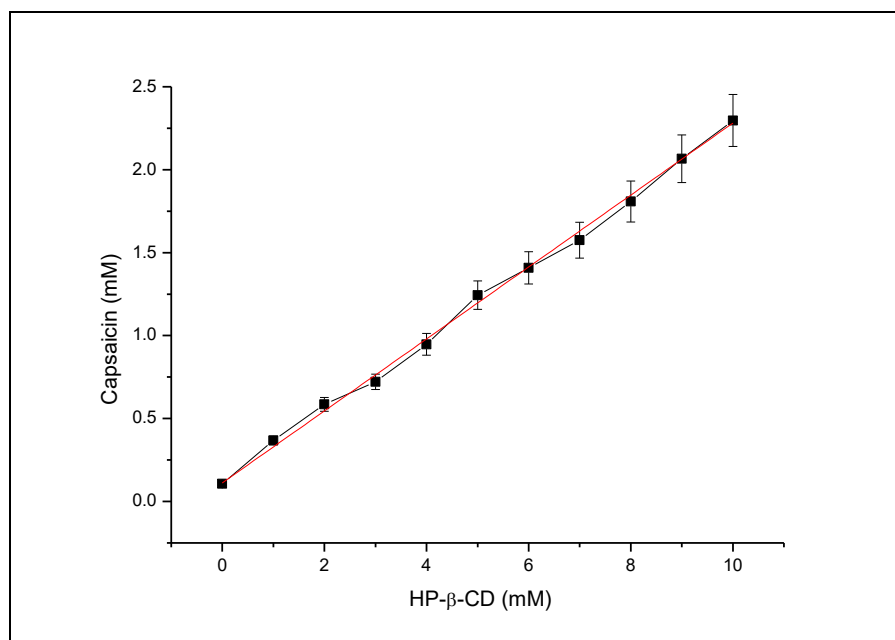
Figure 9- Capsaicin solubility diagram, at different concentrations (0-10 mM) of HP-β-CD, at 25 °C. The results are expressed as mean ± SD (n=3).

The stability constant between HP-β-CD and CAP was Ks = 2400 ± 221 M^{-1}. Usually, drug–cyclodextrin binding constants have values between 10 and 2000 M-1; rarely much higher than 5000 M-1 (Loftsson and Brewster, 2010). Therefore, the Ks of HP-β-CD-CAP shows strong interaction between the CD and CAP. Two previous works in the literature, reported similar Ks values for the HP-β-CD-CAP: 1822 M^{-1} (Zi et al., 2008); and 966 M^{-1} (Shen et al., 2012), using up to 10 times greater HP-β-CD concentrations than here. We did not use such high amount of HP-β-CD because Do and coworkers reported that HP-β-CD at concentrations higher than 12 mM can forms aggregates, that could influence the complexation and Ks values (Do et al., 2017).

The solubilizing effect of CD occurs due the formation of inclusion and non-inclusion complexes. Frequently, when non-inclusion complex occurs there is a formation of dimers, trimers and other soluble oligomers of CD. In this condition, the intercept of the phase solubility diagram is different from the intrinsic solubility of the guest molecule (Loftsson et al., 2005). The curve intercept value of HP-β-CD-CAP diagram (**Figure 9**) and CAP solubility (item 5.1.3.) were very similar, 0.13 ± 0.02 mM and 0.12 ± 0.02mM, respectively. This result indicates that CAP probably form inclusion complexes with HP-β-CD.

Although phase solubility is a very useful tool, it should be considered that the test is performed under drug-saturated media, which is not ideal (Brewster and Loftsson, 2007). Also, Ks values are very sensitive to external conditions (temperature, impurities), method and mathematical interpretation of the experiments (Loftsson and Brewster, 2010). Therefore, different analytical methods should be examined together to assess CD complexes. So far, the most evident information about the HP-β-CD-CAP complexes is that they are water soluble. Following, more specific techniques such as ITC and NMR were used to investigate complexation constants and stoichiometry.

6.1.3. Complexation efficiency

The main goal of adding CDs to medicines is to increase the drug water solubility. CD is strategic to get soluble injectable products has advantages over the co-solvent approach because upon dilution will not precipitate (Strickley, 2004). During formulation development it is important to use the minimum cyclodextrin concentration

necessary to achieve solubilization effect (Loftsson et al., 2005). Thus, determining the complexation efficiency (CE) may be more important than evaluating the absolute value of the drug-cyclodextrin affinity constant (Ks). CE can be calculated from the results of the phase solubility diagram (item 6.1.2.), according to equation 5.

The CE value (**Table 1**) determined for HP-β-CD-CAP was approximately 0.33, indicating that for each complexed cyclodextrin there are 3 free cyclodextrin molecules, assuming the 1:1 stoichiometry of complexation. Loftsson et al. evaluated the CE of 28 different drugs and the mean value found was 0.3 (Loftsson et al., 2005). Thus, CE between CAP and HP-β-CD indicates typical complexing ability, requiring a low amount of CD for the optimal formulation (see item 4.2.2.).

Additionally, it is possible to know the drug:cyclodextrin ratio (D:CD) in the formulation, according to equation 6. The D:CD ratio in Table 1 indicates that each mole of CAP requires 4.2 moles of HP-β-CD to produce the desired soluble formulation. Even though the complex stoichiometry being 1:1 (see item 6.1.4.), the dynamic behavior of the drug-cyclodextrin interaction (weak van der Waals) justifies the need for excess cyclodextrin to keep the complexed fraction (Bouchemal, 2008). The same occurs with other compounds such as terfenadine, miconazole, and clotrimazole that demand 4, 12 and 21 molecules of HP-β-CD, respectively, for optimal complexation (Loftsson et al., 2005). Therefore, to prepare a formulation containing 1.6 mM capsaicin it is necessary to add 6.8 mM HP-β-CD.

Table 1- Parameters evaluated in the phase solubility study of HP-β-CD-CAP complex in solution, at 25 °C: Stability constant (Ks), Complexation efficiency (CE) and drug:cyclodextrin ratio (D: CD). The results are expressed as mean ± SD (n=3).

Ks (M^{-1})	CE	D:CD
2400 ± 221	0.33 ± 0.08	1:4.2±0.7

6.1.4. Determination of the stoichiometry of complexation by isothermal titration calorimetry

ITC measures the heat, generated or absorbed, resulting from the interaction between two molecules or other chemical processes. This technique allows the determination of the stoichiometry of interaction (N) between molecules, and their affinity constant (*Kc*) in a single experiment (Holdgate and Ward, 2005).

The sample cell and the stirring syringe were filled with CAP and HP-β-CD solution, respectively. Each injection of HP-β-CD on CAP solution led to the formation of a complex, and thus to the release of heat. Although the concentration of the applied solution was relatively low, there was still a significant release of heat detectable after injection, as shown in the raw data (**Figure 10A**). This heat release (exothermic reaction) results from the interaction between CAP and HP-β-CD, ΔH= -0.6 kcal/mol. It can be observed that most HP-β-CD molecules bond during the first injections, because of the excess free CAP. As the concentration of free CAP molecules in the cell was decreasing after each injection, heat was diminishing all along the titration, since less and less complexes were formed.
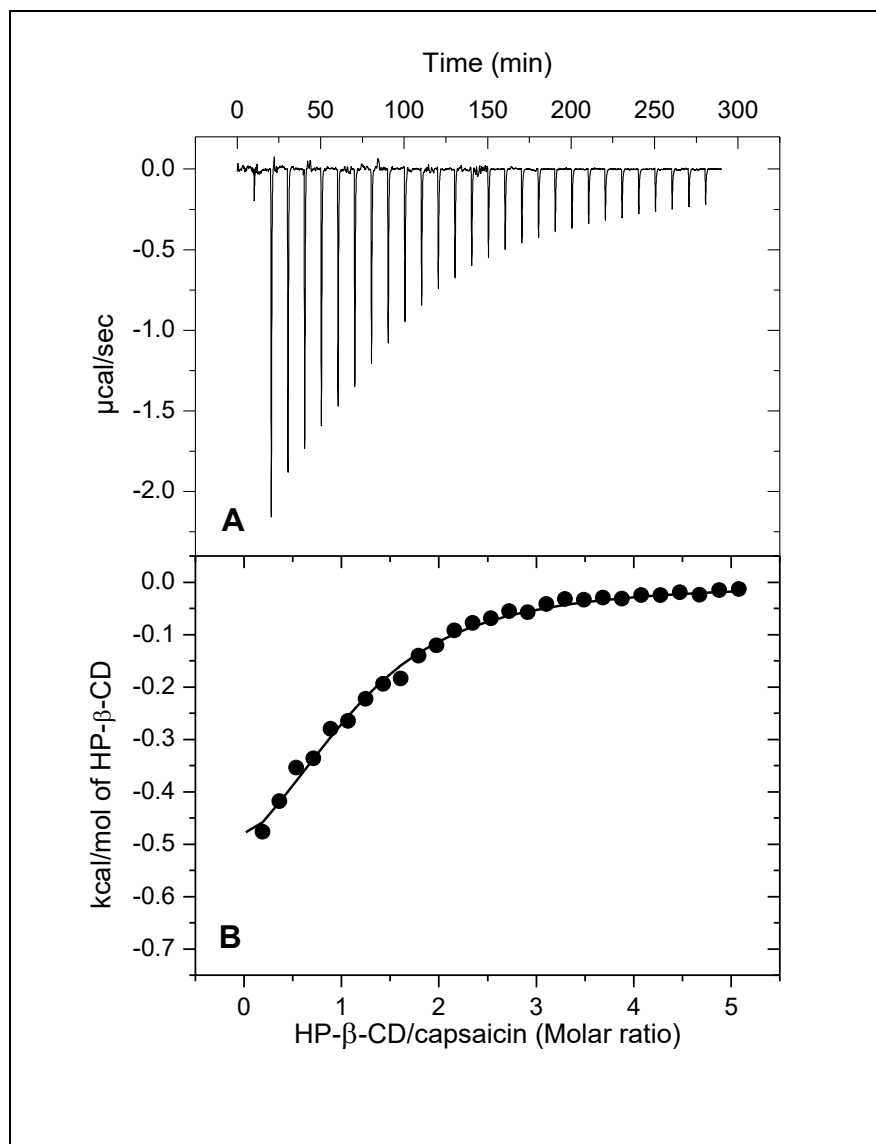
Figure 10- Titration calorimetric curve of HP-β-CD (10 mM) in CAP (0.4 mM) at 25 ° C. A- Raw data of heat flow against time; B- integration of the curve area obtained after correction of the heat of dilution.

Figure 10B shows the results after integration of each peak, in terms of heat (kcal) per mol of HP-β-CD, after subtraction of the heat of dilution. Most thermodynamic studies of the formation of cyclodextrin complexes describe the 1:1 stoichiometry (Bouchemal, 2008). As expected, the data was adjusted using the model of a 1:1 binding site which showed the best fit, in agreement with the phase solubility study. After the stoichiometry is known, the affinity constant could be precisely calculated.

The affinity constant of HP-β-CD-CAP determined by ITC ($Kc = 5100$ M^{-1})

was on the same order of magnitude of that determined from the phase solubility study (K_s=2400 M^{-1}), even though the experiments were performed in different solvent and concentration range. Likewise, ibuprofen/HP-β-CD demonstrated a similar constant value of 5146 M^{-1} and 1080 M^{-1} obtained by ITC and phase solubility study, respectively (Bertaut and Landy, 2014; Felton et al., 2014). However, Rodrigues-Perez et al. found notably different values (two magnitude order) of the affinity constant between sertaconazole/HP-β-CD in both techniques (Rodriguez-Perez et al., 2006).

Since the aim of this thesis is develop a combination drug including LA and CAP, it would be relevant to compare the K_c of HP-β-CD with LA, but it has not been described yet in literature. Only procaine hydrochloride complexation with β-cyclodextrin was investigated describing a K_c of 293.17 M^{-1} (Pîrnău et al., 2014). Generally, hydrochloride LAs show weaker complexes than the base form of LA, considering affinity constant (Dollo et al., 1996).

Overall, ITC confirmed a 1:1 stoichiometry and a strong binding complexation of HP-β-CD-CAP in solution. Following, other techniques in the solid state should help the assessment of the actual inclusion complex formation and appropriate characterization.

6.2.   Freeze-drying

Freeze-drying (or lyophilization) process is commonly used to increase product stability because dehydration decreases the probability of chemical reactions to occur (Franks, 1998). Lyophilization is also one of the methods described for preparation of solid inclusion complexes between drugs and cyclodextrins. Interestingly, the major challenges in the pharmaceutical use of capsaicin is its low stability and water solubility (Costanzo et al., 2014). Consequently, lyophilization of the HP-β-CD-CAP complex is an interesting approach to deliver capsaicin.

6.2.1. Preparation of freeze-dried HP-β-CD-CAP sample

The freeze-drying process removes the water by sublimating the ice of a frozen product (Swarbrick and Boylan, 2000). The freeze-dried samples were prepared with two different techniques. Preparation of the 1:1 HP-β-CD-CAP complex used ethanol (co-solvent) to solubilize CAP in order to produce a 1:1 (molar ratio)

stoichiometry complex. During lyophilization, solutions containing up to 20% ethanol experienced collapsed cakes and are near impossible to dry; solution with 10% ethanol (v/v) appeared to dry slowly and request a freeze-dryer system that reaches -105 °C (not typical commercial freeze-dryer) (Rey and May, 2011; Seager et al., 1985). Therefore, the freezing step was not possible to be performed with the available controlled temperature freeze-dryer (Lyostar 3, SP Scientific) which shelf temperature control range between -70 °C to +60 °C. Instead, the drying was performed in a laboratory bench freeze-dryer (without temperature control) to keep the sample initially at very low temperature (with the help of liquid nitrogen).

The preparation of the 4:1 (molar ratio) HP-β-CD-CAP complex sample did not use any organic solvent. The appropriate amount of cyclodextrin (CE value, item 6.1.3.) and the lyophilization parameters (item 6.2.1.2.) were optimized for this formulation and it is discussed below.

6.2.1.1. Collapse temperature determination

An optimized lyophilization process ensures better product stability, shorter processing cycles and lower costs (Patel et al., 2010). One of the parameters to optimize the freeze-drying cycle is the collapse temperature, determined by freeze-drying microscopy. Meister and coworkers have defined the onset of collapse (Tc) as the temperature in which the first gaps and fissures were visible, adjacent to the sublimation interface; while full collapse describes the complete loss of structure (Meister et al., 2009).

Figure 11 shows the freeze-drying process of HP-β-CD-CAP solution (4:1 HP-β-CD-CAP) under the microscope. In **Figure 11A**, the solution is liquid at 10 °C, then it is cooled down (**Figure 11B**) to the temperature of -60 °C (freezing point at -24 °C). Following, the system was heated up and the Tc event started at -12 °C, showing a subtle rupture of the matrix, as shown in **Figure 11C**. The total collapse occurred at -10 °C as it can be observed (arrows) on **Figure 11D**, exhibiting total loss of the structure.
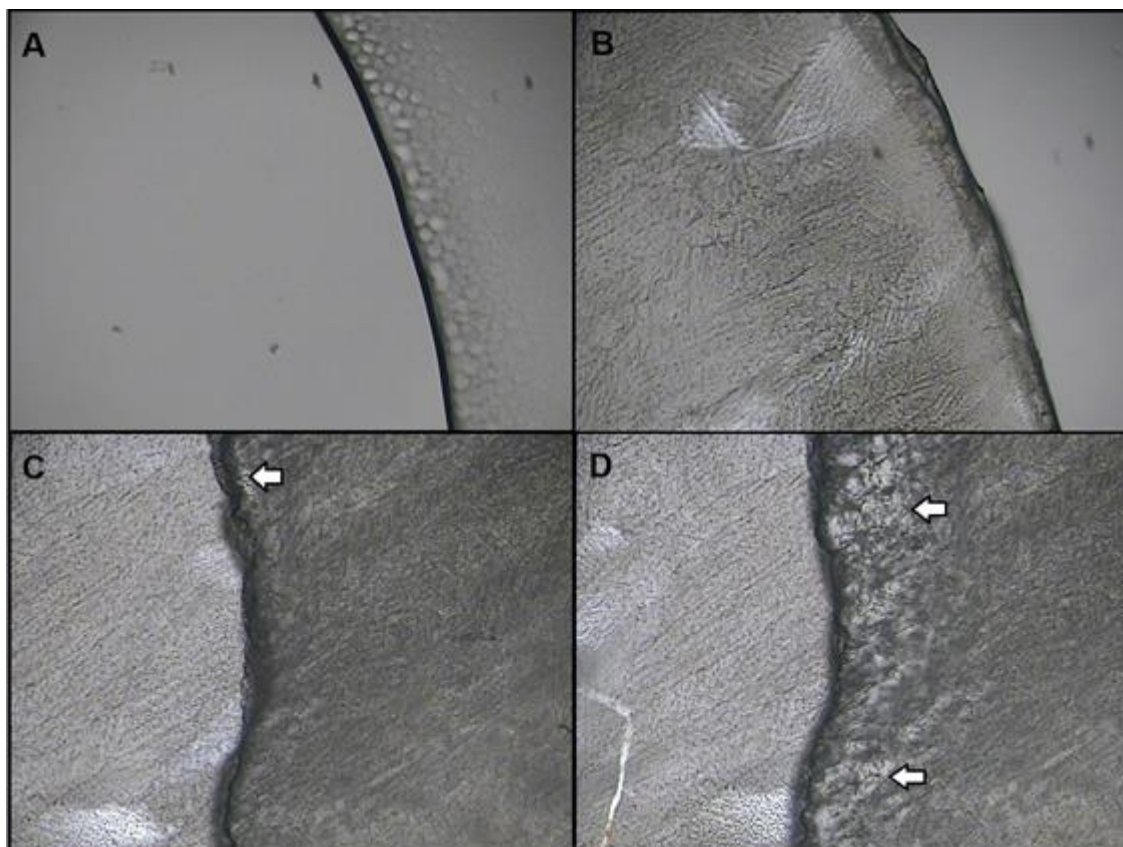
Figure 11- Image obtained during the freeze-drying microscopy test for 4:1 HP-β-CD-CAP formulation. A) The process start at 10 °C; B) the sample is frozen at -24 °C; C) initial zone of collapse (arrow) is seen at -12 ° C; D) total collapse of the sample (arrows) occur at -10ºC.

Tc is an important parameter for the drying process of lyophilization since the beginning of primary drying must occur below such temperature, to ensure adequate residual moisture and reconstitution time (Meister et al., 2009). Besides the Tc, the morphological characterization of the excipients is also critical to establish the proper freeze-drying cycle (Tang and Pikal, 2004). As it will be further shown in SEM (item 6.3.3) and PXRD experiments (item 6.3.2).

6.2.1.2. Freeze-drying process

Lyophilization consists of three steps; freezing, primary drying (sublimation), and secondary drying (desorption). The freeze-drying cycle for the 4:1 HP-β-CD-CAP formulation was established with support of the Smart Freeze Dryer Technology. The

software was set up with information such as: Tc, morphological (crystalline or amorphous) features of excipients and vial information (quantity, weight, area and filled volume). Additionally, the equipment controlled the cycle according to the sublimation rate of the samples during the freeze-drying process. The sublimation vapor flow was detected by the pressure difference between the pyran valve and the gauge valve.

The lyophilization vials were filled up with 4:1 HP-β-CD-CAP solution (prepared according to item 4.4.2.) and placed on the freeze-dryer shelf. The temperature of the shelf and the sample were followed throughout the process, as seen in **Figure 12.** The freezing cycle started at the shelf temperature of 20ºC, with a cooling ramp of 1 ºC/min, remaining at 5 ºC for 30 minutes. Following, the shelf underwent another 30 min-step (at -5 ºC) in order to improve the sample homogeneity of crystallization, intra and intervials (Tang and Pikal, 2004). When the shelf temperature reached -10 °C the sample released heat, raising its temperature up to -5 °C due to ice and vitreous phase (glass) formation. In the time following, the cooling cycle reached -40 ºC remaining at this temperature for 120 minutes, to ensure that the sample was completely frozen. Then, the sample was ready to start the drying process.
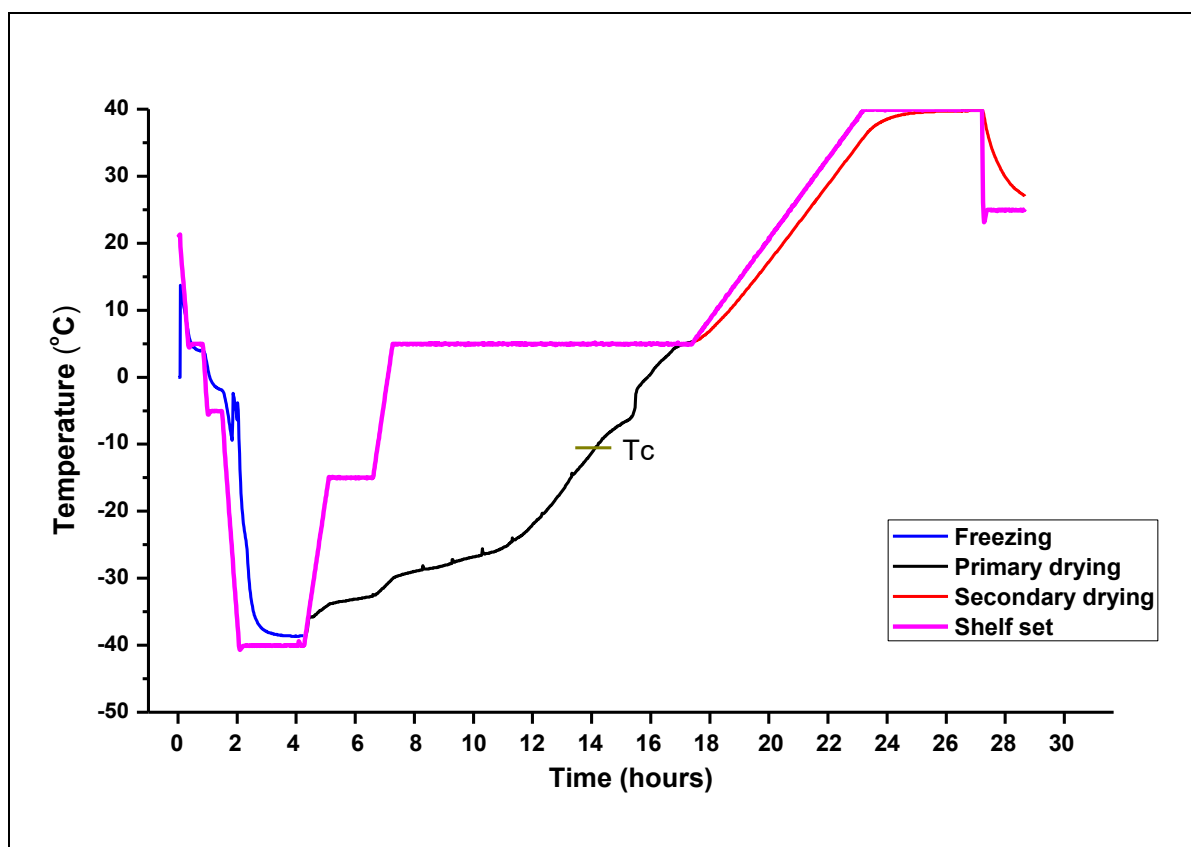
Figure 12- Sample and shelf temperatures during the freeze-drying process of 4:1 HP-β-CD-CAP; Tc= collapse temperature.

Primary drying, or sublimation, is the longest and more critical process of the freeze-drying (Pikal, 1994). This primary drying cycle began when the valve pressure was reduced to 150 mTorr, and the shelf temperature was raised to -15 ° C (0.5 °C/minute), remaining at this temperature for 90 min. This temperature should provide enough heat for sublimation of water, while maintaining the structure of the lyophilizate to avoid sample collapse (5 °C below Tc). Thereafter, the Pirani valve pressure decreased, and the shelf temperature was raised to 5 °C. The product only reached the temperature of Tc (-12 ºC) after 9 hours of the primary drying. Following, both shelf and sample reached the same temperature. This moment marked the end of the primary drying since there is no more ice to be sublimated, therefore the temperature of the product could follow the shelf temperature (Tang and Pikal, 2004).

Secondary drying usually takes place at elevated temperature to remove unfrozen water by desorption (Patel et al., 2010). At this stage, the amorphous products usually have 5 to 20% of residual water. As shown in **Figure 12**, the sample

temperature was raised up to 40 °C with a ramp of 0.1 °C/minute, and remained at this temperature for 4 hours. Amorphous products are harder to dry than crystalline ones, requiring high temperatures and long periods to occur. Also, the ramp of this drying should be slow to avoid sample collapse (Tang and Pikal, 2004). After this process, the samples reached room temperature, the vials were sealed and stored at 25 °C.

Initially, the cakes were white, porous and had a non-adherent structure (**Figure 13**). In addition, they showed a uniform texture, without any shrinkage or collapse, and could be reconstituted in water in less than 10 seconds. Some vials showed minor splashing, primarily due to dripping of solution during the filling, or agitation after filling. Then streaks of dry product appeared on the walls of the vial after freeze drying. Anyhow, minor splashing does not impact on quality of the product and are acceptable (Patel et al., 2017). Besides, the freeze-dried cake had the same size and shape as the liquid that was originally filled into the vial.

Figure 13- Vials containing freeze-dried product of HP-β-CD-CAP (4:1 molar ratio).

6.2.1.3. Stability test

The quality specifications for lyophilized drug products are still not well established by regulatory agencies (Patel et al., 2017). Here, some quality attributes of the HP-β-CD-CAP freeze-dried product were defined, such as cake appearance, reconstitution time, pH, and quantitative assay.

The long-term testing should cover a minimum of 12 months' duration and it is detailed in **Table 2**. The initial samples were visually evaluated in terms of cake appearance, as described above (item 6.2.1.2.), and summarized in the specification (**Table 2**). No changes in the cake appearance should occur during the stability test because it may be an indication of changes in product quality. The dry product should

be reconstituted in less than 10 seconds, to guarantee the fast administration of the injectable formulation. During the stability test the samples met the criteria of cake appearance (white, uniform, no collapse) and reconstitution time (<10 seconds). Generally, the pH is considered a critical parameter of injectable products, and it did not change during 12 month-test. The content of CAP in the reconstituted sample was compared with that determined in fresh samples, showing results within the acceptable range (95-105 %). Overall, these results demonstrated that the lyophilized HP-β-CD-CAP product was stable over up to 12 months, regarding the attributes tested here. It is worthy to mention that it is the first time that the developed of a freeze-dried product containing capsaicin-in-cyclodextrin complexes was proper described in the literature.

Table 2- Stability specifications of 4:1 HP-β-CD-CAP samples during long term condition. The results were described after visual inspection or expressed as mean ± SD (n=3).

Specification	3 months	6 months	9 months	12 months
Cake appearance (white, uniform, no collapse)	met the criteria	met the criteria	met the criteria	met the criteria
Reconstitution time (< 10 seconds)	met the criteria	met the criteria	met the criteria	met the criteria
pH 5-8	6.2 ± 0.1	6.4 ± 0.1	6.5 ± 0.1	6.1 ± 0.0
CAP content 95-105%	99.2 ± 1.5	102.5 ± 0.6	103.2 ± 0.5	96.3 ± 7.4

6.3.   Characterization of freeze-dried HP-β-CD-CAP samples

Up to this point, the characterization of HP-β-CD-CAP complex was performed in liquid state. After the freeze-drying process, it was possible to evaluate the formation of the inclusion complex in the solid state combining the results from several techniques.

6.3.1. Differential scanning calorimetry

DSC is an analytical tool used in product development of cyclodextrin-based DDS, in the solid state (Mura et al., 2003). By comparing the heating curve of pure compounds, cyclodextrin complex, and physical mixture it is possible to indicate interactions between the guest and host molecules due to the preparation methods of complexation and/or inclusion complex formation (Mura, 2015).

Figure 14 shows the heat curve of CAP, HP-β-CD, 1:1 HP-β-CD-CAP, 4:1 HP-β-CD-CAP, and 4:1 physical mixture. The physical mixture contains the same amount of guest and host molecules of the complex, but they were not solubilized in water neither freeze-dried. CAP had a sharp endothermic event at 62.30 °C attributed to its melting point. On the other hand, HP-β-CD exhibited a broad endothermic event, onsetting at 73.75 °C. This broad transition is related to the loss of the water molecules usually absorbed and bonded to inner macrocyclic ring of cyclodextrin (Giordano et al., 2001).
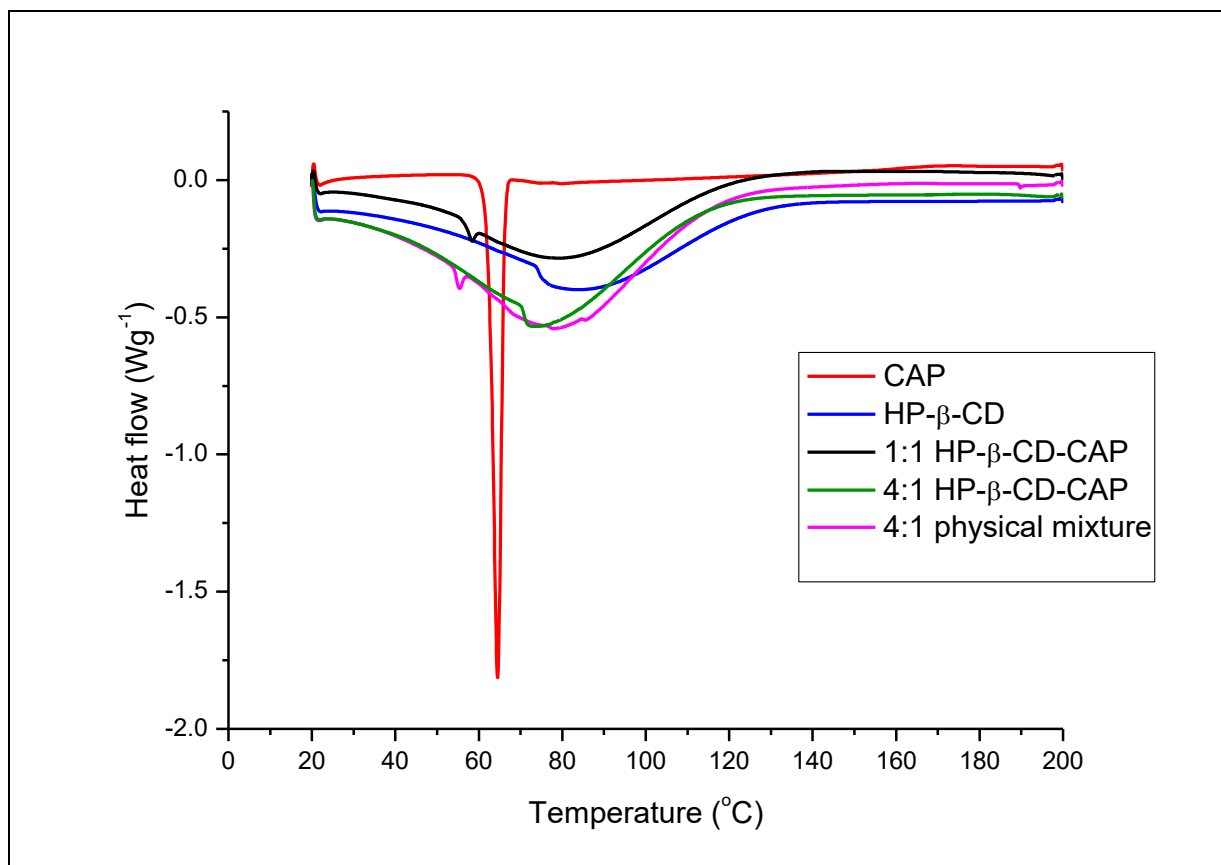
Figure 14- DSC thermograms of CAP, HP-β-CD, 1:1 HP-β-CD-CAP, 4:1 HP-β-CD-CAP and, 4:1 HP-β-CD-CAP physical mixture. First heating cycle from 20 °C to 200 °C, rate 5 °C/min, under inert atmosphere.

The curve of 1:1 HP-β-CD-CAP showed a significant change in the transition temperature of CAP and HP-β-CD to 56.56 °C and 80.39 °C, respectively. This result evidenced that there was some interaction between the two molecules, but it is clear that not all the CAP molecules were complexed. The poor complexation efficiency of the 1:1 HP-β-CD-CAP could be related to the preparation method of the freeze-dried product. The initial solution contained residual ethanol, which has a very low freezing point (-114 °C), probably disturbed the sample sublimation during freeze-drying (Oetjen, 2008). But, most important, the determined CE value (0.33) suggested that a suitable complexation should only be accomplished with 4 times more cyclodextrin than CAP (molar ratios).

As expected, in the freeze-dried 4:1 HP-β-CD-CAP sample there was a complete disappearance of the CAP melting peak, as a result of solid-state interaction between the components. It was observed only a broad endotherm event at 70.03 °C,

suggesting that all CAP molecules were complexed with the cyclodextrin. Following, the physical mixture (4:1 HP-β-CD-CAP) was analyzed at the same concentration and heating condition to investigate if the disappearance of CAP melting point could be due to heating-induced interaction during DSC scan. Contrarily, the 4:1 physical mixture shows a peak relatively to capsaicin (to 54.02 °C) and a slight shift of the HP-β-CD melting temperature, to 76.64 °C.

Considering the DSC results it can be suggested total CAP amorphization due to the formation of inclusion complexes at stoichiometry 4:1 (HP-β-CD-CAP). Further characterization (by PXRD and NMR) were performed to confirm this hypothesis.

6.3.2. Powder X-ray diffraction

PXRD is widely used to characterize the crystallinity and degree of amorphization of cyclodextrin complexes. Differences in the diffraction pattern of the free components, presumed inclusion complex, and physical mixture indicate interactions between components (Mura, 2015).

The diffraction patterns (**Figure 15**) confirmed the crystalline nature of CAP characterized by sharp and well-defined peaks (marked with asterisks). This result is in agreement with previous publications which have shown similar diffraction patterns for CAP (Shen et al., 2012; Zi et al., 2008). In the same figure, HP-β-CD pattern is indicative of an amorphous structure, as previously reported in the literature (Braga et al., 2016; Williams III et al., 1998).
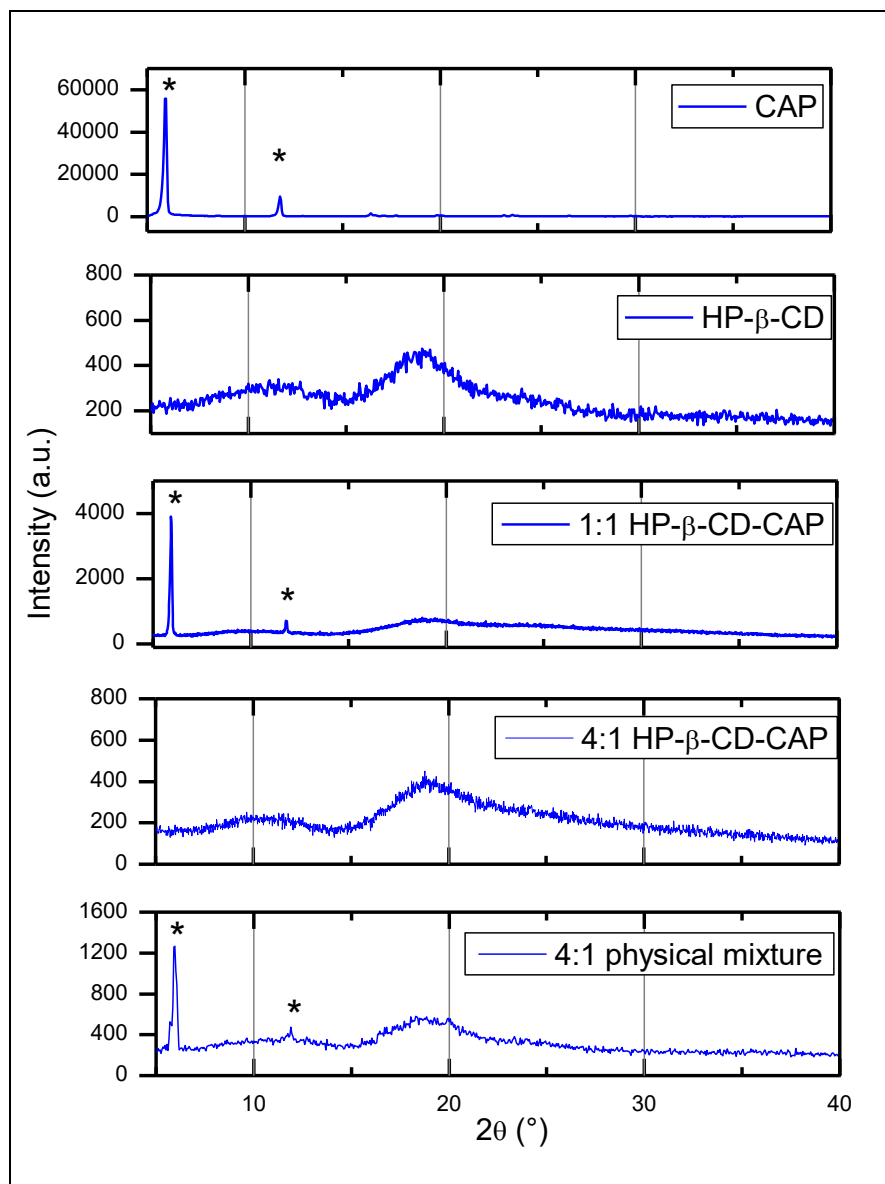
Figure 15- X-ray diffractograms of capsaicin, HP-β-CD, 1:1 HP-β-CD-CAP, 4:1 HP-β-CD-CAP, and 4:1 physical mixture of HP-β-CD and CAP.

PXRD analysis of the 1:1 freeze-dried (HP-β-CD-CAP) complex, prepared using ethanol solvent (item 4.4.1.) showed a reduction on the crystalline pattern of CAP, with decrease in the intensity of its major peaks (marked with asterisks). Although this change in the intensity of the peaks may be an indication of interaction between the compounds, it was less evident than that observed in the 4:1 freeze-dried sample.

In the diffractogram of the 4:1 freeze-dried sample (**Figure 15**) there was a complete disappearance of the CAP crystalline pattern, in a clear contrast to the 4:1 physical mixture. The physical mixture reflected the sum of the crystalline pattern of CAP and the amorphous pattern of HP-β-CD (without complexation). Therefore, the

sample with excess of cyclodextrin probably led to inclusion of all CAP molecules into HP-β-CD cavity, in agreement with DSC results (item 6.3.1.). Nevertheless, this results also corroborated the complexation efficiency test which indicated that each mol of CAP requires 4 moles of HP-β-CD to form a soluble complex.

6.3.3. Scanning electron microscopy

The surface morphology of pure substances (CAP and HP-β-CD), 4:1 physical mixture and freeze-dried HP-β-CD-CAP complex were analyzed by SEM. **Figure 16A** shows the HP-β-CD raw material displaying a spherical structure, with sizes in the range from 10 µm to 150 µm. Capsaicin raw material (**Figure 16B**) displayed a crystalline morphology, corroborating the PXRD results. The physical mixture (4:1 HP-β-CD-CAP) in **Figure 16C** displayed fragments that resemble the pure components. It shows that the simple physical mixture of the CD with CAP does not cause amorphization of the crystalline drug, corroborating the DSC and PXRD results. Contrarily, the 4:1 HP-β-CD-CAP sample (**Figure 16D**) after the freeze-dried process (item 6.2.1.2.) revealed significant morphological chance comparing with raw components. **Figure 16D** displays homogeneous typical freeze-dried cake without any remaining crystalline structure from CAP. This fact supports the hypothesis of the formation of the amorphous state induced by CAP and CD interaction, as described in DSC and PXRD results.
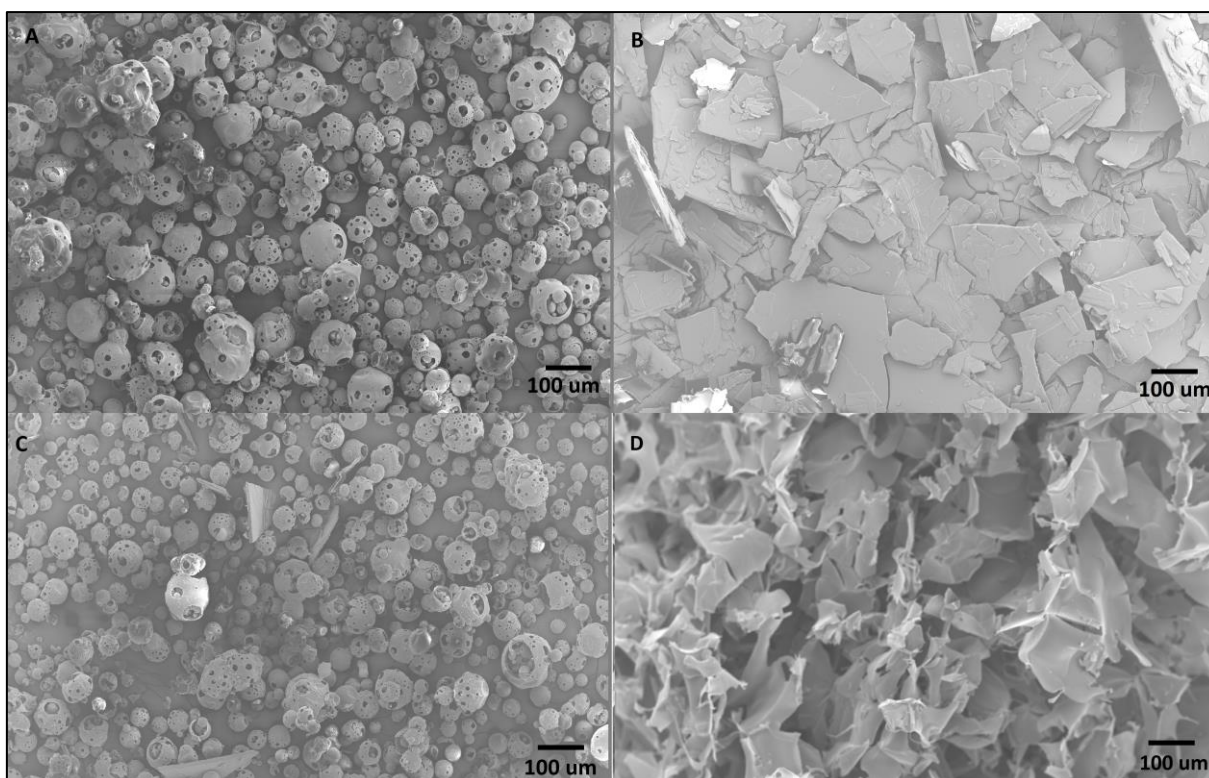
Figure 16- SEM micrographies of: (A) HP-β-CD, (B) CAP, (C) 4:1 physical mixture, and (D) 4:1 HP-β-CD-CAP.

6.3.4. Proton Nuclear Magnetic Resonance

ITC experiments provided thermodynamic information regarding the interaction of capsaicin and HP-β-CD. DSC, XRD and SEM provided evidences of the inclusion complex formation, in the solid state. Subsequently, NMR is the technique that can directly prove the formation of the inclusion complex, either by the chemical displacement (^{1}H-NMR) of the pure compounds or by responses provided by specific pulse-sequences (e.g. NOE and DOSY).

Classical (non-selective pulse sequences) ^{1}H-NMR experiments detect changes in the chemical shift (C.S.) of hydrogens. In the case of CD-based host-guest complexes, C.S. changes to higher fields in hydrogens located inside the cyclodextrin cavity (C and E in Fig. 17) are often seen in the presence of a guest molecule (de Paula et al., 2010b; Mura, 2014).

Figure 17 shows the spectra of CAP, HP-β-CD and HP-β-CD-CAP complex in solution, with peak assignments. The assignment for CAP and HP-β-CD peaks were

consistent with the literature (Kobata et al., 1998; Soares et al., 2009). Observing the spectra in **Figure 17**, it can be noted that CAP peaks are narrow than those of the macrocyclic HP-β-CD molecule. This difference reflects the isotropic motion of CAP molecules in solution. Upon complexation, CAP peaks became broader, indicating immobilization of the molecule due to the inclusion complex formation.

Table 3- ^{1}H-NMR: Chemical shifts (in ppm) of peaks from CAP, in solution or complexed with HP-β-CD. See Figure 17 for assignment.

Capsaicin		HP-β-CD		HP-β-CD-CAP		Δ (ppm)
H atom	ppm	H atom	ppm	H atom	ppm	
9	0.83			9	0.90	**-0.07**
10	0.83			10	0.90	**-0.07**
4	1.24			4	1.24	0
3	1.52			3	1.57	-0.05
5	1.87			5	1.97	-0.1
2	2.19			2	2.24	-0.05
8	2.19			8	2.24	-0.05
		D	3.41		3.42	-0.01
		B	3.65		3.65	0
		E	3.77		-	-
3'a	3.78			3'a	-	-
		C	3.95		3.94	-0.01
7'	4.21			7'	4.24	-0.03
		A	5.18		5.17	-0.01
6	5.32			6	5.33	-0.01
7	5.32			7	5.33	-0.01
Aromatic (2',5',6')	6.89—6.75			Aromatic (2',5',6')	6.88—6.73	-0.01—0.02
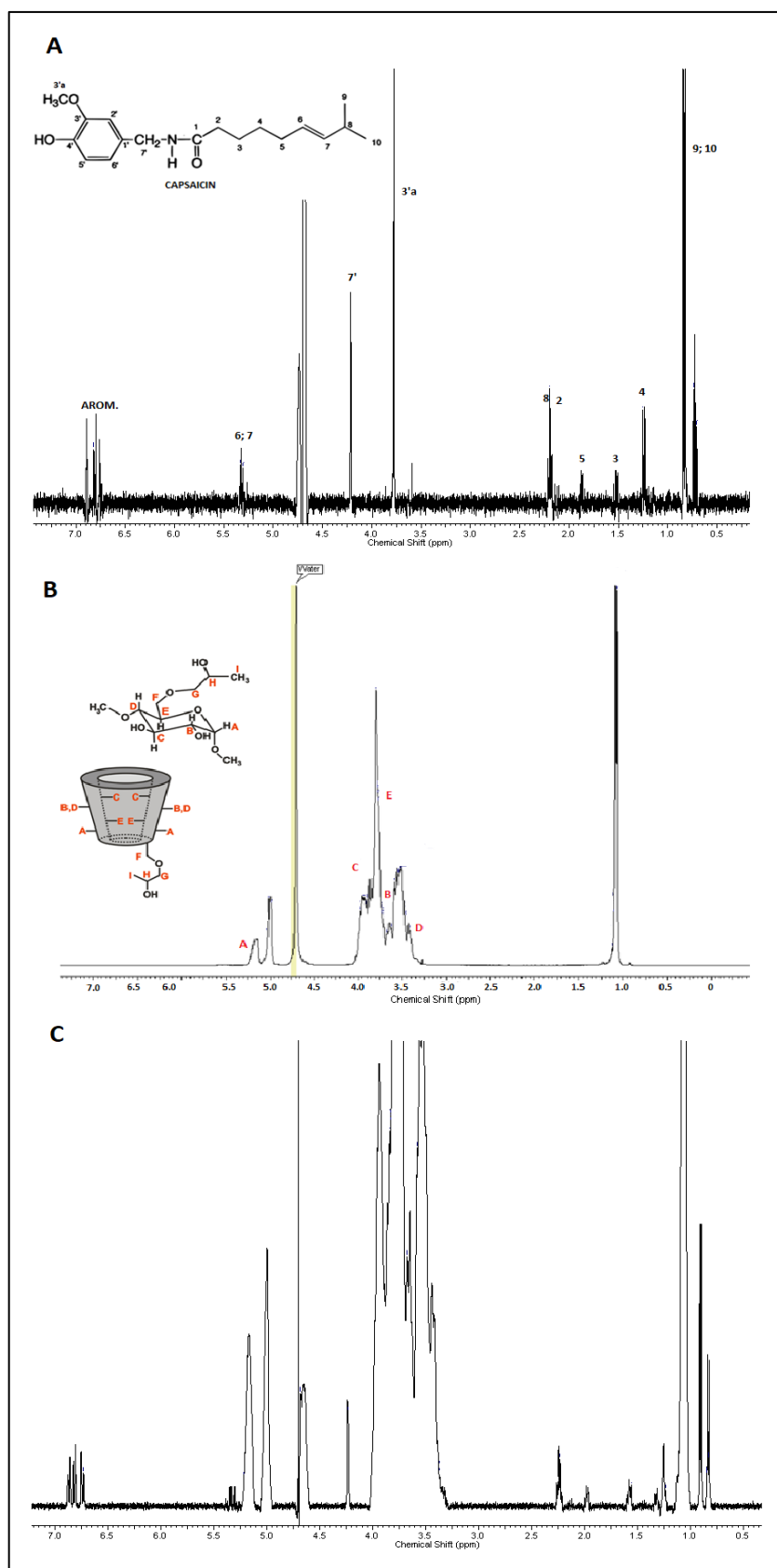
Figure 17- ^{1}H NMR spectra of: A) capsaicin, B) HP-β-CD and C) HP-β-CD-CAP at 400 MHz. D_2O residual hydrogens were referenced at 4.7 ppm.

Table 3 shows the chemical shifts of CAP hydrogens, either in solution or complexed with HP-β-CD, highlighting significant changes observed in some hydrogen's signals. Chemical shifts higher than 0.05 ppm are considered significant (de Paula et al., 2010b). The peaks corresponding to hydrogens 9 and 10 – in the terminal methyl of CAP - displayed higher C.S. variation (Δ = -0.07 ppm), followed by the peaks corresponding to the hydrogen 3 (Δ = -0.05 ppm), also in the aliphatic chain of CAP. Hydrogens 2 and 8 showed variation (0.05 ppm), but their signals are partially overlapped (each other) at 2.19 ppm. In general, the aromatic hydrogens (2',5', 6') showed small displacements. Unfortunately, the signal of the methyl-ether hydrogens (3'a) got superposed with signals from HP-β-CD hydrogen E, restricting determination of changes in their chemical shift upon complexation. Therefore, the chemical displacements suggest insertion of hydrogens from the long hydrophobic chain of CAP (e.g. methyl hydrogens 9, 10) into the HP-β-CD cavity. To further elucidate the interaction between CAP and HP-β-CD, ROESY-2D experiment was performed.

6.3.4.1. Rotating Frame Nuclear Overhauser effect

The structure elucidation of a drug-in-cyclodextrin complex can be obtained by the ROESY spectra. The ROESY sequence allows detection of cross-peak correlations in the spectrum, representing hydrogens from the guest and host molecules that are close in space (less than 6 angstrons apart) but not covalently linked (de Paula et al., 2010b; Mura, 2014).

In the first expansion of the ROESY two-dimensional spectrum (**Figure 18B**) it is possible to observe the Nuclear Overhauser effect cross-peaks – green circles – that reveal spatial and non-scalar proximities between nuclei. The upper circle corresponds to the (intramolecular) interaction between aromatic hydrogens 2', 5', 6' at 6.88 ppm and the methyl-ether hydrogens of capsaicin (3a') at 3.75 ppm. Also, the lower green circle corresponds to an intramolecular interaction between the aromatic 2', 5', 6' hydrogens of capsaicin (6.88 ppm) and hydrogen 7' of capsaicin (4.24 ppm).
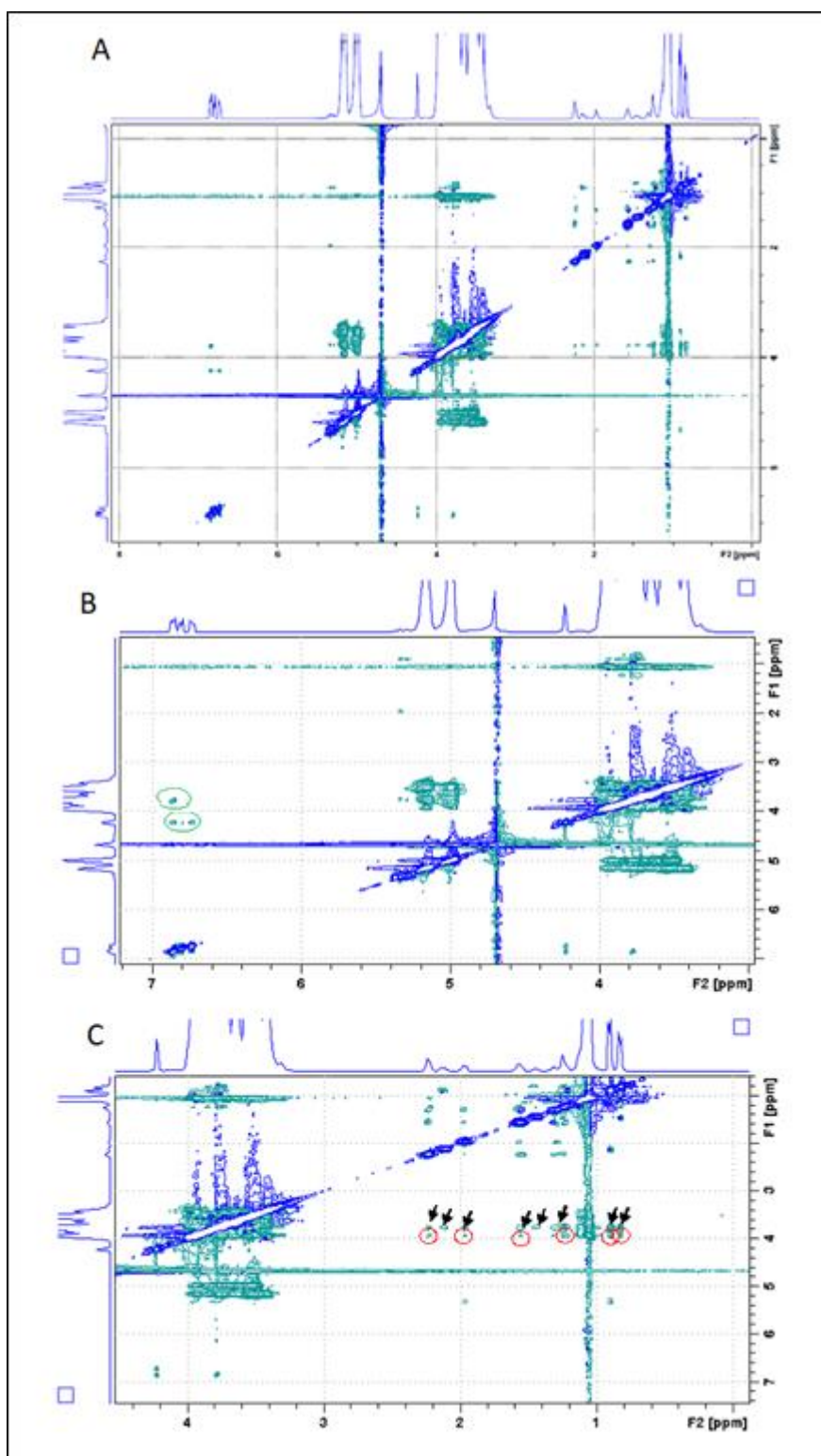
Figure 18- A: Two-dimensional ROESY spectrum (400 MHz) of HP-β-CD-CAP sample. B: first spectrum expansion, in the region between 3 and 7 ppm, C: second spectrum expansion, in the region between 1 and 4 ppm.

Most interestingly, in the second expansion (**Figure 18C**) intermolecular interactions were detected (red circles) between hydrogens 2 = 2.24 ppm; 5 = 1.97 ppm; 3 = 1.57 ppm; 4 = 1.24 ppm, 9,10 = 0.90 ppm of CAP and hydrogen C = 3.94 ppm of HP-β-CD. Hydrogen C is located in the inner cavity of HP-β-CD macrocyclic ring and, along with hydrogen E is very sensitive to changes in the chemical environment provoked by insertion of the guest molecules (de Paula et al., 2010b). In fact, additional cross-peaks - indicated by the black arrows in **Figure 18C** could be seen between the same hydrogens of CAP (2, 5, 3, 4, 9, 10) and hydrogen E of HP-β-CD, at 3.79 ppm. It is therefore very likely that upon complexation, the aliphatic portion of capsaicin gets inserted into the CD cavity, justifying their spatial proximity with hydrogens C and E of ROESY spectra confirmed the Δ C.S. results so that NMR results confirmed the inclusion complex formation between CAP and HP-β-CD and also revealed details on the topology of the 1:1 stoichiometry complexation (**Figure 19**).
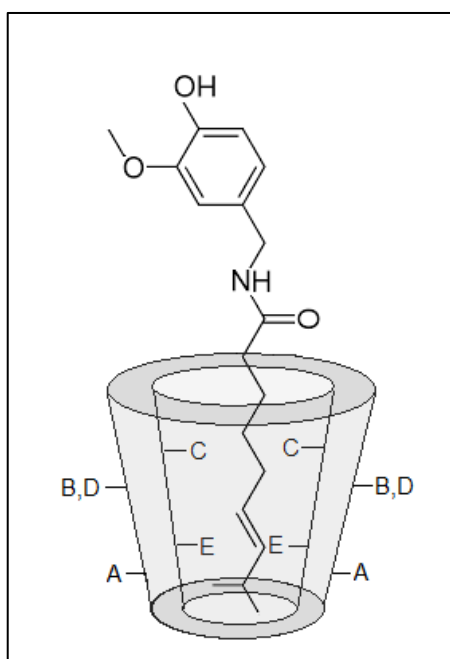
Figure 19- Proposed topology of the HP-β-CD-CAP complex.

6.3.4.2. DOSY and determination of HP-β-CD-CAP affinity constant

The DOSY gradient-field pulse sequence measures differences in the diffusion coefficient (D_c) of molecules and provide information such as the molar fraction ($F_{complexed}$) and association constant (Ka) between small ligands and macromolecules such as cyclodextrins, liposomes, protein (Cabeça et al., 2009).

The D_c is especially attractive when there is large difference between the molecular masses of two interacting molecules, e.g. in cyclodextrins complex (Simova and Berger, 2005). As expected, the DOSY spectra of the free compounds (**Figure 20A, B**) revealed quite different D_c for HP-β-CD ($2.00\ 10^{-10} m^2 s^{-1}$) and CAP ($4.94 \times 10^{-10}\ m^2 s^{-1}$). The slower diffusion of HP-β-CD reflects its larger structure when compared to free CAP. Similar D_c values for CAP ($4.81 \times 10^{-10}\ m^2 s^{-1}$) and HP-β-CD ($2.21 \times 10^{-10}\ m^2 s^{-1}$) were reported in the literature (Prado et al., 2017; Liu et al, 2013). Small molecules such as CAP have a high D_c, however, when complexed, their diffusion is retarded. This can be observed for the HP-β-CD-CAP complex (**Figure 20C**) which D_c value ($2.35 \times 10^{-10} m^2 s^{-1)}$ is suggestive of the complex formation.

From the D_c values it was possible to determine the CAP complexed fraction and the Ka, using equations 9 and 10. The $F_{complexed}$ of capsaicin bound to the complex was very high ($F_{complexed}$ = 88%) and the Ka was 1079 M^{-1}. Our group has measured $F_{complexed}$ and association constants for the complexation of different LA and cyclodextrins, using DOSY-NMR. For the complexation with HP-β-CD of the local anesthetic S-bupivacaine $F_{complexed}$ = 57% and Ka = 91 M^{-1} (de Paula et al., 2010b), for oxetazaine, $F_{complexed}$ = 38% and Ka = 198 M^{-1} (Prado et al., 2017). Comparing to those LA, HP-β-CD-CAP complex has a Ka and $F_{complexed}$ notably higher.

Together, all analytical techniques for characterization of HP-β-CD-CAP complex in aqueous solution revealed a strong intermolecular interaction between the components, despite the fact that constant value is not the same. It is worth mentioning that phase solubility studies are performed under saturated solutions (excess drug) to maintain a high thermodynamic activity of the complex (Brewster and Loftsson, 2007). As for ITC measurements, very diluted concentrations are used, often solubilized in co-solvent. On the other hand, DOSY experiment by NMR is intuitively related to the formation of the complexes, not being affected by intra and intermolecular events (Simova and Berger, 2005). Overall, there is still the need to improve the available

methods and developing new techniques, in order to obtain a more reliable determination of the stability constants of CD complexes (Mura, 2014).
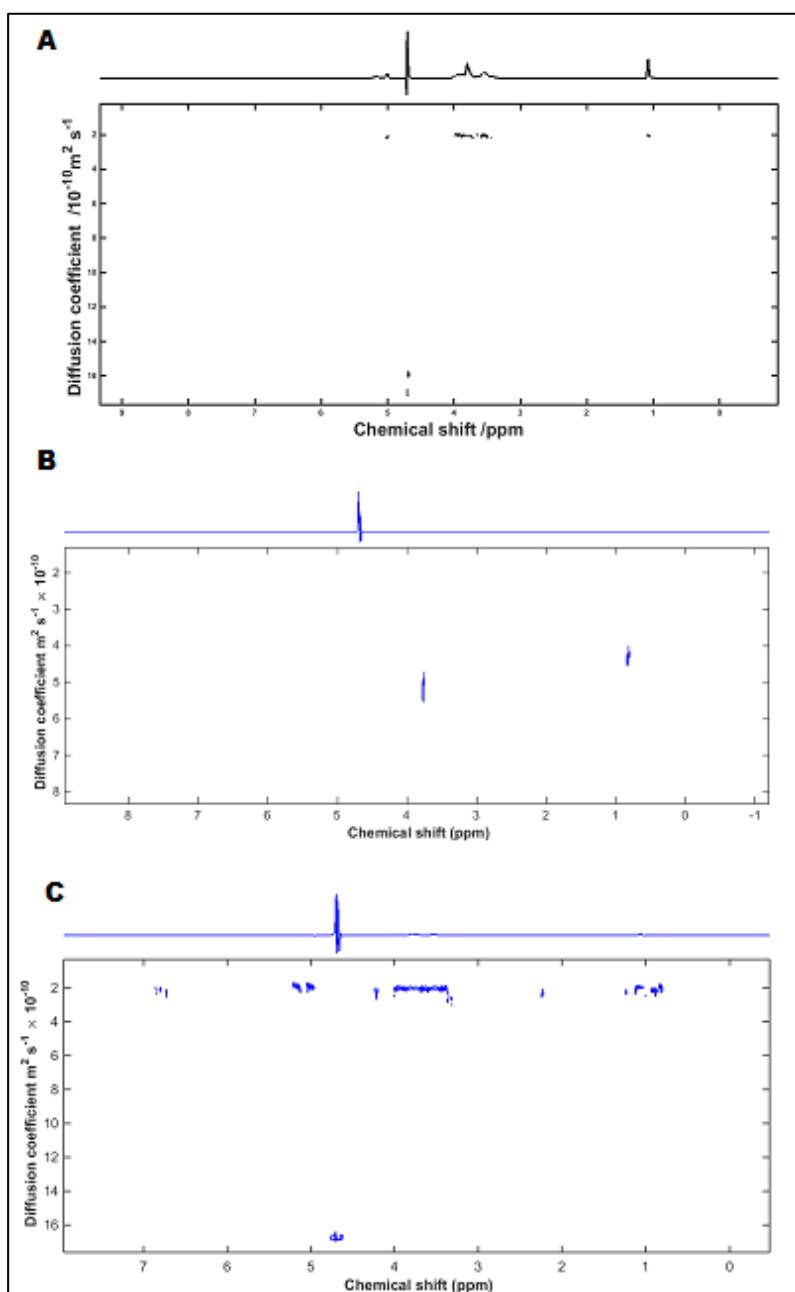
Figure 20- ^{1}H-NMR: DOSY spectra of: A) HP-β-CD [10mmol L^{-1}]; B) CAP and C) HP-β-CD-CAP (4:1). 400 MHz, H$_2$O residual peak at 4.7 ppm.

6.3.5. *In vitro release*

According to Gerner and coworkers, lidocaine and QX-314 can elicit a predominantly sensory selective block when their administration was followed (10 min later) by injection of capsaicin (Gerner et al., 2008); while others found that the co-administration of LA and CAP at the same time led to improved sensory block (C. H. Wang et al., 2014). Here, it was evaluated if the strong interaction in HP-β-CD-CAP complex could influence the release of the drug, hoping to better understand the following *in vivo* result.

Once a complex is formed and freeze-dried it only dissociated by heating or in water, which can displace the drug from the CD cavity (Del Valle, 2004). In this test, vertical diffusion (Franz) cells were used as a tool to assess the drug release rate of DDS in comparison to the CAP (dissolved in ethanolic solution 20% v/v).

First, the lyophilized cake (4:1 HP-β-CD-CAP) was dissolved in deionized water. Equilibrium should be established between free and complexed cyclodextrin; and the drug. Once 4:1 HP-β-CD-CAP solution was transferred to the Franz cell system, then the diffusion to the medium is involved in disturbing this equilibrium, releasing of the complexed drug. Here the dilution factor of the Franz cell system was small (12 times from donor to receptor compartments) but adequate to alter dissociation event of highly bond drugs from CD (Stella, 1999).

According to **Figure 21**, the formulation containing HP-β-CD-CAP complex induced the release of capsaicin in a sustained manner, if compared to CAP in solution. The total release (ca. 100%) of capsaicin from the solution and formulation complex occurred after 3 and 5 hours, respectively.
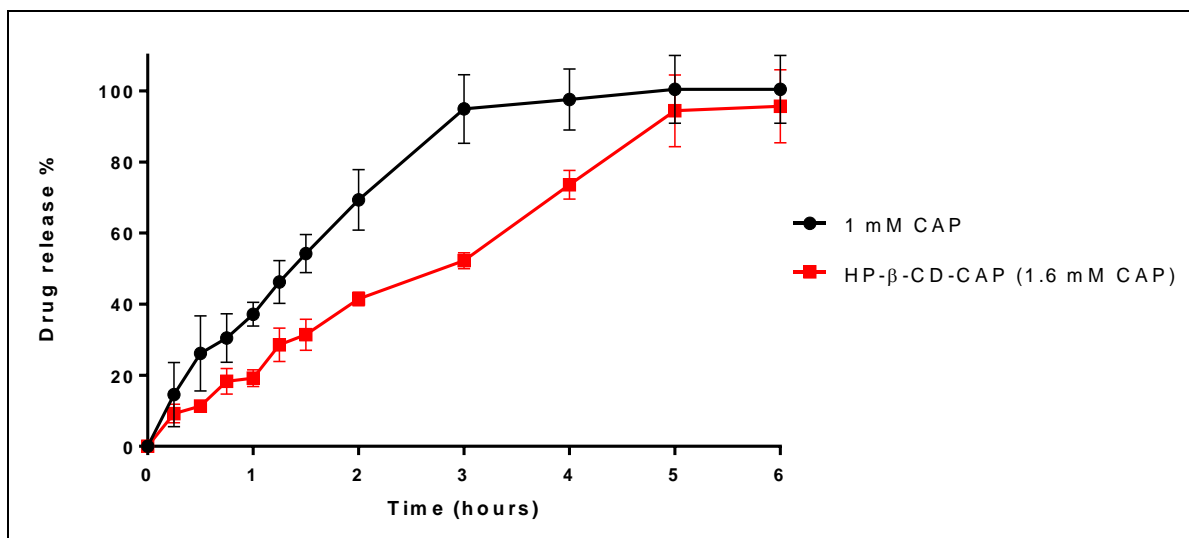
Figure 21- Cumulative release of capsaicin, free and complex with HP-β-CD, at 37 °C Results are expressed in mean ± n = 3.

In solution, the interaction of the drug with the cyclodextrin cavity depends on weak non-covalent interactions, and therefore the complex continuously form and dissociate (Shimpi et al., 2005). The high association constant between HP-β-CD and CAP, which it was described here by different techniques, evidenced by sustained the release profile demonstrated by the HP-β-CD-CAP formulation. Also, the 4:1 HP-β-CD-CAP formulation has an excess of CD, which results in a higher probability of CAP binding to other cyclodextrins, in this dynamic association/dissociation regimen.

In Franz cells, the diffusion seems to be the greatest force for the release of the CAP from the complex. However, it is important to bear in mind that, when a formulation is injected into tissue, as in a local anesthetic infiltration, other factors affect the release of the drug such as drug-protein binding; partition of the drug into the tissue; endogenous competitors for the cyclodextrin site; elimination of cyclodextrin; effects related to pH or temperature (Stella, 1999). Here, the system has also the LA molecules as a competitor for the cyclodextrin cavity.

The final objective of Part 1 of this thesis is to evaluated HP-β-CD-CAP freeze-dried, reconstituted in LA (hydrochloride MVC) solution to improve anesthesia. Accordingly, the injection solution would contain: HP-β-CD-CAP (complex); excess HP-β-CD; and MVC molecules that could interact with the excess CD or displace CAP from the complex. Dollo et al. reported *Ks* (from phase solubility study) values for LA

(base form) system with HP-β-CD as bupivacaine (95 M^{-1}), lidocaine (19 M^{-1}), and mepivacaine (38 M^{-1}) (Dollo et al., 1996). Therefore, the affinity of HP-β-CD with LA is far smaller than with CAP. Also, the salt form of LA in aqueous solution contain mostly ionized drug which forms even less stable CD complexes than those described by Dollo (Loftsson and Brewster, 2010). Consequently, it is expected that MVC molecules or any other LA discussed here do not disturb HP-β-CD-CAP complex stability.

6.4. *In vivo* evaluation of the effect of HP-β-CD-CAP complex with LA

Since the lyophilized formulation of HP-β-CD-CAP (resuspended in water) showed *in vitro* sustained release profile (**Figure 21**), we expected that when suspended in a mepivacaine hydrochloride solution (single dose application) it would have an similar effect to that reported by Gerner. This combined formulation was evaluated *in vivo* for the sciatic nerve block and analgesia, in inflamed tissue.

6.4.1. Sciatic nerve block

The paw pressure experiment allows the evaluation of the intensity of sensory block. According to **Figure 22**, the sensory block elicited by 2% (w/v) MVC solution and 0.05% (w/v) HP-β-CD-CAP + 2% (w/v) MVC is similar, for up to 120 minutes. After that (between 150 and 180 minutes) the anesthesia of the combined formulation is significantly more intense than that of the LA alone.
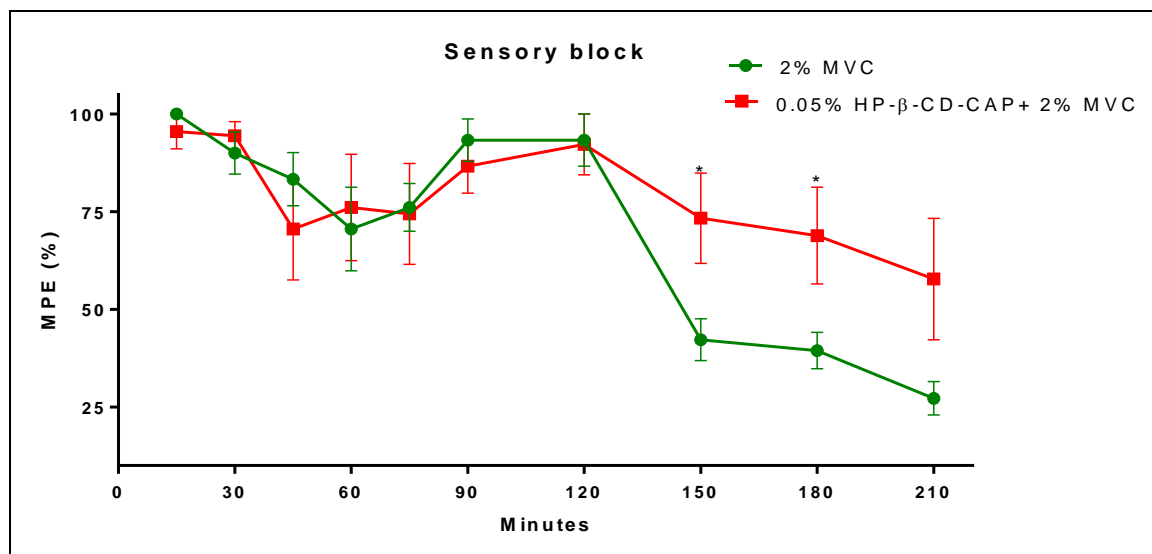
Figure 22- Sensory block, evaluated by the paw pressure test, in mice, after administration of 2% MVC or 0.05% HP-β-CD-CAP + 2% MVC. MPE= maximum possible effect. Statistics: Student t-Test, *p<0.05.

In general, the animals in the 0.05% HP-β-CD-CAP + 2% MVC group had a less intense motor block than those in the 2% MVC group (**Table 4**). The motor function of all mice was compromised at Level 2, shortly after injection of the 2% MVC solution, and persisted for 30 minutes, while in the 0.05% HP-β-CD-CAP + 2% MVC group only half of the animals exhibited motor alteration up to Level 2 during the first 30 minutes. All animal recovered motor function after 90 and 75 min for 2% MVC and the combined formulation group, respectively.

Table 4- Percentage of animals with motor block, according to level, after administration of 2% MVC and 0.05% HP-β-CD-CAP + 2% MVC solution. Statistical analysis was performed by Multiple t test, statistical significance: *p<0.05.

		Motor block						
Group	Level	5 min	15 min	30 min	45 min	60 min	75 min	90 min
2% MVC	2	*100%	*100%	*100%	16%	-	-	-
	1	-	-	-	67%	33%	16%	-
	0	-	-	-	16%	67%	84%	100%
0.05% HP-β-CD-CAP+ 2% MVC	2	50%	50%	50%	-	-	-	-
	1	50%	50%	50%	84%	16%	-	-
	0	-	-	-	16%	84%	100%	100%

Binshtok et al. (2007) tested the administration of QX-314 (lidocaine quaternary analogue), followed by the application of CAP in a region close to the sciatic nerve of rats. Co-administration of these drugs promoted reduction of the pain response by mechanical stimulation, without significantly affecting the motor block (Binshtok et al., 2007). In 2008, Gerner et al. evaluated the combination of LA (bupivacaine and lidocaine) with capsaicin (mixed or injected apart) in a similar animal model. They observed a prolonged nociceptive blockade when bupivacaine and CAP were injected 10 min apart, but no selective block was observed. The combination of lidocaine and CAP administrated together or 10 min apart increased the nociceptive blockage, but there was no decrease in duration of motor blockade (Gerner et al., 2008). In 2014, Wang and coworkers injected LA (bupivacaine, lidocaine or articaine) mixed with CAP and reported a reduced motor blockade produced by intrathecal anesthesia in rats, when compared with LA administration alone (C. H. Wang et al., 2014).

Although the sensory block results found here were not as expressive as we expected, the motor block results were very promising. Altogether, the literature and these results have shown that the association of CAP and LA might be route- and LA- dependent and should be further explored in future studies. Following, the analgesia effect of the combined administration of CAP and LA was evaluated for the first time in an inflamed tissue.

6.4.2. Evaluation of analgesia in inflamed tissue

The presence of inflammation considerably decreases the potency of the local anesthetic mainly in dental procedures (Ueno et al., 2008). The carrageenan-induced hyperalgesia model was used to evaluate the anesthetic action in the presence of acute inflammation. Pain threshold was measured against a mechanical stimulus on the inflamed plantar surface of a mice.

According to the results in **Figure 23**, injection of the 2% MVC solution did not induced anesthesia at any time tested, being the result similar to that elicited by the control (saline solution). The reason for LA failure in inflamed tissue is not fully understood, but can be interpreted as a combination of factors: inflammatory acidosis; pH change - favoring the protonated fraction in relation to the neutral species of the LA; hyperalgesia, increased nerve sensitization; and peripheral vasodilation, increased blood flow and LA clearance (Miller, 2010; Tsuchiya, 2016). Larger doses of LA can be administered to induce anesthesia, but the risk of systemic toxicity limits the total dose administered (Grant et al., 1997).

The formulation containing 0.05% HP-β-CD-CAP + 2% MVC significantly induced analgesia in the first 30 min compared to control (saline), despite of the presence of inflammation. Moreover, the combined formulation was significantly more efficient than 2% MVC for the first 45 min. Probably, TRPV1 channels activated by CAP allowed the cell uptake of MVC in the protonated form, which is normally not permeable to the neuronal membrane (Puopolo et al., 2013). Consequently, in the presence of CAP the prevalence of the protonated form of the LA in the inflamed tissue (low pH) was not anymore a limitation for the anesthetic action (Tsesis, 2014).

It is worth mentioning that other strategies such as buffering or addition of vasoconstrictors in the injection solution; pre-treatment with anti-inflammatories; DDS and supplemental anesthesia (administration of other LA agents) did not satisfactorily increase the effect of LA in inflamed tissues (Tsuchiya, 2016). Therefore, the antinociceptive effect achieved with HP-β-CD-CAP formulation associated with MVC emerges as an innovative strategy to improve LA efficiency in inflammatory condition.
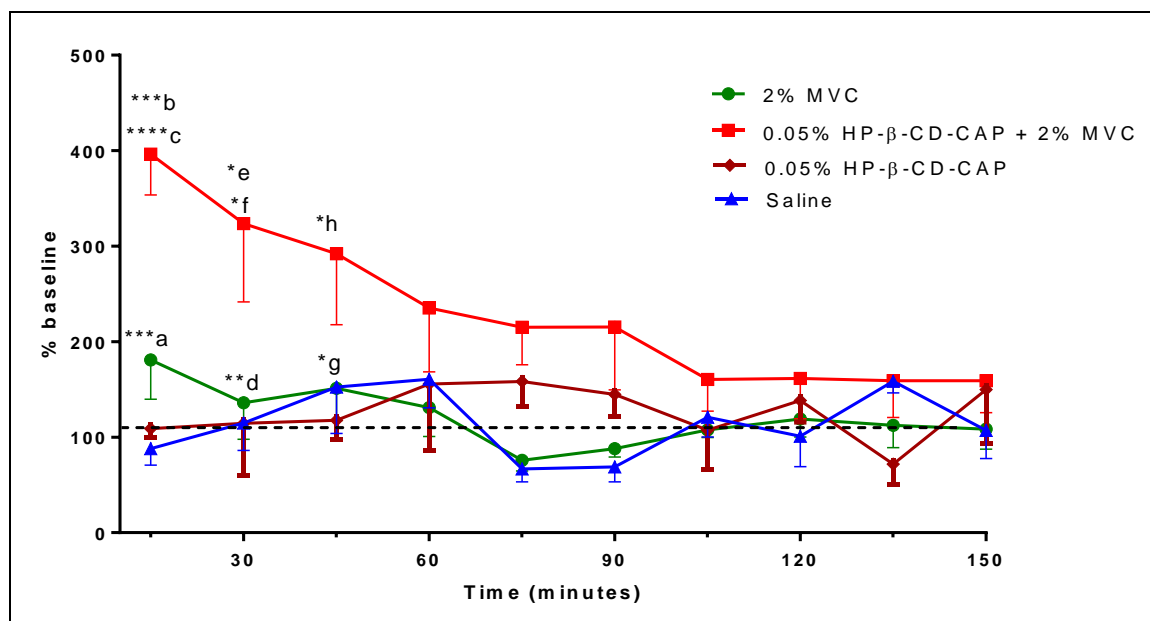
Figure 23- Effect of injection of 2% MVC, 0.05% HP-β-CD-CAP + 2% MVC, 0.05% HP-β-CD-CAP and saline (control) on the mechanical sensitivity of mice, measured after carrageenan-induced hyperalgesia. Basal was tested after 4 hours of carrageenan injection. Statistics: One-Way Anova/Tukey Test, *p<0.05, **p<0.01, ***p<0.0005 and ****p<0.0001. (a) 0.05% HP-β-CD-CAP + 2% MVC x 2% MVC; (b) 0.05% HP-β-CD-CAP + 2% MVC x 0.05% HP-β-CD-CAP; (c) 0.05% HP-β-CD-CAP + 2% MVC 2% x Saline; (d) 0.05% HP-β-CD-CAP + 2% MVC x MVC 2%; (e) 0.05% HP-β-CD-CAP+ 2% MVC x 0.05% HP-β-CD-CAP; (f) 0.05% HP-β-CD-CAP + 2% MVC x Saline; (g) 0.05% HP-β-CD-CAP+ 2% MVC x 2% MVC; (h) 0.05% HP-β-CD-CAP+ 2% MVC x 0.05% HP-β-CD-CAP.

PART 2

6.5. Screening of LA for IL/DEM preparation, using DSC

BVC, MVC, LDC (base) and LDC.HCl (salt) were tested for their ability to form IL/DEM with CAP by thermal analysis. DSC is a highly sensitive technique widely used to determine the melting temperature and other thermodynamic parameters of compounds. The physical state of the prepared IL/DEM can be determined from the first heating cycle. The cooling cycle can assess the propensity to crystallization, and the second heating cycle provide information of glass transition temperatures.

DSC measurements were performed on mixtures of several LAs (BVC, MVC, LDC base, LDC hydrochloride) and CAP. The thermograms obtained during heating of the LA:CAP mixtures are shown in **Figure 24**. For the pure components only one endothermic melting peak was found for each compound (CAP = 64.15 °C, BVC = 106.76 °C, MVC = 152.58 °C, LDC-HCl = 75.11 °C, and LDC = 68.25 °C), in good agreement with data found in literature (Hayman and Kam, 2008; Schmidt, 2005). In the case of MVC, besides the main melting peak (at 152.58 °C) another endothermic event occurred at the temperature of 105.87 °C, due to impurity (2',6'-Picolinoxylidide).

It can be observed in **Figure 24** that CAP diminished the melting event of all LA agents, even at the lowest molar fraction investigated: $[BVC]_8[CAP]_2$; $[MVC]_8[CAP]_2$; $[LDC-HCl]_9[CAP]_1$; $[LDC]_9[CAP]_1$. In the binary mixtures containing 0.8 molar ratio or less of the anesthetics BVC and MVC, it was easy to observe the appearance of a new peak at lower temperature. This endothermic event (ca. 50 °C) is attributed, at least partially, to the presence of a eutectics phase since it has a lower melting point than either of the pure components. Although CAP also diminished LDC-HCl melting event in the mixtures, LA peak is found in almost all mixtures, even at the lowest concentration ($[LDC]_1[CAP]_9$). Therefore, this result suggests that the electrostatic interaction within the LDC salt is stronger enough to affect the eutectic phase formation.
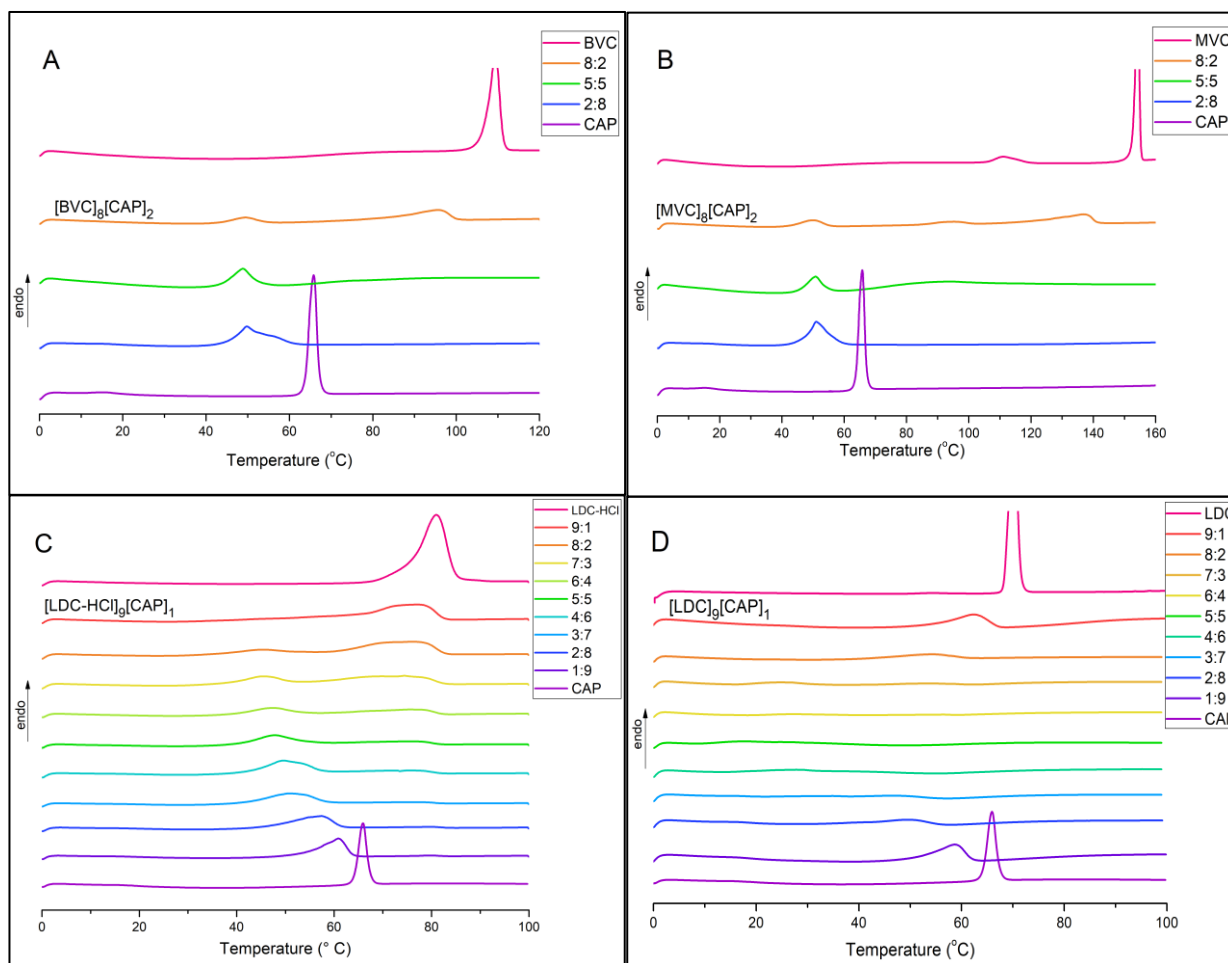
Figure 24- DSC first heating curves of binary mixtures of BVC:CAP(A), MVC:CAP (B), LDC-HCl:CAP (C), and LDC:CAP (D). Ratios in the legends are in mole ratios of the LA to CAP.

The representative thermograms of the LDC:CAP mixtures displayed a pronounced reduction of Tm starting from the pure LDC or CAP towards the equimolar composition. Unlike the mixtures of CAP with BVC and MVC, the eutectic temperature of the LDC:CAP mixtures was not clearly notable from the experimental data. In that case, the eutectic event most likely occurs below 25° C since the equimolar mixture of LDC and CAP readily turns into a liquid at room temperature or upon gentle grinding.

The main reason to prepare ionic liquids and eutectic mixtures formulation is to reduce the API melting temperature to overcome problems related with the solid form, such as low solubility, polymorphism, and permeability (Kelley et al., 2013). The

mixture between LDC (base) and CAP produced liquefaction at the lowest temperature (room temperature) among all mixtures, therefore this binary system (LDC:CAP) was selected to further characterization.

6.6. Physicochemical characterization of LDC:CAP deep eutectic mixture

6.6.1. Thermal analysis

It can be noticed from the second heating curves (**Figure 25**) that a crystallization (exothermic event) occurred at -13.55 °C for the sample containing $[LDC]_8[CAP]_2$, and at 1.88 °C for that with $[LDC]_7[CAP]_3$. Those peaks can be attributed to LDC that crystallized out of the mixture, resulting in an endothermic event close to the pure LDC melting point, on the second heating cycle. The same happened to $[LDC]_9[CAP]_1$ however the crystallization occurred during super-cooling step (from 100 °C to -65 °C). Moreover, for the equimolar composition and the binary mixtures with excess CAP (**Figure 25**) there was no evidence of transitions during the second heating cycle, therefore, suggesting a disordered (liquid or amorphous) state of the samples. It also indicates that, in order to suppress LDC tendency to crystallization, it is necessary to mix the anesthetic with at least an equivalent molar ratio of CAP. No cold crystallization was found upon storage of the 7:3 and 3:7 LDC:CAP mixtures up to -20 °C for 2 months, suggesting excellent physical stability of the samples.
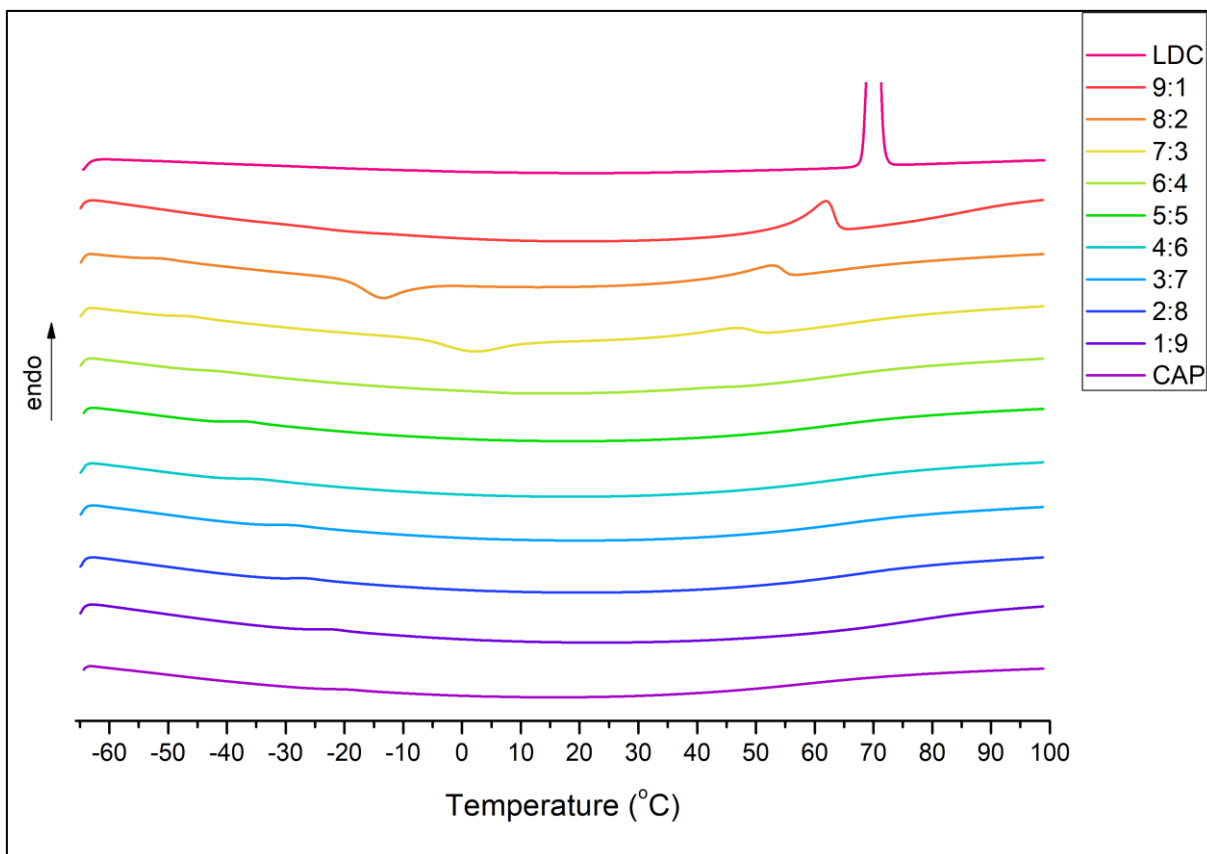
Figure 25- DSC second heating curves of binary LDC:CAP mixtures. Ratios in the legends are in molar LDC:CAP fraction.

The series of DSC heating curves of LDC:CAP mixtures have demonstrated a behavior similar to those observed for LDC binary systems with ibuprofen, decanoic acid and oleic acid (Bica et al., 2011; H. Wang et al., 2014). In all systems, the pure compounds have an expected reduction of Tm until a specific range of the composition, close to equimolar concentration. At this range, the LDC:CAP sample did not crystallize at the cooling and heating rates investigated, and only a glass transition event (-39.35 °C) was observed (**Figure 25**).

Considering that the temperature of the eutectic event is not evident from the experimental DSC curves, its composition and melting temperature (Tm) were calculated based on the ideal behavior described by the Schröder–van Laar equation (Ivashenko et al., 1976; Schröder Iw., 1893) (Equation 11), and the full phase diagram obtained is shown in **Figure 26**.
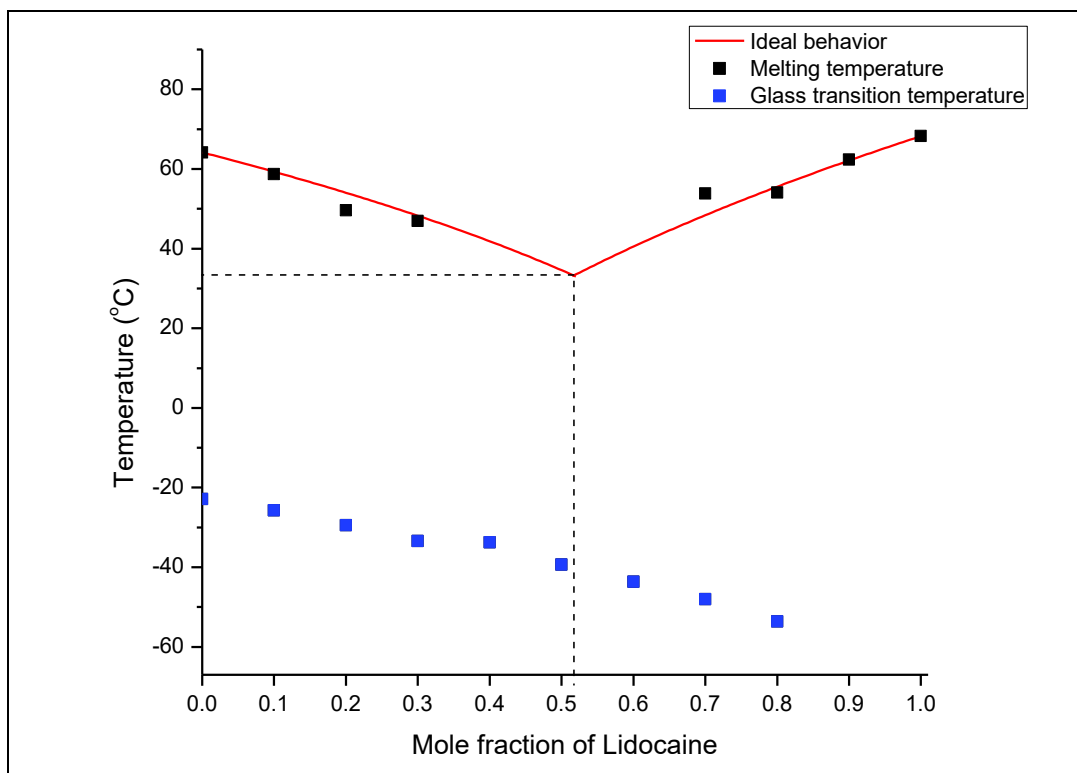
Figure 26- Melting and glass transition temperature from DSC curves of LDC:CAP mixtures, and ideal behavior curve, fitted according to the Schröder–van Laar equation.

In **Figure 26** the theoretically determined Tm(x) lines do coincide well with the experimental points of the binary mixtures. The predicted eutectic temperature was found to be 33.05 °C, so that it would be expected that all of the LDC:CAP mixture would be solid at room temperature. The theoretical eutectic composition for LDC:CAP found by the Schröder–van Laar model was 0.515:0.485. Thus, mixing approximately 1 mole of LDC and 1 mole of CAP results in a single eutectic mixture, which melts at 33.05 °C. However, in contrast to the prediction, some of the mixtures turned to be liquid when prepared at room temperature. The reason for such behavior of the LDC:CAP system might be the presence of an intermolecular interaction, probably a hydrogen bond that prevents crystallization of the eutectic.

The glass transition temperature (Tg) of LDC:CAP composition decreased with increasing LDC mole fraction. The maximum Tg was -25.72 °C for 0.1 molar fraction LDC, reaching a minimum of -53.58 °C for 0.8 LDC mole fraction. It should be noticed that the sample containing 0.9 LDC mole fraction did not show a Tg due to crystallization during super-cooling (data not shown). This finding evidenced that it is possible to obtain an amorphous system for the majority of LDC:CAP binary mixtures.

These results corroborate the hypothesis of Martins et al. (2018) who defined a DEM as a mixture of pure compounds for which the eutectic point temperature is below that of an ideal liquid mixture. Also, it was described that usually the compounds forming DEM are very strongly hydrogen-bonded. Following, the intermolecular interaction between CAP and LDC was investigated through IR and NMR spectroscopies (Martins et al., 2018) and X-ray diffractometry.

6.6.2. Powder X-Ray diffraction

PXRD is a non-destructive characterization method that gives information about the crystallinity of a sample. This technique can be helpful to distinguish between an amorphous form and different multicomponent crystalline forms (Cherukuvada and Nangia, 2014).

Figure 27 confirmed that pure LDC and CAP starting materials were crystalline (their main peaks are highlighted with a start or hash symbol). The equimolar composition was analyzed at cold condition (below Tm), and at room temperature. The cold sample (below Tm) has shown all the main peaks of the pure LDC and CAP, which is an evidence of a eutectic mixture formation. According to Cherukuvada and Nangia (2014), the crystalline pattern of a eutectic mixture should be similar to the patterns of the pure APIs because it is not a new phase but a binary crystalline mixture. This is in contrast to co-crystals, which are also composed of neutral molecules, but have a unique crystal packing. The same $[LDC]_1[CAP]_1$ mixture was analyzed above Tm and it has not shown any crystalline peak. As a DEM, LDC and CAP have a disorganized lattice structure, demonstrating the amorphous pattern and supporting the DSC results.

As shown in **Figure 27**, $[LDC]_6[CAP]_4$ and $[LDC]_4[CAP]_6$ samples exhibited the main peaks of the major compound. Besides, the binary mixture with 0.6 LDC partly displayed an amorphous pattern. Thus, any slight change away from the equimolar concentration results in the appearance of a crystalline phase. This finding supports the theoretical eutectic composition being 1:1 LDC:CAP (molar ratio), as calculated by the Schröder–van Laar equation.
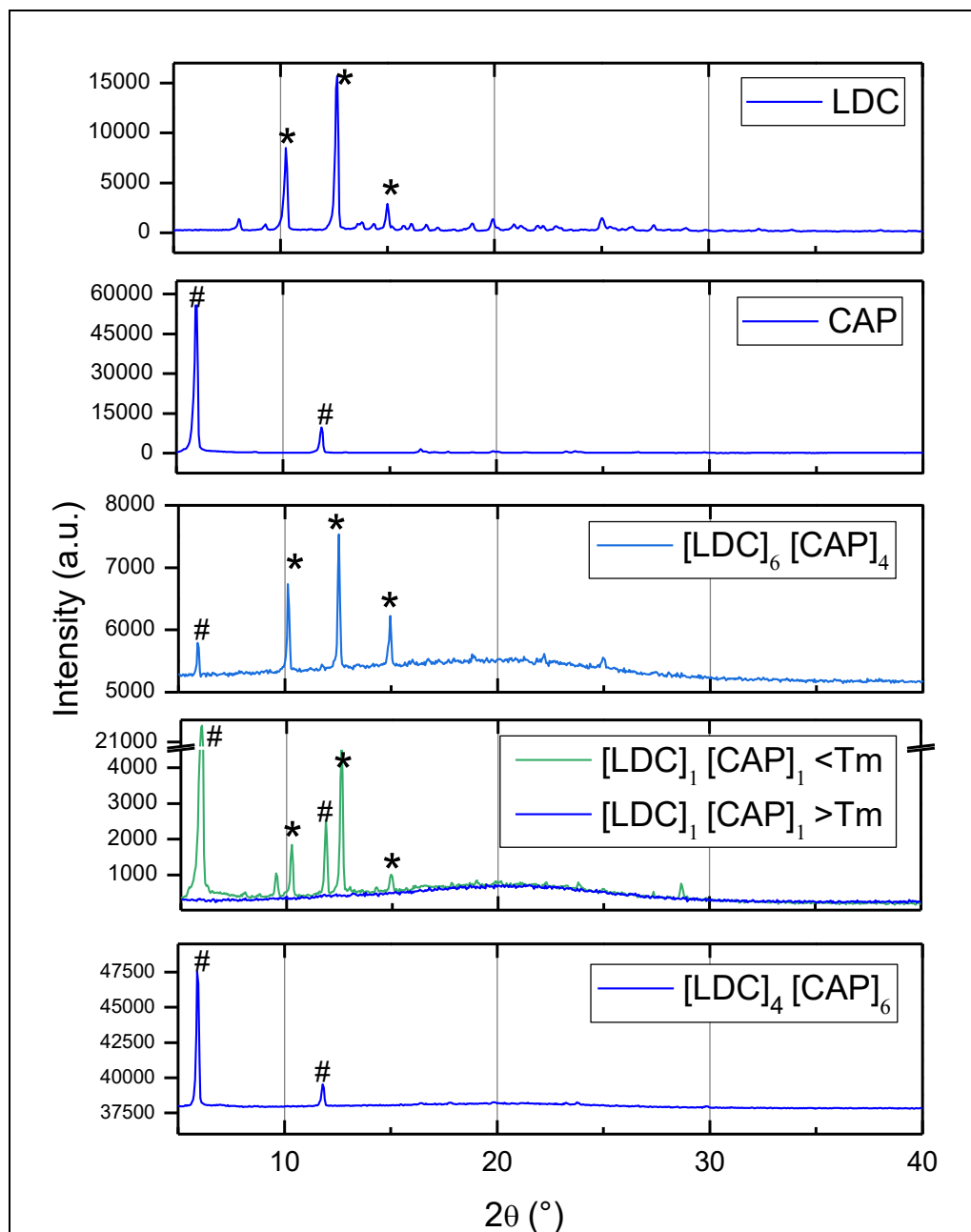
Figure 27- Power X-ray diffraction patterns of LDC, CAP and [LDC] [CAP] mixture, at different molar ratios.

6.7.   Investigation of intermolecular interactions

Most APIs have a hydrophobic nature and this property makes it difficult for them to reach the site of action and stay there long enough to exert the therapeutic effect (Aulton and Taylor, 2013; Tamjidi et al., 2013). Among different strategies applied to increase drug solubility, salt formation is one of most used. Recently, ionic liquids (ILs) comprised of cations and anions and combining two APIs have been

studied as a potential strategy to improve pharmacokinetics and pharmacodynamics properties of both drugs. The degree of ionization between anion and cation is critical to determine the type of DDS produced. From a mixture of two APIs (with melting points below 100°C) it is possible to get a mostly ionized combination, called an ionic liquid, and a mostly unionized complex, called deep eutectic mixture. Also, a variety of salt-neutral compounds with intermediate ionization degree can be obtained. In this section, the intermolecular interactions between LDC and CAP and the degree of ionization of the mixture was analyzed using FT-IR and NMR.

6.7.1. Fourier Transform Infrared spectroscopy

In a mixture of weak acids and bases, a ΔpKa of at least three units should result in efficient ionization of the compounds. The reason for this minimal (3 pH units) interval is that one would expect a 1 to 1000 acid-conjugated base molar ratio difference (99.9% complete proton transfer) for the ionization in aqueous solution (Kelley et al., 2013). However, ILs very often do not follow this rule, since the pKa is evaluated in aqueous solution, and not in the solid state (Braga et al., 2013).

The ΔpKa between LDC (tertiary amine, pKa= 7.92) and CAP (phenol, pKa= 9.95) is approximately 2 log units, so that salt formation is not expected to form between them (Brown et al., 2014; Powell, 1986). However, since the two APIs exhibit nearly an immediate conversion into a liquid at room temperature, possible intermolecular interactions between them were investigated by FTIR.

Figure 28 presents the FT-IR spectra of pure LDC, pure CAP and LDC:CAP binary mixtures. Secondary amides show a single N-H stretching in the region of 3200–3400 cm^{-1}, and this stretching was observed at 3245 cm^{-1} and 3287 cm^{-1}, respectively, for LDC and CAP. The O-H (3200-3500 cm^{-1}) and N-H stretching bands became broader and shift to longer wavenumbers when they take part in hydrogen bonding. However, from the spectra of the LDC:CAP mixtures no shift of the N-H stretching bands was noticeable.
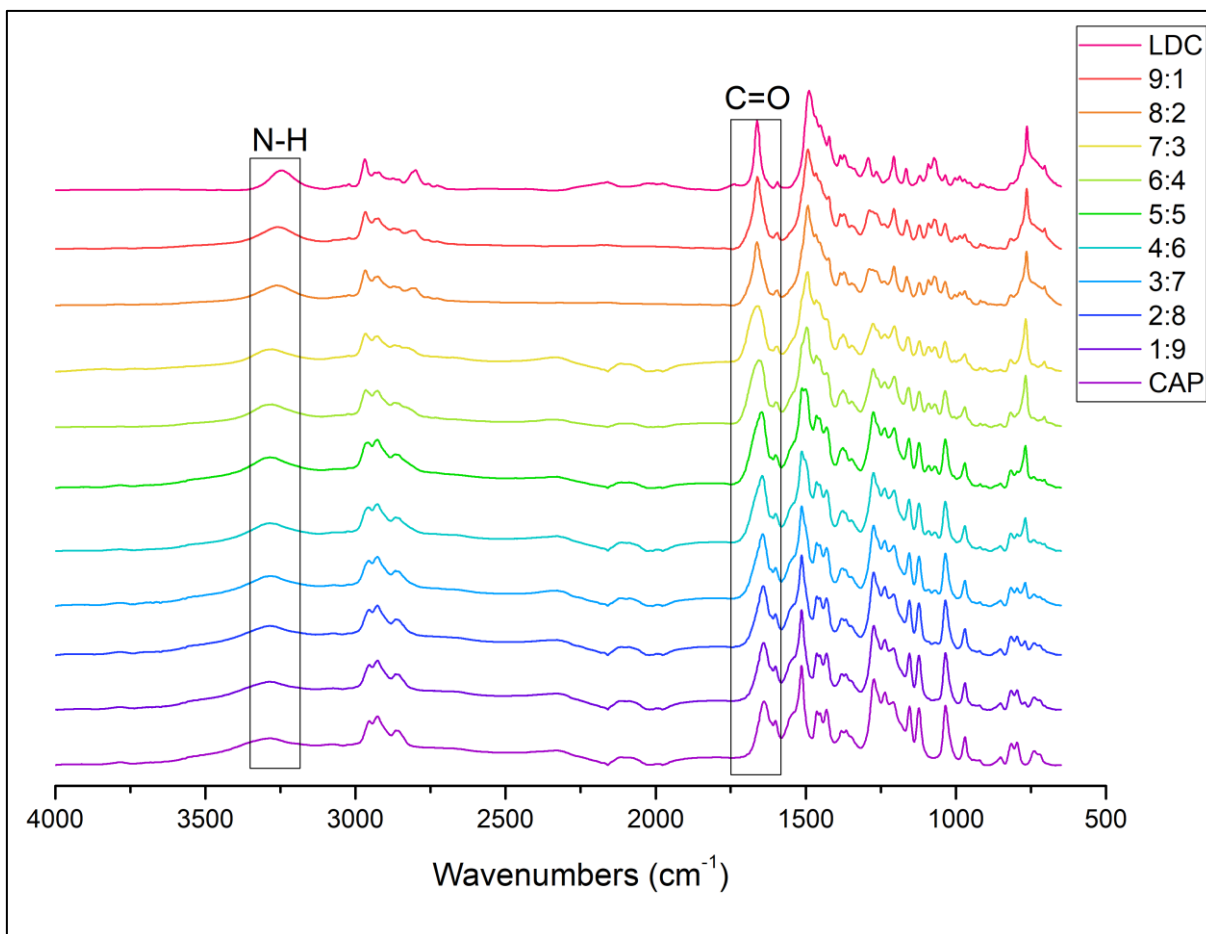
Figure 28- FT-IR spectra of LDC, CAP and LDC:CAP mixtures. LA:CAP molar ratios are given in the legends.

Tertiary amines have no N-H bonds and therefore no band appears in this region (3100–3550 cm^{-1}) of the infrared spectrum (Brown et al., 2014). Although, Regnier and Neville observed that when hydrohalide salts of LDC (tertiary amine) were produced the N^+-H stretching occurred in a range of 3367-2500 cm^{-1}, depending on the anion size (Regnier and Neville, 1969). The LDC:CAP binary mixture did not show any new peak related to ionization of the amine group. The phenol (pKa = 9.95) is the ionizable group of CAP and the position of the O-H stretching absorption, as well as its intensity depends on the extent of hydrogen bonding. In a concentrated solution (extensive hydrogen bonding) the O-H stretching absorption occurs as a broad peak at 3200–3500 cm^{-1} (Brown et al., 2014). The formation of hydrogen bonds between phenols and aliphatic amines was studied by Farah (Farah et al., 1979). These authors found that two ortho groups on the phenol group prevents any hydrogen bond formation with amines, while a single ortho group has no effect on such a reaction. The

authors discussed that the observed results might be due to the fact that tertiary aliphatic amines are sterically hindered to react.

In the FT-IR region, the carbonyl stretching peak of amides is observed between 1630–1680 cm^{-1}; for LDC it occurs at 1661 cm^{-1} and for CAP at 1639 cm^{-1}. The mixture containing 0.5, 0.6 and 0.7 LDC mole fractions showed the C=O band split into three. A shoulder appeared at 1652 cm^{-1} (**Figure 29**) and the peak became broader, possibly indicating an intermolecular interaction between LDC and CAP in the carbonyl.
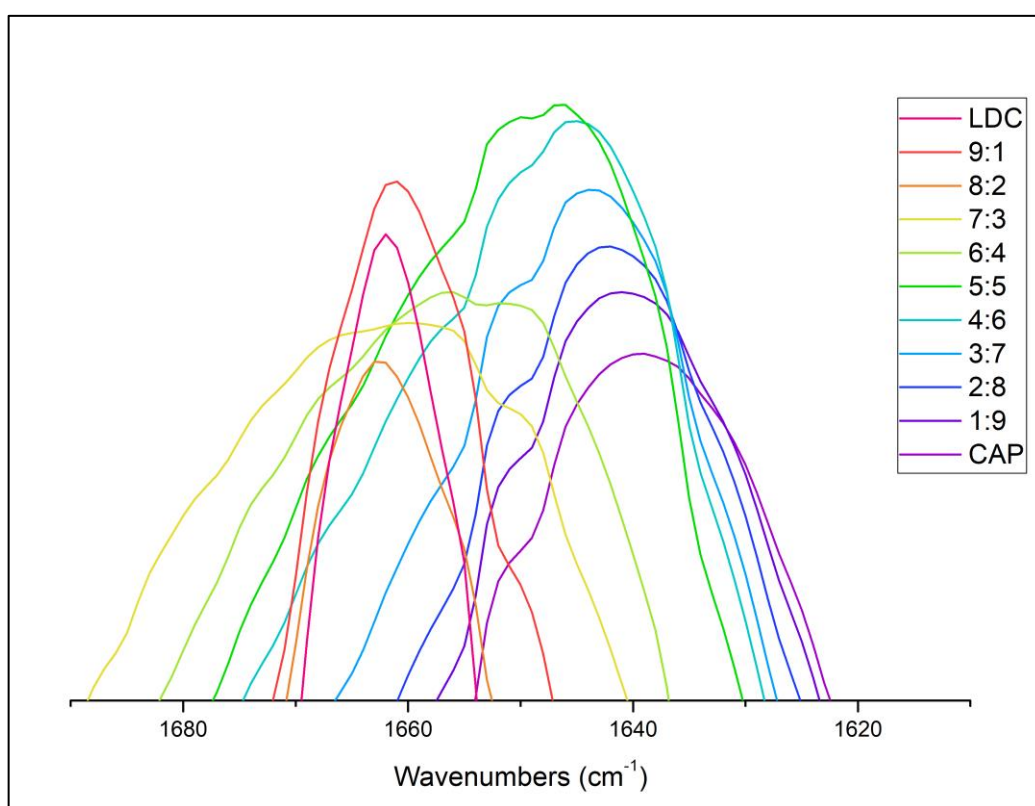
Figure 29- Overlay FT-IR spectra of LDC:CAP mixtures at the range of carbonyl stretching band. LDC:CAP molar ratios are seen in the legends.

Aromatic rings show a medium to weak band in the C-H stretching region at approximately 3030 cm^{-1}, and these stretching bands are seen at 2969 cm^{-1} and 2926 cm^{-1} for LDC, and at 2922 cm^{-1} and 2866 cm^{-1} for CAP. The equimolar mixture of LDC and CAP showed the same bands as pure CAP. Aromatic rings show a strong absorption in the region of 690–900 cm^{-1} as a result of out-of-plane C-H bending, which for LDC occurred at 763 cm^{-1}, and for CAP at 738 cm^{-1}. Also, these compounds showed absorptions owing to aromatic C=C stretching between 1450 and 1600 cm^{-1}: for LDC

it occurred at 1489 cm^{-1}, and CAP at 1515 cm^{-1}. The binary mixtures of LDC:CAP did not show any new band in the aromatic ring spectrum range.

Finally, -CH$_3$ groups shows a weak to medium stretching bands in the region of 1375–1450 cm^{-1}, which were registered at 1385 cm^{-1} and 1372 cm^{-1} for LDC, and at at 1366 cm^{-1} and 1381 cm^{-1}, for CAP. Surprisingly, in the samples with 0.5, 0.6 and 0.7 LDC molar fraction, a new absorption was detected at 1376 cm^{-1}, as shown in **Figure 30**.
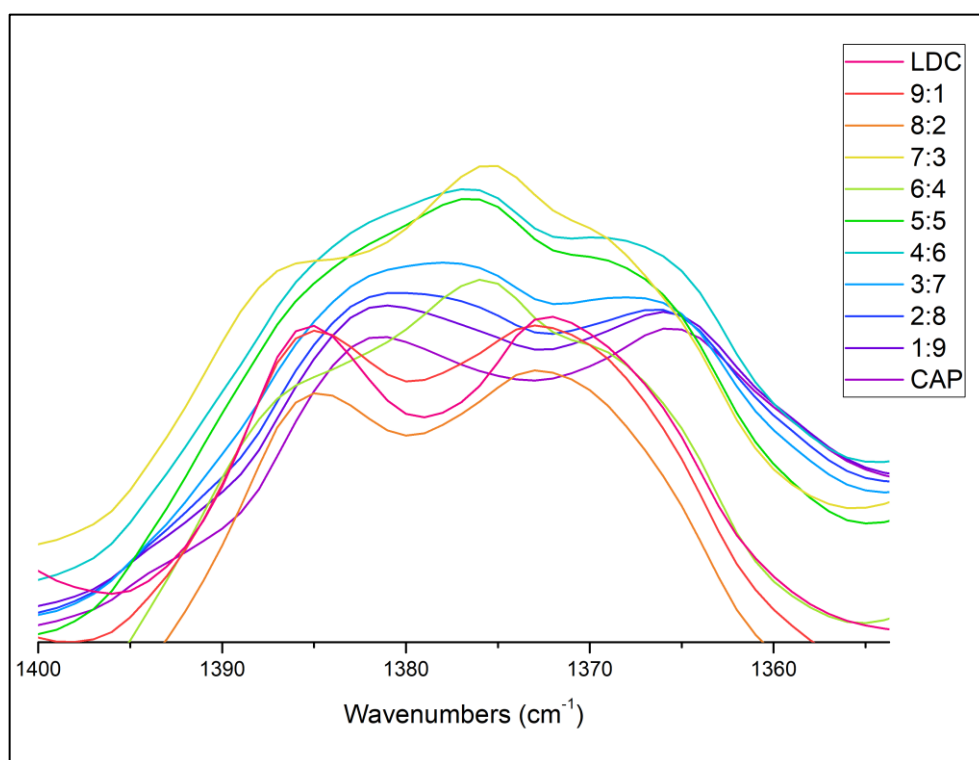
Figure 30- Overlay of FTIR spectra of LDC:CAP mixture at the range of methyl stretching bands (1400 - 1360 cm^{-1}). LDC:CAP molar ratios are seen in the legends.

FTIR spectroscopy indicated no salt formation between LDC and CAP, so that LDC:CAP mixture most probably do not form an ionic liquid, but rather a DEM liquid. The results suggest the existence of an intermolecular interaction, seen as a new peak around the carbonyl stretching band of amides. NMR analysis was performed to confirm such intermolecular interaction, and to identify the groups involved in it.

6.7.2. Nuclear Magnetic Resonance

Nuclear Magnetic Resonance is the dominant structural elucidation method for complex molecules that have many functional groups (Gerothanassis et al., 2002). This technique can be helpful to define whether the compounds (LDC and CAP) remain as a neutral molecular DEM, or as an IL in the $[LDC]_1[CAP]_1$ mixture.

The chemical structures of the two compounds (CAP and LDC) are shown at **Figure 31** and they were used to assign the protons and carbons to their corresponding peaks on the ^{1}H-NMR and ^{13}C-NMR spectra, respectively.
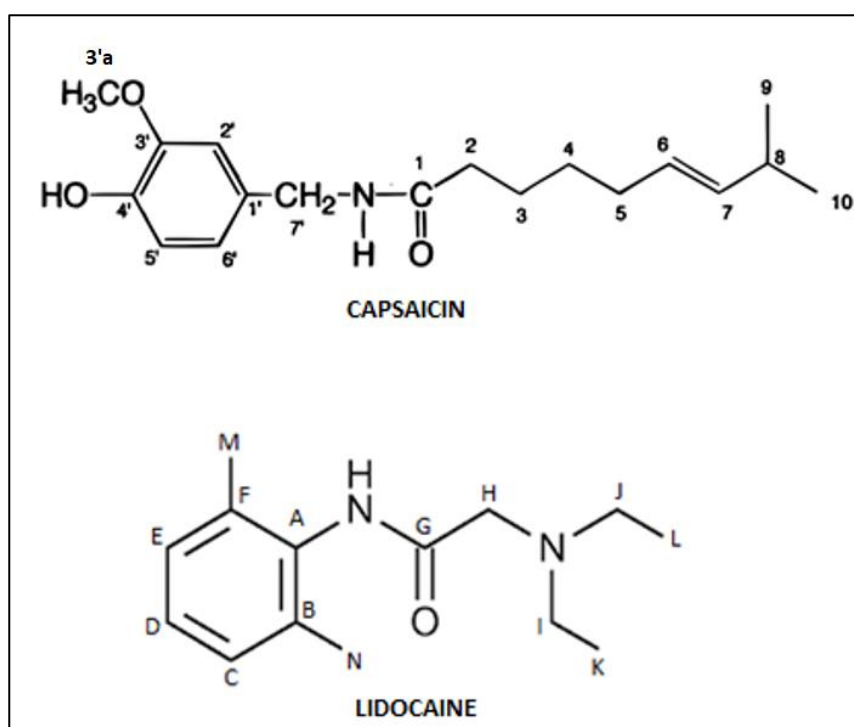
Figure 31- Chemical structure and atom numbering of CAP and LDC molecules.

The first NMR spectra technique performed was ^{1}H-NMR, using deuterated chloroform as solvent, as shown at **Figure 32**. Also, the list of all ^{1}H chemical shifts for CAP, LDC and $[LDC]_1[CAP]_1$ samples is given in **Table 5**. Hydrogen atoms with higher chemical shift values tend to be hydrogens in functional groups such amides (Brown et al., 2014). The amide NH signal of LDC can be seen at 8.94 ppm, and only

a small signal was detected for the amide NH of CAP at 5.63 ppm, near the OH signal (5.66 ppm).
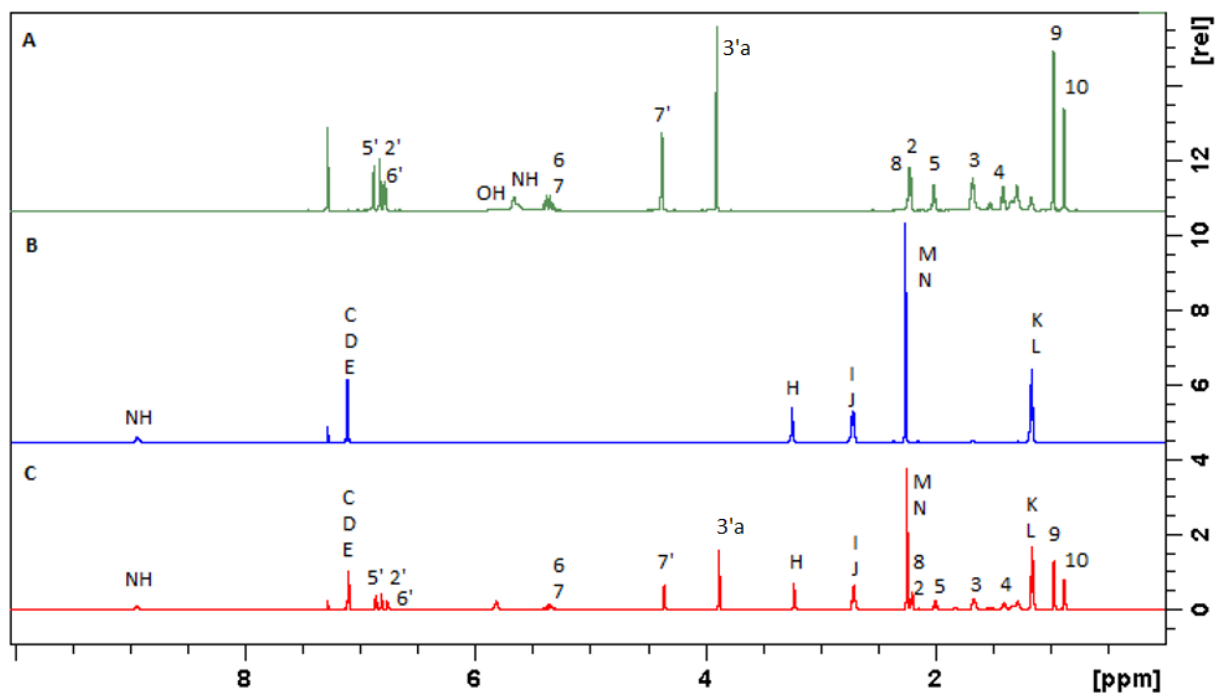
Figure 32- ^{1}H NMR spectrum of: A) capsaicin, B) lidocaine, and C) [LDC]$_1$:[CAP]$_1$. Samples in deuterated chloroform; the residual CDCl$_3$ was used as a reference - at 7.28 ppm. 600 MHz and 25°C; ^{1}H-NMR peak assignment as in Figure 31.

In the [LDC]$_1$[CAP]$_1$ spectrum, the NH signal of LDC kept the same chemical shift (8.94 ppm) of the pure anesthetic (**Table 5**). Contrarily, the NH signal of CAP (5.63 ppm) moved low field, to 5.81 ppm. In the spectrum of the equimolar mixture, hydrogens of NH and OH (from CAP) were superimposed on each other. So, the OH signal (5.66 ppm) also moved downfield to 5.81 ppm. Since changes in chemical shift higher than 0.05 ppm are considered significant (Fraceto et al., 2005, 2002), we can say that the NH and OH groups of CAP were significantly affected by the interaction with LDC, although no change was observed, for any LDC hydrogen.

Table 5- ^{1}H-NMR: Chemical shifts, δ (ppm) of capsaicin, lidocaine and [LDC]$_1$[CAP]$_1$ hydrogens. Samples in deuterated chloroform, at 25°C and 600 MHz; the residual CDCl$_3$ signal was used as a chemical shift reference, at 7.28 ppm. ^{1}H-NMR peak assignment as in 31. * = superimposed peaks.

Capsaicin		Lidocaine		[LDC]$_1$[CAP]$_1$			$\Delta \delta$.
H atom	ppm	H atom	ppm	H atom	ppm	Integrated area	(ppm)
		NH$_{LDC}$	8.937	NH$_{LDC}$	8.941	1.060	0.004
		C; D; E	7.108	C; D; E	7.099	3.086	-0.009
5'	6.889			5'	6.870	1.000	-0.019
2'	6.828			2'	6.813	1.020	-0.015
6'	6.789			6'	6.767	1.048	-0.022
OH	**5.660**			**OH***	**5.815**	**1.984**	**0.155**
NH	**5.626**			**NH***	**5.815**	**1.984**	**0.189**
6; 7	5.408			6; 7	5.402	1.288	-0.005
7'	4.381			7'	4.357	2.219	-0.024
3'a	3.897			3'a	3.877	3.236	-0.020
		H	3.243	H	3.225	2.151	-0.018
		I; J	2.731	I; J	2.722	4.350	-0.009
		M; N	2.255	M; N	2.244	6.574	-0.011
8	2.231			8	2.214	0.850	-0.017
2	2.218			2	2.201	1.803	-0.017
5	2.007			5	2.015	0.850	0.008
3	1.676			3	1.676	1.803	-0.000
4	1.406			4	1.406	1.347	0.000
		K; L	1.173	K; L	1.164	7.336	-0.009
9	0.970			9	0.971	3.842	0.001
10	0.876			10	0.877	2.631	0.001

^{13}C-NMR is particularly useful to assign shifts in the carbonyl groups (e.g. from amide groups where the carbon has no hydrogens and are thus not visible by ^{1}H-

NMR). As one can notice from **Figure 33**, the ^{13}C belonging to the carbonyl group was found at 172.77 ppm and 170.29 ppm, for CAP and LDC, respectively. In the [LDC]$_1$[CAP]$_1$ spectrum, there was a change in the position of those carbon atoms: to 172.86 ppm and 170.37 ppm, respectively (**Table 6**).

In the case of LDC protonation, a shift in the carbonyl signal as well in carbon "H" of LDC (57.56 ppm) would be noticed (Badawi et al., 2016). However, in the equimolar mixture there were no significant changes in the position of carbon "H" nor in amine carbons "I" and "J". Despite the changes in the position of the carbonyl peaks, no other chemical shifts were observed in the spectrum of the binary mixture. Therefore, ^{13}C-NMR spectrum of the binary mixture indicated that hydrogen bond formation is most likely to be happening between the APIs, rather than ionization of LDC (IL formation).
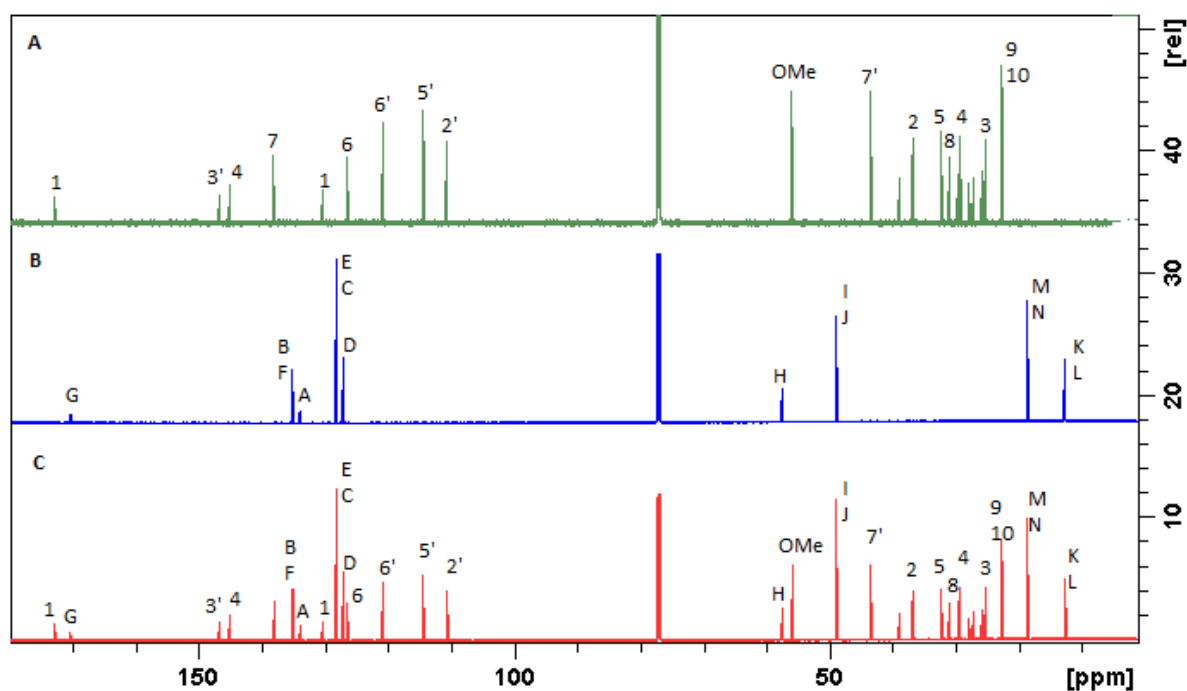
Figure 33- ^{13}C-NMR spectrum of: A) capsaicin, B) lidocaine, and C) [LDC]$_1$:[CAP]$_1$. Samples in chloroform, residual CHCl$_3$ was used as a reference at 77.23 ppm, 25°C, and 600 MHz; ^{13}C NMR peak assignment as in Figure 31.

Table 6- Observed ^{13}C chemical shifts δ (ppm) of neat capsaicin, lidocaine and [LDC]₁[CAP]₁. Samples in chloroform, residual $CDCl_3$ was used as a reference at 77.23 ppm, 25°C, and 600 MHz; ^{13}C NMR peak assignment as in Figure 31.

Capsaicin		Lidocaine		[LDC]₁[CAP]₁		$\Delta\,\delta$.
C atom	ppm	C atom	ppm	C atom	ppm	(ppm)
1	**172.766**			**1**	**172.858**	**0.092**
		G	**170.289**	**G**	**170.370**	**0.081**
3'	146.691			3'	146.746	0.055
4'	145.127			4'	145.147	0.020
7	138.105			7	138.069	-0.036
		A	135.098	A	135.088	-0.010
		B; F	133.992	B; F	133.957	-0.035
1'	130.409			1'	130.416	0.007
		C; E	128.236	C; E	128.229	-0.007
		D	127.076	D	127.090	0.014
6	126.485			6	126.508	0.023
6'	120.824			6'	120.770	-0.054
5'	114.351			5'	114.393	0.042
2'	110.670			2'	110.713	0.044
		H	57.562	H	57.518	-0.044
3'a	55.948			3'a	55.926	-0.022
		I; J	48.969	I; J	48.967	-0.002
7'	43.547			7'	43.500	-0.047
2	36.739			2	36.684	-0.056
5	32.232			5	32.241	0.008
8	30.978			8	30.975	-0.003
4	29.292			4	29.296	0.004
3	25.281			3	25.294	0.013
9; 10	22.658			9; 10	22.661	0.003
		M; N	18.587	M; N	18.574	-0.013
		K; L	12.682	K; L	12.669	-0.013

Altogether, the ^1H-NMR and ^{13}C-NMR results, collected with the samples in chloroform provided evidences of an interaction between LDC and CAP, probably by hydrogen bonds. The main limitation of this method is that the solvent could break up the bond, since both APIs are very soluble in this solvent. Thereupon, the NMR

analysis was performed using neat (solvent-free) samples. The samples should be liquid during analysis, so the spectra were run at 70 °C, a temperature that is above Tm of capsaicin and lidocaine.

Figure 34 shows the ^{1}H-NMR spectra of neat CAP, LDC and the [LDC][1][CAP][1] mixture, at 70 °C. LDC and the mixture showed sharp and well-defined chemical shifts that are characteristic of liquid samples. On the other hand, the broad peaks of CAP revealed its high viscosity at 70 °C, which restrains the rotation of the hydrogens. Most interestingly, the spectra of the mixture showed sharp chemical shifts, as in a liquid sample, showing that LDC can change the physical state of CAP in the binary mixture.

No absolute references were used in the neat samples experiment at 70 °C. The chemical shift of the peaks was mainly dependent on the concentration of the sample, and on how did the molecules interact with each other. After integration and peak assignment (Table 7) of the pure components, hydrogen signals that were less likely to interact in the mixture were used as standard references for the binary mixture: "OCH$_3$ (4.18 ppm) and "M, N" hydrogens (2.71 ppm), were used as a reference for CAP and LDC, respectively.
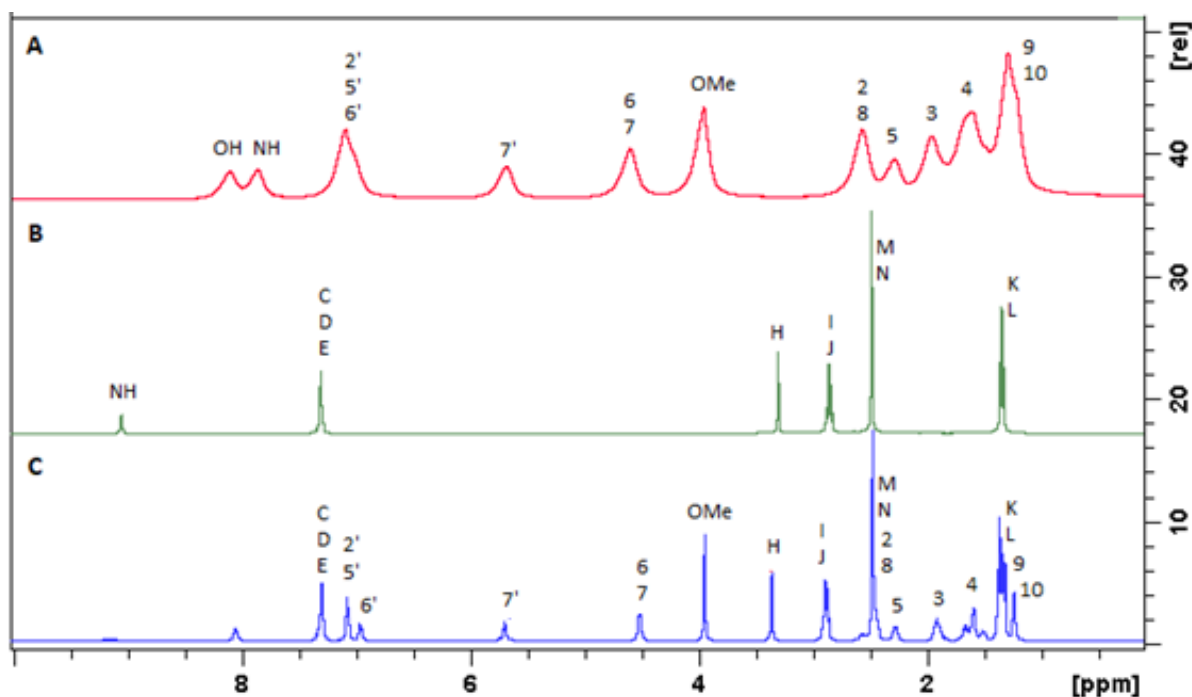
Figure 34- ^{1}H-NMR spectrum of neat capsaicin, lidocaine and [LDC]$_1$:[CAP]$_1$ at 70 °C, and 400 MHz. Assignment as in Figure 31.

As seen in the [LDC]₁[CAP]₁ spectrum, the amide NH peak from LDC disappeared, while there was only one peak at 8.283 ppm that could be assigned to either NH or OH, from CAP (**Table 7**). The above evidences strongly indicate that these hydrogens are in fast exchange in the NMR timescale. The formation of DEM are associated to hydrogen bonds between compounds (Abbott et al., 2003). To further study the dynamics of hydrogen bonds, hydrogens NMR spectra of [LDC]₁[CAP]₁ were performed at a range of 25 °C to 70°C.

Table 7- Observed ¹H-NMR chemical shifts δ (ppm) of neat capsaicin, lidocaine and [LDC]₁[CAP]₁ at 70 °C, and 400 MHz. The signal of the "OCH₃" hydrogens (at 4.18 ppm) was used as a reference for CAP; "M, N" hydrogens (2.71 ppm) were used as references for LDC. Assignment as in Figure 31. *= superposed peaks; n.o.= not observed.

Capsaicin			Lidocaine		[LDC]₁[CAP]₁			
H atom	ppm	Integrated area	H atom	ppm	H atom	ppm	Integrated area	Δ δ. (ppm)
			NH$_{LDC}$	9.275	n.o.			
OH	8.327	0.781			OH*	8.283	1.047	-0.044
NH	8.083	0.877			NH*	8.283	1.047	0.200
			C; D; E	7.526	C; D; E	7.532	3.139	0.006
2'; 5'; 6'	7.316	2.905			2'; 5'	7.314	2.045	-0.002
					6'	7.203	1.103	**-0.113**
7'	5.909	1.119			7'	5.936	1.170	0.026
6; 7	4.822	1.975			6; 7	4.755	1.962	-0.066
3'a	4.181	3.000			3'a	4.181	3.000	0.000
			H	3.530	H	3.593	2.041	0.064
			I; J	3.109	I; J	3.148	4.172	0.040
2; 8	2.792	2.771	M; N	2.711	M; N; 2; 8	2.711	8.807	-0.081
5	2.508	1.442			5	2.521	1.373	0.013
3	2.181	2.472			3	2.151	2.435	-0.030
4	1.824	2.806			4	1.827	1.367	0.004
9; 10	1.848	5.822			K; L; 9; 10	1.617	12.311	0.031

Temperature variation has been one of the most used approaches to study the presence of hydrogen bond (Gellman et al., 1991). **Figure 35** shows that an increase in temperature was accompanied by the disappearance of the NH signal of LDC in the neat mixture (black arrows). While, OH/NH superposed peaks (CAP) changed upfield (to lower ppm) in [LDC]$_1$[CAP]$_1$ spectrum (black line). This behavior is related to a large conformational changes that take place with the temperature which decrease the intermolecular hydrogen bonding (Duarte et al., 2017). On the contrary, when the [LDC]$_1$[CAP]$_1$ sample were diluted in chloroform at 25° C, OH and NH superimposed peak showed a downfield shift (higher ppm), indicating hydrogen bond formation. Together, neat and chloroform spectra corroborated to confirm the formation of hydrogen bond between LDC and CAP, at 25 °C.
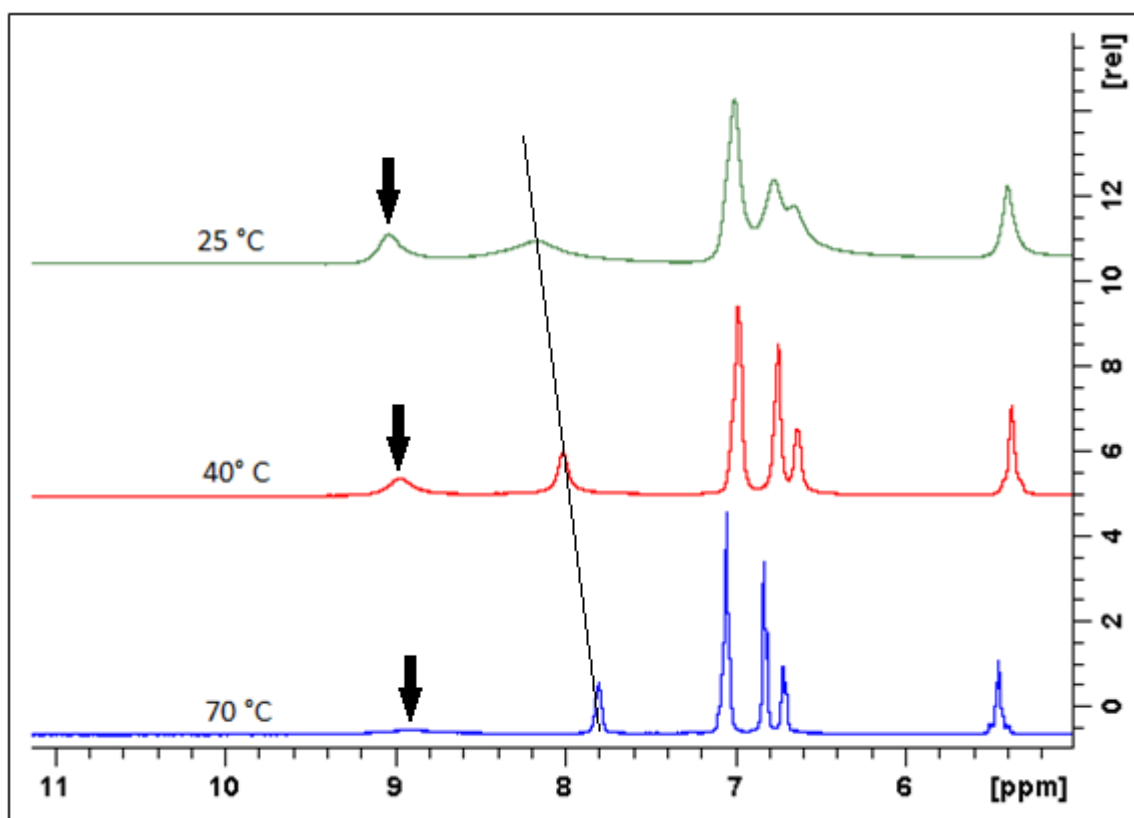
Figure 35- Representative expansion of the ^{1}H-NMR spectra of neat [LDC]$_1$[CAP]$_1$ as function of temperature. Black arrows indicate proton of NH chemical shift (LDC) and the black line show displacement of OH/NH superposed peaks (CAP).

Figure 36 shows the carbon NMR spectra of neat samples, whose chemical shifts are listed in **Table 9**. It can be observed that the peak corresponding to LDC carbon "G" (at 168.754 ppm) had a significant shift to 170.245 ppm, in the presence of CAP. Also, CAP peak at 174.173 ppm significantly changed position to 173.412 ppm. Both signals belong to the carbonyl group of LDC and CAP. Therefore, this result is in agreement with the results obtained with ^{13}C-NMR for the samples in chloroform.
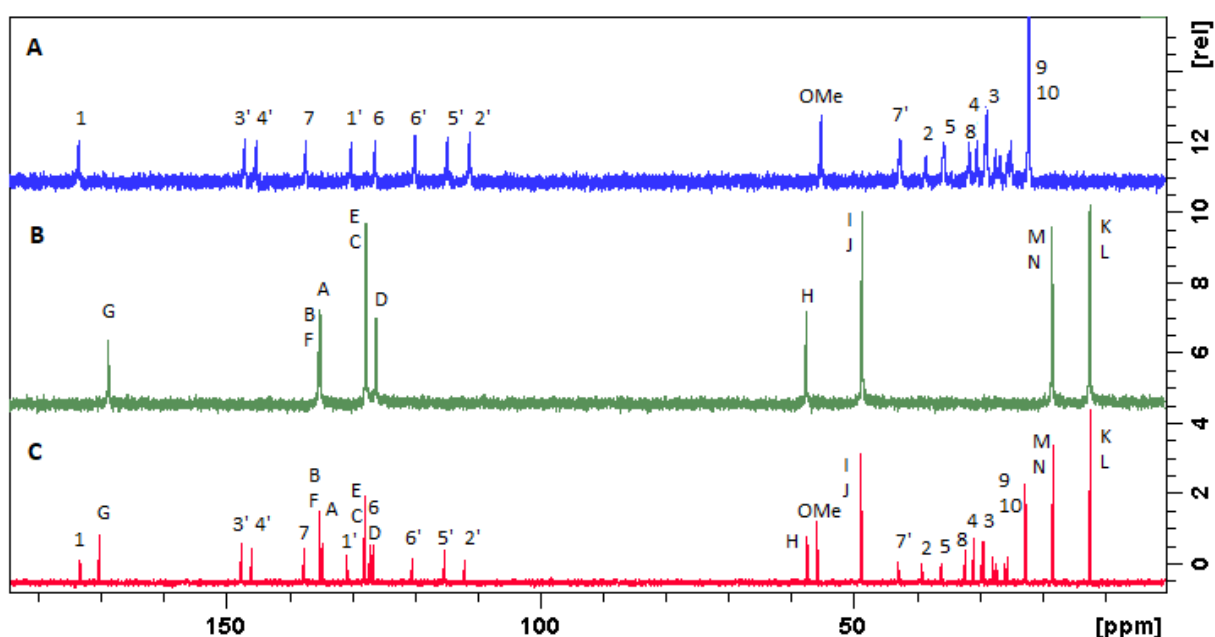
Figure 36- ^{13}C-NMR spectrum of neat capsaicin, lidocaine and [LDC]$_1$[CAP]$_1$ at 70 °C. Peak assignment as in Figure 34.

The purpose of the current NMR analysis was to confirm if the interaction between LDC and CAP in the liquid mixture was due to hydrogen binding (DEM) rather than proton transfer (IL). All the NMR data strongly supported hydrogen bond formation between CAP (carbonyl) and LDC (amide) groups. No sign of protonation was observed, in agreement to FTIR results, confirming that [LDC]$_1$[CAP]$_1$ as a DEM system.

Table 8- ^{13}C chemical shifts δ (ppm) of neat capsaicin, lidocaine and [LDC]1[CAP]1 at 70 °C, and 400 MHz. Carbon "OCH$_3$" (55.864 ppm) was used as a reference for CAP; and carbons "M, N" (18.311 ppm) were used as references for LDC. Assignment as in Figure 31.

Capsaicin		Lidocaine		[LDC]$_1$[CAP]$_1$		Δ δ (ppm)
C atom	ppm	C atom	ppm	C atom	ppm	
1	**174.173**			**1**	**173.412**	**-0.760**
		G	**168.754**	**G**	**170.245**	**1.491**
3'	147.697			3'	147.677	-0.021
4'	145.873			4'	146.030	0.157
7	137.942			7	137.663	-0.278
		B; F	135.284	B; F	135.115	-0.169
		A	134.989	A	134.771	-0.218
1'	130.780			1'	130.849	0.069
		C; E	127.687	C; E	127.959	0.272
6	126.953			6	127.080	0.128
		D	126.069	D	126.674	0.605
6'	120.578			6'	120.428	-0.149
5'	115.411			5'	115.222	-0.189
2'	111.843			2'	112.063	0.219
		H	57.789	H	57.438	-0.051
3'a	55.864			3'a	55.864	0.000
		I; J	48.599	I; J	48.833	0.235
7'	43.318			7'	42.962	-0.356
2	39.125			2	39.123	-0.002
5	36.280			5	36.163	-0.118
8	32.277			8	31.968	0.309
4	30.976			4	30.918	-0.058
3	29.483			3	29.740	0.257
9; 10	22.754			9; 10	22.729	-0.025
		M; N	18.311	M; N	18.311	0.000
		K; L	12.308	K; L	12.363	0.055

6.8. Stability studies

Water sorption of pharmaceutical products is a concern limiting dosing accuracy, the chemical stability, and compatibility (Zografi, 1988). LDC free base is not hygroscopic, in contrast LDC hydrochloride is very hygroscopic. It adsorbs 1 mol of water per mole of lidocaine at 80% relative humidity (25 °C) (Powell, 1986). Capsaicin is unlikely to form hydrates and is non-hygroscopic.

Figure 37 shows the dynamic vapor sorption behavior of the $[LDC]_1[CAP]_1$ sample at 25 °C. The weight of the sample was monitored during the process. The mass increase is associated with vapor sorption whereas a decrease is due to vapor desorption (Sheokand et al., 2014). It can be seen that the equilibrium on sorption and desorption was established in a similar period of time. The sorption kinetic showed that the sample was capable of sorbing a small amount of water, with a change in mass of approximately 1.8% at 80% relative humidity. According to the criteria of the European Pharmacopoeia (Ph. Eur., 2010), substances are classified "slightly hygroscopic" if water sorption after 24 h at 80% relative humidity (25 °C) ranges between 0.2% and 2%.
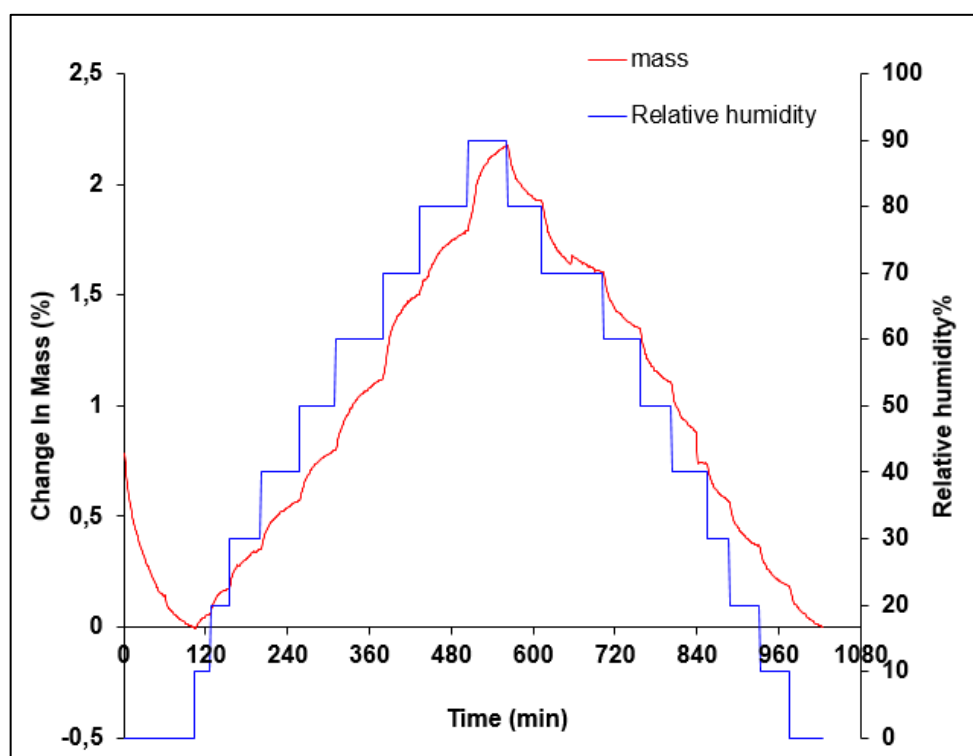
Figure 37- Sorption kinetic plot for the $[LDC]_1[CAP]_1$ sample, at 25.0 °C.

Most ILs/DEMs are hygroscopic and absorb moisture as soon as they are exposed to atmosphere (Ma et al., 2018). Wiest et al. synthesized a library of 36 different ILs for poor water soluble drug Selurampanel reaching moisture range between 5% to 18% change in mass, for 80% relative humidity (Wiest et al., 2017). As expected, transforming the APIs LDC and CAP into DEM slightly increased their hygroscopicity. Nevertheless, $[LDC]_1[CAP]_1$ water sorption was below values that have been described for IL/DEM.

The sorption-desorption isotherm described the amount of vapor sorbed or desorbed, as a function of the concentration of vapor at 25 °C. The hysteresis is the difference in water vapor uptake between the sorption and desorption isotherms. As shown in **Figure 38**, the isotherm demonstrated a slight sigmoidal shape and the sorption and desorption isotherm coincided (no hysteresis). Therefore, it revealed that the absorption and desorption of water is completely reversible.
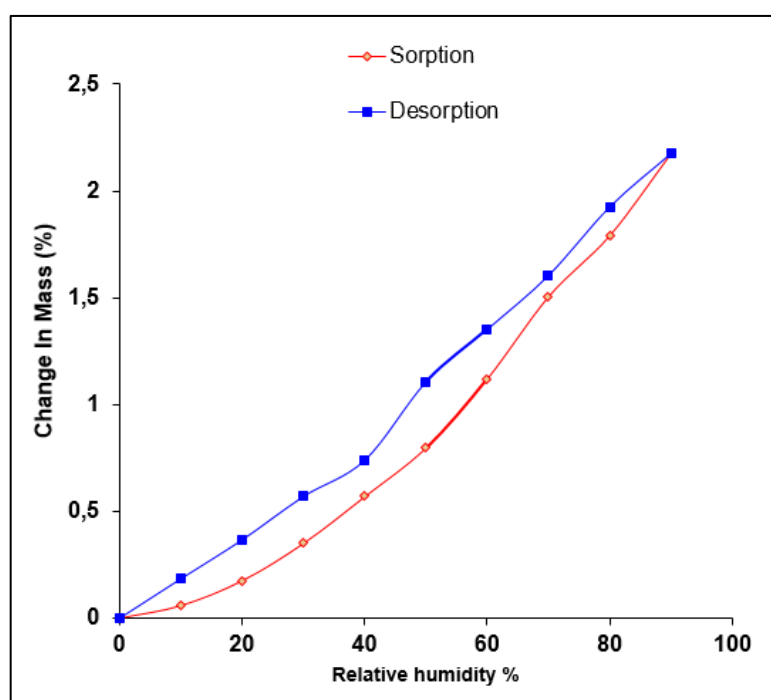
Figure 38- Water vapor isotherm for $[LDC]_1[CAP]_1$ sample, at 25.0 °C.

An amorphous standard sample would gain weight due to surface adsorption as well as to bulk absorption, while crystalline samples would gain weight because of surface adsorption (Sheokand et al., 2014). Consequently, crystallization occurring in a pure amorphous sample would be seen as an abrupt weight change.

This event was not observed for the $[LDC]_1[CAP]_1$ mixture, since the sample remained amorphous throughout DVS analysis, as shown by PXRD (**Figure 39**). The amorphous arrangement can be explained by the formation of a strong hydrogen bond between LDC and CAP, stabilizing the $[LDC]_1[CAP]_1$ sample, and restraining water absorption and thus preventing crystallization.
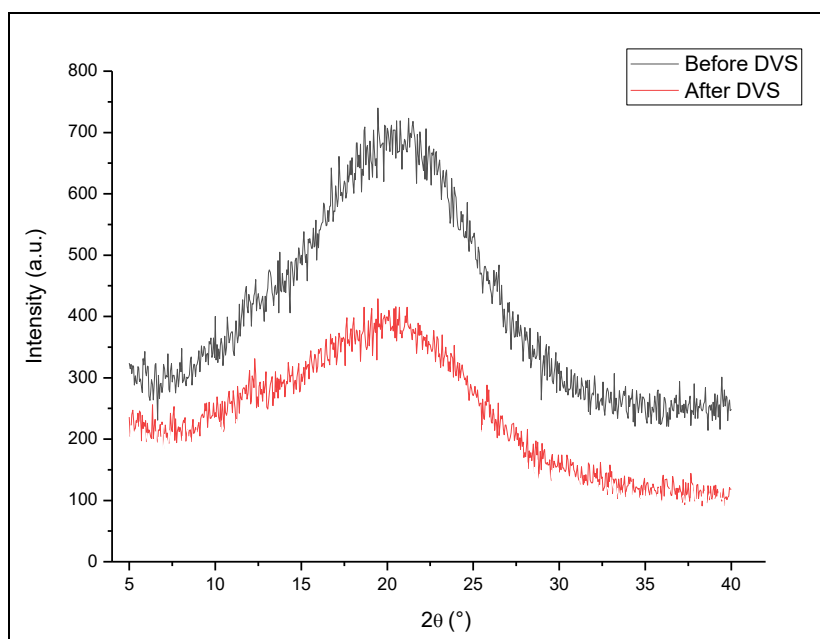
Figure 39- Power X-Ray Diffraction pattern of $[LDC]_1[CAP]_1$ sample, before and after the DVS analysis.

The results obtained from the DVS analysis suggests that $[LDC]_1[CAP]_1$ is a stable formulation since the intermolecular interaction between LDC and CAP was sufficient to prevent any crystallization, when exposed to high humidity stress.

6.9.   Solubility studies

The major challenge in drug development is to overcome the low water solubility and/or low permeability of compounds. In order to study the changes in hydrophilicity of the APIs (LDC and CAP) upon DEM formation, the saturation solubility was investigated in water, at 37 °C (**Figure 40**).

The maximum water solubility of LDC (14.09 ± 0.34 mM) was reached after 2 hours of stirring, and similar value (14 mM) was reported in the literature, for the

same temperature (Powell, 1986). The water solubility of LDC decreased to 4.26 ± 0.82 mM when in [LDC]₁[CAP]₁ mixture. CAP might have increased the hydrophobicity of LDC resulting an increased saturation solubility of LDC in water.

According to Turgut and coworkers, under saturated conditions, the water solubility of CAP is around 0.19 mM (Turgut et al., 2004). The determined water solubility of CAP was 0.223± 0.004 mM and 0.210 ± 0.036, for pure CAP and the binary system, respectively. Accordingly, the solubility of CAP was not significant affected in the [LDC]₁[CAP]₁ formulation.
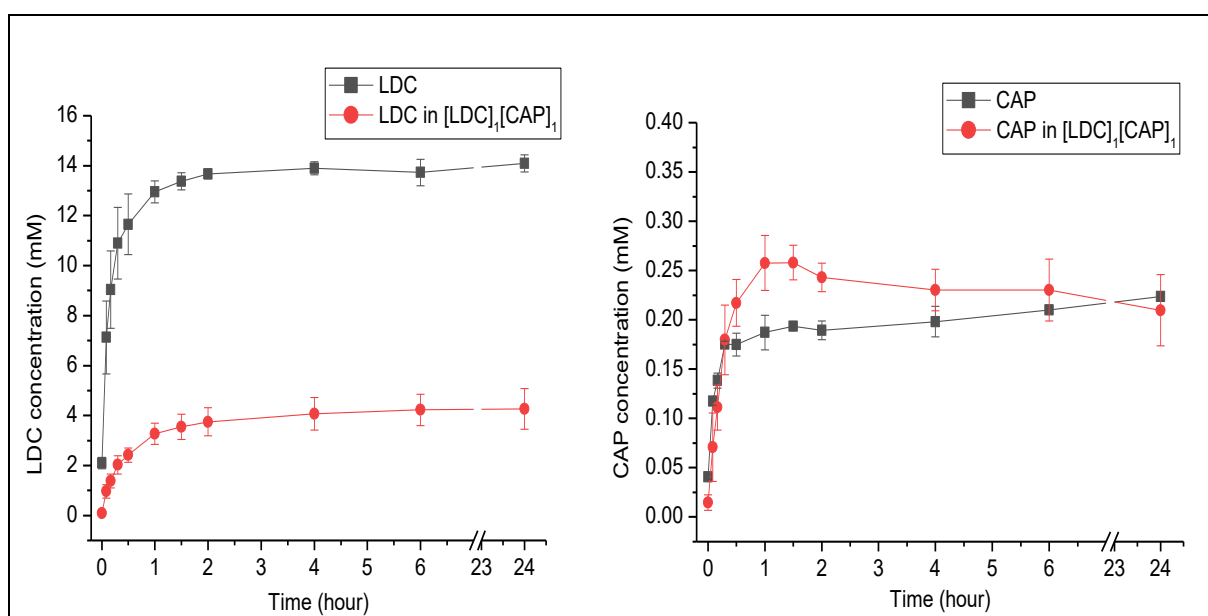
Figure 40- Saturated solubility study of LDC, CAP and [LDC]₁[CAP]₁ in water, at 37 °C. Results are expressed in mean (± SD) of 3 experiments. The LDC and CAP solubility was plotted in a different panel due to differences in scale. The average pH of the water solutions at the end of the study were 9.22 for LDC, 5.80 for CAP and 8.27 for [LDC]₁[CAP]₁ formulation.

[LDC]₁[CAP]₁ presented as a homogenous liquid not miscible in water, and the vial showed no sign of precipitation after the experiment. Additionally, the remaining formulation was characterized by PXRD demonstrating a liquid/amorphous pattern with no signs of crystallization. This may indicate that the interactions established between LDC and CAP upon [LDC]₁[CAP]₁ formation were not fully

disrupted in an aqueous solution. This result is in agreement with the DVS analysis that has shown excellent stability of the formulation upon extreme relative humidity conditions (90%).

Interestingly, upon addition of powdered CAP to a suspension of LDC in water, $[LDC]_1[CAP]_1$ formed spontaneously, showing a great affinity of CAP to LDC. This result indicates that the equimolar mixture of the two components is truly stable and suitable for further development.

A very soluble formulation would be suitable for parental delivery, while a hydrophobic DEM could be exploited to achieve better skin permeation. The lower ionicity of this system is highly desirable for topical applications, as the DEM may cross the membrane barrier more easily than the more ionized compounds (Cruz-Cabeza, 2012).

The lidocaine patch (Lidoderm) and capsaicin products are the only topical treatment available for postherpetic neuralgia, a severe chronic neuropathic pain condition (Shrestha and Chen, 2018; Suzuki et al., 2019). Accordingly, a therapy that combines the effects of lidocaine and capsaicin could possibly have synergistic effects of the drugs. Additionally, this system could reduce the CAP burning sensation and increase LDC potency in a topical delivery approach.

Whilst this study did not investigate the permeation of the mixture (LDC:CAP), the literature supports that DEM promotes better skin delivery (Caparica, 2017; Duarte et al., 2017; H. Wang et al., 2014). Further investigation should be performed to incorporate $[LDC]_1[CAP]_1$ into a final product and assess the drugs permeation into the skin.

7.   CONCLUSIONS

In the first part of this thesis, we developed, characterized, and evaluated a parental formulation of HP-β-CD-CAP. Initially, methods for capsaicin quantification, by UV/Vis and HPLC, were determined. Then, the HP-β-CD-CAP complex was characterized in solution to establish an optimized preparation method. In order to achieve full complexation, the HP-β-CD-CAP solution was prepared under magnetic stirring (350 rpm) for at least 20 hours, at room temperature. A phase solubility study showed that complexation was able to increase the apparent solubility of CAP up to 20 times, with a strong stability constant between HP-β-CD and CAP (K_s = 2400 ± 221 M^{-1}). The Complexation efficiency study established that each mole of capsaicin requires 4.2 moles of HP-β-CD to produce a soluble formulation (4:1 HP-β-CD-CAP). Following, ITC technique confirmed the 1:1 stoichiometry of HP-β-CD-CAP, and high association constant (K_c = 5100 M^{-1}).

After that, the collapse temperature (-12 °C) of the 4:1 HP-β-CD-CAP sample was determined, to set the freeze-drying cycle. The freeze-dried product demonstrated to be stable for at least 12 months.

The solid 4:1 HP-β-CD-CAP sample was characterized by DSC and X-ray diffraction, evidencing the complexation between CAP and HP-β-CD. Finally, ^{1}H-NMR measurements with the ressuspensed freeze-dried sample: i) confirmed the formation of an inclusion complex through the interaction of the aliphatic portion of capsaicin with the inner hydrogens of CD cavity, and ii) indicated that a large fraction of capsaicin (88%) was complexed with HP-β-CD, with high affinity constant (K = 1079 M^{-1}), corroborating the phase solubility and ITC data.

In vitro tests demonstrated the sustained release of CAP by the 4:1 HP-β-CD-CAP formulation. *In vivo* experiments showed that 0.05% HP-β-CD-CAP + 2% MVC significantly diminished motor blockade, after regional anesthesia in mice. Moreover, the formulation was two times more efficient that 2% mepivacaine to anesthetize inflamed tissue.

In the second part, it was reported a new liquid formulation, combining a local anesthetic agent and capsaicin, by a straightforward synthesis. Based on the screening studies, lidocaine was selected as the most promising local anesthetic compound to interact with CAP. The thermodynamic properties of the LDC:CAP mixture were explored; phase diagrams revealed that at room temperature a liquid

formulation was formed, at equimolar concentration of LDC and CAP. The experimental data followed the theoretical Schröder–Van Laar predictions, and some mixtures did not crystallize upon two cycles of heating.

Low temperature PXRD revealed that LDC:CAP mixtures had the same crystalline pattern as the pure compounds. Besides, $[LDC]_1[CAP]_1$ showed a liquid/amorphous pattern above the melting temperature. LDC:CAP mixtures were analyzed by FTIR and the carbonyl stretching bands of the amide group band gave indication of intermolecular interaction (hydrogen bond) between the compounds. When $[LDC]_1[CAP]_1$ samples (in chloroform) were analyzed by ^1H- and ^{13}C-NMR spectroscopy, chemical shits reflected the hydrogen bonds formation. Similar results were found on neat samples, and confirmed that a strong hydrogen bond, between CAP (carbonyl) and LDC (amide) groups, was responsible for the reduced melting temperature that characterizes the formed $([LDC]_1[CAP]_1)$ DEM.

The stability of $[LDC]_1[CAP]_1$ composition was tested by vapor sorption that revealed a highly stable formulation that did not crystallize, and sorbed only low humidity (c.a. 1.8%). The solubility study showed that the hydrophobic binary mixture has strong interaction that might not be disrupted even in an aqueous medium. Since DEM usually show a good permeation through the skin, $[LDC]_1[CAP]_1$ can be a promising system to be applied in topical anesthesia.

Both part 1 and 2 of this thesis, successfully investigated the combination between LA and CAP. In Part 1 of this project, the solubility of CAP was increased by complexation with HP-β-CD and greatly improved infiltration anesthesia of MVC, in inflamed tissue. Further studies should be performed to address the toxicity of this novel parental formulation. Also, this work described for the first time the combination of CAP and LA as a strategic to overcome LA failure upon inflammation. In Part 2, it was performed a pre-formulation study of a DEM that combines the hydrophobic drugs LDC and CAP into liquefied delivery system that can be a promising new topical formulation. In the future, this DEM should be formulated in a solution, emulsion, spray, or be embedded in a patch. Then, more research is required to determine the efficiency of this topical formulation as an alternative treatment for neuropathic pain.

8. REFERENCES

Abbott, A.P., Capper, G., Davies, D.L., Rasheed, R.K., Tambyrajah, V., 2003. Novel solvent properties of choline chloride/urea mixtures. Chem. Commun. 70–71. https://doi.org/10.1039/b210714g

Agência Nacional de Vigilância Sanitária (Brazil), Fundação Oswaldo Cruz, 2010. Farmacopeia brasileira. Agência Nacional de Vigilância Sanitária : Fundação Oswaldo Cruz, Brasília.

Agrawal, U., Gupta, M., Vyas, S.P., 2015. Capsaicin delivery into the skin with lipidic nanoparticles for the treatment of psoriasis. Artif. Cells Nanomedicine Biotechnol. 43, 33–39. https://doi.org/10.3109/21691401.2013.832683

Allen, L.V., Alsen, H.C., 2013. Introduction to Drugs, Drug Dosage Form, and Drug Delivery System, in: Ansel's Pharmaceutical Dosage Forms and Drug Delivery Systems. Wolters Kluwer Health, Philadelphia, pp. 2–76.

Anand, P., Bley, K., 2011. Topical capsaicin for pain management: therapeutic potential and mechanisms of action of the new high-concentration capsaicin 8% patch. Br. J. Anaesth. 107, 490–502. https://doi.org/10.1093/bja/aer260

Aulton, M.E., Taylor, K.M.G., 2013. Biopharmaceutical principles of drug delivery, in: Aulton's Pharmaceutics: The Design and Manufacture of Medicines. Elsevier Health Sciences, London, pp. 292–355.

Avula, S.G., Alexander, K., Riga, A., 2010. Predicting eutectic behavior of drugs and excipients by unique calculations. J. Therm. Anal. Calorim. 99, 655–658. https://doi.org/10.1007/s10973-009-0595-1

Badawi, H.M., Förner, W., Ali, S.A., 2016. The molecular structure and vibrational, 1H and 13C NMR spectra of lidocaine hydrochloride monohydrate. Spectrochim. Acta. A. Mol. Biomol. Spectrosc. 152, 92–100. https://doi.org/10.1016/j.saa.2015.07.060

Bagnéris, C., DeCaen, P.G., Naylor, C.E., Pryde, D.C., Nobeli, I., Clapham, D.E., Wallace, B.A., 2014. Prokaryotic NavMs channel as a structural and functional model for eukaryotic sodium channel antagonism. Proc. Natl. Acad. Sci. 111, 8428–8433. https://doi.org/10.1073/pnas.1406855111

Balk, A., Holzgrabe, U., Meinel, L., 2015. 'Pro et contra' ionic liquid drugs – Challenges and opportunities for pharmaceutical translation. Eur. J. Pharm. Biopharm. 94, 291–304. https://doi.org/10.1016/j.ejpb.2015.05.027

Barash, P., Cullen, B.F., Stoelting, R.K., Cahalan, M., Stock, C., Ortega, R., 2013. Anesthetic agents, adjuvants, and drug interaction, in: Handbook of Clinical Anesthesia. Wolters Kluwer Health, Philadelphia, pp. 227–310.

Becker, D.E., Reed, K.L., 2012. Local anesthetics: review of pharmacological considerations. Anesth. Prog. 59, 90–102.

Bertaut, E., Landy, D., 2014. Improving ITC studies of cyclodextrin inclusion compounds by global analysis of conventional and non-conventional experiments. Beilstein J. Org. Chem. 10, 2630–2641. https://doi.org/10.3762/bjoc.10.275

Bica, K., Shamshina, J., Hough, W.L., MacFarlane, D.R., Rogers, R.D., 2011. Liquid forms of pharmaceutical co-crystals: exploring the boundaries of salt formation. Chem. Commun. 47, 2267–2269. https://doi.org/10.1039/C0CC04485G

Binshtok, A.M., Bean, B.P., Woolf, C.J., 2007. Inhibition of nociceptors by TRPV1-mediated entry of impermeant sodium channel blockers. Nature 449, 607–610. https://doi.org/10.1038/nature06191

Binshtok, A.M., Gerner, P., Oh, S.B., Puopolo, M., Suzuki, S., Roberson, D.P., Herbert, T., Wang, C.-F., Kim, D., Chung, G., Mitani, A.A., Wang, G.K., Bean, B.P., Woolf, C.J., 2009. Coapplication of Lidocaine and the Permanently Charged Sodium Channel Blocker QX-314 Produces a Long-lasting Nociceptive Blockade in Rodents: Anesthesiology 111, 127–137. https://doi.org/10.1097/ALN.0b013e3181a915e7

Bouchemal, K., 2008. New challenges for pharmaceutical formulations and drug delivery systems characterization using isothermal titration calorimetry 13, 960–972. https://doi.org/10.1016/j.drudis.2008.06.004

Bouchemal, K., Mazzaferro, S., 2012. How to conduct and interpret ITC experiments accurately for cyclodextrin–guest interactions. Drug Discov. Today 17, 623–629. https://doi.org/10.1016/j.drudis.2012.01.023

Braga, D., Chelazzi, L., Grepioni, F., Dichiarante, E., Chierotti, M.R., Gobetto, R., 2013. Molecular Salts of Anesthetic Lidocaine with Dicarboxylic Acids: Solid-State Properties and a Combined Structural and Spectroscopic Study. Cryst. Growth Des. 13, 2564–2572. https://doi.org/10.1021/cg400331h

Braga, M.A., Martini, M.F., Pickholz, M., Yokaichiya, F., Franco, M.K.D., Cabeça, L.F., Guilherme, V.A., Silva, C.M.G., Limia, C.E.G., de Paula, E., 2016. Clonidine complexation with hydroxypropyl-beta-cyclodextrin: From physico-chemical characterization to in vivo adjuvant effect in local anesthesia. J. Pharm. Biomed. Anal. 119, 27–36. https://doi.org/10.1016/j.jpba.2015.11.015

Brewster, M.E., Loftsson, T., 2007. Cyclodextrins as pharmaceutical solubilizers. Adv. Drug Deliv. Rev. 59, 645–666. https://doi.org/10.1016/j.addr.2007.05.012

Broberg, B.F.J., Evers, H.C.A., 1985. Topical application and method for obtaning local anesthesia. US4529601A.

Brodin, A., Nyqvist-Mayer, A., Wadsten, T., Forslund, B., Broberg, F., 1984. Phase Diagram and Aqueous Solubility of the Lidocaine-Prilocaine Binary System. J. Pharm. Sci. 73, 481–484. https://doi.org/10.1002/jps.2600730413

Brown, W.H., Iverson, B.L., Anslyn, E.V., Foote, C.S., 2014. Reaction Mechanisms, in: Organic Chemistry. Wadsworth Cengage, Belmont, pp. 491–556.

Cabeça, L.F., Pickholz, M., de Paula, E., Marsaioli, A.J., 2009. Liposome−Prilocaine Interaction Mapping Evaluated through STD NMR and Molecular Dynamics Simulations. J. Phys. Chem. B 113, 2365–2370. https://doi.org/10.1021/jp8069496

Caparica, R., 2017. Applicability of Ionic Liquids in Topical Drug Delivery Systems: A Mini Review. J. Pharmacol. Clin. Res. 4, 1–7. https://doi.org/10.19080/JPCR.2018.04.555649

Casale, R., Symeonidou, Z., Bartolo, M., 2017. Topical Treatments for Localized Neuropathic Pain. Curr. Pain Headache Rep. 21, 15–24. https://doi.org/10.1007/s11916-017-0615-y

Caterina, M.J., Schumacher, M.A., Tominaga, M., Rosen, T.A., Levine, J.D., Julius, D., 1997. The capsaicin receptor: a heat-activated ion channel in the pain pathway. Nature 389, 816–824.

Challa, R., Ahuja, A., Ali, J., Khar, R.K., 2005. Cyclodextrins in drug delivery: An updated review. AAPS PharmSciTech 6, 329–357. https://doi.org/10.1208/pt060243

Cherukuvada, S., Nangia, A., 2014. Eutectics as improved pharmaceutical materials: design, properties and characterization. Chem Commun 50, 906–923. https://doi.org/10.1039/C3CC47521B

Clapham, D.E., Runnels, L.W., Strubing, C., 2001. The trp ion channel family. Nat Rev Neurosci 2, 387–396. https://doi.org/10.1038/35077544

Costanzo, M.T., Yost, R.A., Davenport, P.W., 2014. Standardized method for solubility and storage of capsaicin-based solutions for cough induction. Cough 10, 1–8. https://doi.org/10.1186/1745-9974-10-6

Covino, B.G., Giddon, D.B., 1981. Pharmacology of local anesthetic agents. J. Dent. Res. 60, 1454–1459. https://doi.org/10.1177/00220345810600080903

Covino, B.G., Vassallo, H.G., 1976. Local Anesthetics: Mechanics of Action and Clinical Use, The Scientific Basis of Clinical Anesthesia Series. Grune & Stratton.

Cruz-Cabeza, A.J., 2012. Acid–base crystalline complexes and the pKa rule. Cryst Eng Comm 14, 6362–6365. https://doi.org/10.1039/c2ce26055g

Cui, L., Zhang, Z.-H., Sun, E., Jia, X.-B., 2012. Effect of β-Cyclodextrin Complexation on Solubility and Enzymatic Conversion of Naringin. Int. J. Mol. Sci. 13, 14251–14261. https://doi.org/10.3390/ijms131114251

Daneshkazemi, A., Abrisham, S.M., Daneshkazemi, P., Davoudi, A., 2016. The efficacy of eutectic mixture of local anesthetics as a topical anesthetic agent used for dental procedures: A brief review. Anesth. Essays Res. 10, 383–387. https://doi.org/10.4103/0259-1162.172342

Davis, M.E., Brewster, M.E., 2004. Cyclodextrin-based pharmaceutics: past, present and future. Nat. Rev. Drug Discov. 3, 1023–1035. https://doi.org/10.1038/nrd1576

de Araújo, D.R., Cereda, C.M., Brunetto, G.B., Pinto, L.M., Santana, M.H.A., de Paula, E., 2004. Encapsulation of mepivacaine prolongs the analgesia provided by sciatic nerve blockade in mice. Can. J. Anesth. 51, 566–572.

de Araújo, D.R., de Paula, E., Fraceto, L.F., 2008. Anestésicos locais: interação com membranas biológicas e com o canal de sódio voltagem-dependente. Quím. Nova 1775–1783.

de León-Casasola, O.A., Mayoral, V., 2016. The topical 5% lidocaine medicated plaster in localized neuropathic pain: a reappraisal of the clinical evidence. J. Pain Res. 9, 67–79. https://doi.org/10.2147/JPR.S99231

de Paula, E., Cereda, C., Tofoli, G.R., Franz-Montan, M., Fraceto, L.F., de Araujo, D.R., 2010a. Drug delivery systems for local anesthetics. Recent Pat. Drug Deliv. Formul. 4, 23–34.

de Paula, E., Cereda, C.M., Fraceto, L.F., de Araújo, D.R., Franz-Montan, M., Tofoli, G.R., Ranali, J., Volpato, M.C., Groppo, F.C., 2012. Micro and nanosystems for delivering local anesthetics. Expert Opin. Drug Deliv. 9, 1505–1524. https://doi.org/10.1517/17425247.2012.738664

de Paula, E., de Araújo, D.R., Fraceto, L.F., 2010b. Nuclear magnetic resonance spectroscopy tools for the physicochemical characterization of cyclodextrins inclusion complexes. In: Cyclodextrins: chemistry and physics. Transworld Research Network, Kerala.

de Paula, E., Schreier, S., 1996. Molecular and physicochemical aspects of local anesthetic-membrane interaction. Braz. J. Med. Biol. Res. 29, 877–894.

de Paula, E., Schreier, S., Jarrell, H.C., Fraceto, L.F., 2008. Preferential location of lidocaine and etidocaine in lecithin bilayers as determined by EPR, fluorescence and 2H NMR. Biophys. Chem. 132, 47–54. https://doi.org/10.1016/j.bpc.2007.10.004

Del Valle, E.M.M., 2004. Cyclodextrins and their uses: a review. Process Biochem. 39, 1033–1046. https://doi.org/10.1016/S0032-9592(03)00258-9

Do, T.T., Van Hooghten, R., Van den Mooter, G., 2017. A study of the aggregation of cyclodextrins: Determination of the critical aggregation concentration, size of aggregates and thermodynamics using isodesmic and K 2 –K models. Int. J. Pharm. 521, 318–326. https://doi.org/10.1016/j.ijpharm.2017.02.037

Dollo, G., Le Corre, P., Chevanne, F., Le Verge, R., 1996. Inclusion complexation of amide-typed local anaesthetics with β-cyclodextrin and its derivatives. ii. evaluation of affinity constants and in vitro transfer rate constants. Int. J. Pharm. 136, 165–174.

Duarte, A.R.C., Ferreira, A.S.D., Barreiros, S., Cabrita, E., Reis, R.L., Paiva, A., 2017. A comparison between pure active pharmaceutical ingredients and therapeutic deep eutectic solvents: Solubility and permeability studies. Eur. J. Pharm. Biopharm. 114, 296–304. https://doi.org/10.1016/j.ejpb.2017.02.003

Duchêne, D., 2011. Cyclodextrins and Their Inclusion Complexes, in: Cyclodextrins in Pharmaceutics, Cosmetics, and Biomedicine. John Wiley & Sons, Inc., pp. 1–18. https://doi.org/10.1002/9780470926819.ch1

Duchêne, D., 1987. Cyclodextrins and Their Industrial Uses. Editions de Santé, Paris.

Dunbar, D., Reader, A., Nist, R., Beck, M., Meyers, W.J., 1996. Anesthetic efficacy of the intraosseous injection after an inferior alveolar nerve block. J. Endod. 22, 481–486. https://doi.org/10.1016/S0099-2399(96)80083-5

Dworkin, R.H., O'Connor, A.B., Audette, J., Baron, R., Gourlay, G.K., Haanpää, M.L., Kent, J.L., Krane, E.J., LeBel, A.A., Levy, R.M., Mackey, S.C., Mayer, J., Miaskowski, C., Raja, S.N., Rice, A.S.C., Schmader, K.E., Stacey, B., Stanos, S., Treede, R.-D., Turk, D.C., Walco, G.A., Wells, C.D., 2010. Recommendations for the Pharmacological Management of Neuropathic Pain: An Overview and Literature Update. Mayo Clin. Proc. 85, 3–14. https://doi.org/10.4065/mcp.2009.0649

Egorova, K.S., Gordeev, E.G., Ananikov, V.P., 2017. Biological Activity of Ionic Liquids and Their Application in Pharmaceutics and Medicine. Chem. Rev. 117, 7132–7189. https://doi.org/10.1021/acs.chemrev.6b00562

Farah, Louis., Giles, George., Wilson, Donna., Ohno, Agnes., Scott, R.M., 1979. Hydrogen bonding interactions of aliphatic amines with ortho-substituted phenols. J. Phys. Chem. 83, 2455–2458. https://doi.org/10.1021/j100482a007

Fattori, V., Hohmann, M., Rossaneis, A., Pinho-Ribeiro, F., Verri, W., 2016. Capsaicin: Current Understanding of Its Mechanisms and Therapy of Pain and Other Pre-Clinical and Clinical Uses. Molecules 21, 1–33. https://doi.org/10.3390/molecules21070844

Fehrenbacher, J.C., Vasko, M.R., Duarte, D.B., 2012. Models of Inflammation: Carrageenan- or Complete Freund's Adjuvant-Induced Edema and Hypersensitivity in the Rat, in: Current Protocols in Pharmacology. John Wiley & Sons, Inc., Hoboken. https://doi.org/10.1002/0471141755.ph0504s56

Felton, L.A., Popescu, C., Wiley, C., Esposito, E.X., Lefevre, P., Hopfinger, A.J., 2014. Experimental and Computational Studies of Physicochemical Properties Influence NSAID-Cyclodextrin Complexation. AAPS Pharm Sci Tech 15, 872–881. https://doi.org/10.1208/s12249-014-0110-2

Fletcher, D., Le Corre, P., Guilbaud, G., Le Verge, R., 1997. Antinociceptive effect of bupivacaine encapsulated in poly (D, L)-lactide-co-glycolide microspheres in the acute inflammatory pain model of carrageenin-injected rats. Anesth. Analg. 84, 90–94.

Fraceto, L.F., de Matos Alves Pinto, L., Franzoni, L., Albert Carmo Braga, A., Spisni, A., Schreier, S., de Paula, E., 2002. Spectroscopic evidence for a preferential

location of lidocaine inside phospholipid bilayers. Biophys. Chem. 99, 229–243. https://doi.org/10.1016/S0301-4622(02)00202-8

Fraceto, L.F., Spisni, A., Schreier, S., de Paula, E., 2005. Differential effects of uncharged aminoamide local anesthetics on phospholipid bilayers, as monitored by 1H-NMR measurements. Biophys. Chem. 115, 11–18. https://doi.org/10.1016/j.bpc.2004.12.003

Franks, F., 1998. Freeze-drying of bioproducts: putting principles into practice. Eur. J. Pharm. Biopharm. 45, 221–229.

Franz, T.J., 1975. Percutaneous absorption on the relevance of in vitro data. J Investig Dermatol 64, 190–195.

Gantenbein, M., Abat, C., Attolini, L., Pisano, P., Emperaire, N., Bruguerolle, B., 1997. Ketamine effects on bupivacaine local anaesthetic activity and pharmacokinetics of bupivacaine in mice. Life Sci. 61, 2027–2033.

Gellman, S.H., Dado, G.P., Liang, G.B., Adams, B.R., 1991. Conformation-directing effects of a single intramolecular amide-amide hydrogen bond: variable-temperature NMR and IR studies on a homologous diamide series. J. Am. Chem. Soc. 113, 1164–1173. https://doi.org/10.1021/ja00004a016

Gerner, P., Binshtok, A.M., Wang, C.-F., Hevelone, N.D., Bean, B.P., Woolf, C.J., Wang, G.K., 2008. Capsaicin Combined with Local Anesthetics Preferentially Prolongs Sensory/Nociceptive Block in Rat Sciatic Nerve: Anesthesiology 109, 872–878. https://doi.org/10.1097/ALN.0b013e31818958f7

Gerothanassis, I.P., Troganis, A., Exarchou, V., Barbarossou, K., 2002. Nuclear Magnetic Resonance Spectroscopy: Basic Principles and Phenomena, ande their applications to Chemistry, Biology and Medicine. Chem Educ Res Pr. 3, 229–252. https://doi.org/10.1039/B2RP90018A

Giordano, F., Novak, C., Moyano, J.R., 2001. Thermal analysis of cyclodextrins and their inclusion compounds. Thermochim. Acta 380, 123–151. http://dx.doi.org/10.1016/S0040-6031(01)00665-7

Gould, S., Scott, R.C., 2005. 2-Hydroxypropyl-β-cyclodextrin (HP-β-CD): A toxicology review. Food Chem. Toxicol. 43, 1451–1459. https://doi.org/10.1016/j.fct.2005.03.007

Gounarides, J.S., Chen, A., Shapiro, M.J., 1999. Nuclear magnetic resonance chromatography: applications of pulse field gradient diffusion NMR to mixture analysis and ligand–receptor interactions. J. Chromatogr. B. Biomed. Sci. App. 725, 79–90. http://dx.doi.org/10.1016/S0378-4347(98)00512-X

Grant, G.J., Lax, J., Susser, L., Zakowski, M., Weissman, E., 1997. Wound infiltration with liposomal bupivacaine prolongs analgesia in rats. Acta Anaesthesiol. Scand. 41, 204–207.

Grichnik, K., Ferrante, F., 1991. The difference between acute and chronic pain. Mt. Sinai J. Med. N. Y. 58, 217—220.

Hayman, M., Kam, P.C.A., 2008. Capsaicin: A review of its pharmacology and clinical applications. Curr. Anaesth. Crit. Care 19, 338–343. https://doi.org/10.1016/j.cacc.2008.07.003

Higuchi, T., Connors, K.A., 1965. Phase-solubility techniques. Adv. Anal. Chem. Instrum. 4, 117–210.

Holdgate, G.A., Ward, W.H.J., 2005. Measurements of binding thermodynamics in drug discovery. Drug Discov. Today 10, 1543–1550. http://dx.doi.org/10.1016/S1359-6446(05)03610-X

Hough, W.L., Smiglak, M., Rodriguez, H., Swatloski, R.P., Spear, S.K., Daly, D.T., Pernak, J., Grisel, J.E., Carliss, R.D., Soutullo, M.D., Davis, Jr., J.H., Rogers,

R.D., 2007. The third evolution of ionic liquids: active pharmaceutical ingredients. New J. Chem. 31, 1429–1436. https://doi.org/10.1039/b706677p

Hung, Y.-C., 2011. Method and composition for prolonging analgesic effect of local anesthetic. US8779003B2.

ICH Q1A(R2), 2003. Stability testing of new drug substances and products. Int. Conf. Harmon. Tech. Requir. Regist. Pharm. Hum.

Ivashenko, A.V., Titov, V.V., Kovshev, E.I., 1976. Liquid Crystalline Compounds: III On Applicability of Schröder-Van Laar Equations to Liquid Crystals Mixtures. Mol. Cryst. Liq. Cryst. 33, 195–200. https://doi.org/10.1080/15421407608084295

Jensen, T.S., Høye, K., Fricová, J., Vanelderen, P., Ernault, E., Siciliano, T., Marques, S., 2014. Tolerability of the capsaicin 8% patch following pretreatment with lidocaine or tramadol in patients with peripheral neuropathic pain: A multicentre, randomized, assessor-blinded study: Capsaicin patch tolerability after lidocaine/tramadol. Eur. J. Pain 18, 1240–1247. https://doi.org/10.1002/j.1532-2149.2014.00479.x

Jensen, T.S., Madsen, C.S., Finnerup, N.B., 2009. Pharmacology and treatment of neuropathic pains: Curr. Opin. Neurol. 22, 467–474. https://doi.org/10.1097/WCO.0b013e3283311e13

Kelley, S.P., Narita, A., Holbrey, J.D., Green, K.D., Reichert, W.M., Rogers, R.D., 2013. Understanding the Effects of Ionicity in Salts, Solvates, Co-Crystals, Ionic Co-Crystals, and Ionic Liquids, Rather than Nomenclature, Is Critical to Understanding Their Behavior. Cryst. Growth Des. 13, 965–975. https://doi.org/10.1021/cg4000439

Kim, H.Y., Kim, K., Li, H.Y., Chung, G., Park, C.-K., Kim, J.S., Jung, S.J., Lee, M.K., Ahn, D.K., Hwang, S.J., Kang, Y., Binshtok, A.M., Bean, B.P., Woolf, C.J., Oh, S.B., 2010. Selectively targeting pain in the trigeminal system: Pain 150, 29–40. https://doi.org/10.1016/j.pain.2010.02.016

Kissin, I., 2008. Vanilloid-induced conduction analgesia: selective, dose-dependent, long-lasting, with a low level of potential neurotoxicity. Anesth. Analg. 107, 271–281.

Knotkova, H., Pappagallo, M., Szallasi, A., 2008. Capsaicin (TRPV1 Agonist) therapy for pain relief: farewell or revival? Clin. J. Pain 24, 142–154.

Kobata, K., Todo, T., Yazawa, S., Iwai, K., Watanabe, T., 1998. Novel Capsaicinoid-like Substances, Capsiate and Dihydrocapsiate, from the Fruits of a Nonpungent Cultivar, CH-19 Sweet, of Pepper. J. Agric. Food Chem. 46, 1695–1697. https://doi.org/10.1021/jf980135c

Kurkov, S.V., Loftsson, T., 2013. Cyclodextrins. Int. J. Pharm. 453, 167–180. https://doi.org/10.1016/j.ijpharm.2012.06.055

Lagan, G., McLure, H.A., 2004. Review of local anaesthetic agents. Curr. Anaesth. Crit. Care 15, 247–254. https://doi.org/10.1016/j.cacc.2004.08.007

Leszczynska, K., Kau, S.T., 1992. A sciatic nerve blockade method to differentiate drug-induced local anesthesia from neuromuscular blockade in mice. J. Pharmacol. Toxicol. Methods 27, 85–93. http://dx.doi.org/10.1016/1056-8719(92)90026-W

Loftsson, T., Brewster, M.E., 2012. Cyclodextrins as Functional Excipients: Methods to Enhance Complexation Efficiency. J. Pharm. Sci. 101, 3019–3032. https://doi.org/10.1002/jps.23077

Loftsson, T., Brewster, M.E., 2010. Pharmaceutical applications of cyclodextrins: basic science and product development: Pharmaceutical applications of

cyclodextrins. J. Pharm. Pharmacol. 62, 1607–1621. https://doi.org/10.1111/j.2042-7158.2010.01030.x

Loftsson, T., Duchene, D., 2007. Cyclodextrins and their pharmaceutical applications. Int. J. Pharm. 329, 1–11. https://doi.org/10.1016/j.ijpharm.2006.10.044

Loftsson, T., Hreinsdóttir, D., Másson, M., 2005. Evaluation of cyclodextrin solubilization of drugs. Int. J. Pharm. 302, 18–28. https://doi.org/10.1016/j.ijpharm.2005.05.042

Luduena, F.P., Hoppe, J.O., Coulston, F., Drobeck, H.P., 1960. The pharmacology and toxicology of mepivacaine, a new local anesthetic. Toxicol. Appl. Pharmacol. 2, 295–315. https://doi.org/10.1016/0041-008X(60)90059-4

Ma, C., Laaksonen, A., Liu, C., Lu, X., Ji, X., 2018. The peculiar effect of water on ionic liquids and deep eutectic solvents. Chem. Soc. Rev. 47, 8685–8720. https://doi.org/10.1039/C8CS00325D

Malamed, S.F., 2014. Handbook of Local Anesthesia, 6th ed. Elsevier Health Sciences, St. Louis.

Martins, I.C.B., Oliveira, M.C., Diogo, H.P., Branco, L.C., Duarte, M.T., 2017. MechanoAPI-ILs: Pharmaceutical Ionic Liquids Obtained through Mechanochemical Synthesis. ChemSusChem 10, 1360–1363. https://doi.org/10.1002/cssc.201700153

Martins, M.A.R., Pinho, S.P., Coutinho, J.A.P., 2018. Insights into the Nature of Eutectic and Deep Eutectic Mixtures. J. Solut. Chem. 1–21. https://doi.org/10.1007/s10953-018-0793-1

McCormack, P.L., 2010. Capsaicin Dermal Patch: In Non-Diabetic Peripheral Neuropathic Pain. Drugs 70, 1831–1842. https://doi.org/10.2165/11206050-000000000-00000

McLure, H.A., Rubin, A.P., 2005. Review of local anaesthetic agents. Minerva Anestesiol 71, 59–74.

Meister, E., Šaši, S., Gieseler, H., 2009. Freeze-Dry Microscopy: Impact of Nucleation Temperature and Excipient Concentration on Collapse Temperature Data. AAPS PharmSciTech 10, 582–588. https://doi.org/10.1208/s12249-009-9245-y

Mense, S., 1983. Basic neurobiologic mechanisms of pain and analgesia. Antipyretic Analg. Ther. 75, 4–14. https://doi.org/10.1016/0002-9343(83)90226-7

Messner, M., Kurkov, S.V., Jansook, P., Loftsson, T., 2010. Self-assembled cyclodextrin aggregates and nanoparticles. Int. J. Pharm. 387, 199–208. http://dx.doi.org/10.1016/j.ijpharm.2009.11.035

Miller, R.D., 2010. Local Anesthetics, in: Anesthesia. Elsevier, San Francisco.

Miwa, Y., Hamamoto, H., Ishida, T., 2016. Lidocaine self-sacrificially improves the skin permeation of the acidic and poorly water-soluble drug etodolac via its transformation into an ionic liquid. Eur. J. Pharm. Biopharm. 102, 92–100. https://doi.org/10.1016/j.ejpb.2016.03.003

Moore, P.A., Hersh, E.V., 2010. Local Anesthetics: Pharmacology and Toxicity. Dent. Clin. North Am. 54, 587–599. https://doi.org/10.1016/j.cden.2010.06.015

Moreira, D.N., Fresno, N., Pérez-Fernández, R., Frizzo, C.P., Goya, P., Marco, C., Martins, M.A.P., Elguero, J., 2015. Brønsted acid–base pairs of drugs as dual ionic liquids: NMR ionicity studies. Tetrahedron 71, 676–685. https://doi.org/10.1016/j.tet.2014.12.003

Morris, K.F., Johnson, C.S., 1992. Diffusion-ordered two-dimensional nuclear magnetic resonance spectroscopy. J. Am. Chem. Soc. 114, 3139–3141. https://doi.org/10.1021/ja00034a071

Mura, P., 2015. Analytical techniques for characterization of cyclodextrin complexes in the solid state: A review. J. Pharm. Biomed. Anal. 113, 226–238. https://doi.org/10.1016/j.jpba.2015.01.058

Mura, P., 2014. Analytical techniques for characterization of cyclodextrin complexes in aqueous solution: A review. J. Pharm. Biomed. Anal. 101, 238–250. https://doi.org/10.1016/j.jpba.2014.02.022

Mura, P., Maestrelli, F., Cirri, M., Furlanetto, S., Pinzauti, S., 2003. Differential scanning calorimetry as an analytical tool in the study of drug-cyclodextrin interactions. J. Therm. Anal. Calorim. 73, 635–646. https://doi.org/10.1023/A:1025494500283

Murnion, B., 2018. Neuropathic pain: current definition and review of drug treatment. Aust. Prescr. 41, 60–63. https://doi.org/10.18773/austprescr.2018.022

Narahashi, T., Frazier, D., Yamada, M., 1970. The site of action and active form of local anesthetics. I. Theory and pH experiments with tertiary compounds. J. Pharmacol. Exp. Ther. 171, 32–44.

Oetjen, G.W., 2008. Freeze-Drying. Wiley, Hoboken.

O'Neill, J., Brock, C., Olesen, A.E., Andresen, T., Nilsson, M., Dickenson, A.H., 2012. Unravelling the Mystery of Capsaicin: A Tool to Understand and Treat Pain. Pharmacol. Rev. 64, 939–971. https://doi.org/10.1124/pr.112.006163

Palazzo, E., Luongo, L., de Novellis, V., Rossi, F., Marabese, I., Maione, S., 2012. Transient receptor potential vanilloid type 1 and pain development. Curr. Opin. Pharmacol. 12, 9–17. https://doi.org/10.1016/j.coph.2011.10.022

Patel, S.M., Doen, T., Pikal, M.J., 2010. Determination of End Point of Primary Drying in Freeze-Drying Process Control. AAPS PharmSciTech 11, 73–84. https://doi.org/10.1208/s12249-009-9362-7

Patel, S.M., Nail, S.L., Pikal, M.J., Geidobler, R., Winter, G., Hawe, A., Davagnino, J., Rambhatla Gupta, S., 2017. Lyophilized Drug Product Cake Appearance: What Is Acceptable? J. Pharm. Sci. 106, 1706–1721. https://doi.org/10.1016/j.xphs.2017.03.014

Pessine, F.B., Calderini, A., Alexandrino, G.L., 2012. Review: cyclodextrin inclusion complexes probed by NMR techniques, in: NMR Techniques, Magnetic Resonance Spectroscopy. INTECH.

Ph. Eur., 2010. Characters Section. Eur. Dir. Qual. Med. Healthc., Section 5.

Pikal, M.J., 1994. Freeze-Drying of Proteins, in: Formulation and Delivery of Proteins and Peptides. pp. 120–133. https://doi.org/10.1021/bk-1994-0567.ch008

Pîrnău, A., Mic, M., Bogdan, M., Turcu, I., 2014. Characterization of β-cyclodextrin inclusion complex with procaine hydrochloride by 1H NMR and ITC. J. Incl. Phenom. Macrocycl. Chem. 79, 283–289. https://doi.org/10.1007/s10847-013-0350-x

Powell, M.F., 1986. Lidocaine and Lidocaine Hydrochloride, in: Analytical Profiles of Drug Substances. Elsevier, pp. 761–779. https://doi.org/10.1016/S0099-5428(08)60428-1

Prado, A.R., Yokaichiya, F., Franco, M.K.K.D., Silva, C.M.G. da, Oliveira-Nascimento, L., Franz-Montan, M., Volpato, M.C., Cabeça, L.F., de Paula, E., 2017. Complexation of oxethazaine with 2-hydroxypropyl-β-cyclodextrin: increased drug solubility, decreased cytotoxicity and analgesia at inflamed tissues. J. Pharm. Pharmacol. 69, 652–662. https://doi.org/10.1111/jphp.12703

Puopolo, M., Binshtok, A.M., Yao, G.-L., Oh, S.B., Woolf, C.J., Bean, B.P., 2013. Permeation and block of TRPV1 channels by the cationic lidocaine derivative

QX-314. J. Neurophysiol. 109, 1704–1712. https://doi.org/10.1152/jn.00012.2013

Ragsdale, D.S., McPhee, J.C., Scheuer, T., Catterall, W.A., 1996. Common molecular determinants of local anesthetic, antiarrhythmic, and anticonvulsant block of voltage-gated Na+ channels. Proc. Natl. Acad. Sci. 93, 9270–9275.

Regnier, Z., Neville, G., 1969. Hydrogen bonding in lidocaine salts. I. The NH stretching band and its dependence on the associated anion. Canadian Journal of Chemistry 4229–4235.

Reisman, D., Reader, A., Nist, R., Beck, M., Weaver, J., 1997. Anesthetic efficacy of the supplemental intraosseous injection of 3% mepivacaine in irreversible pulpitis. Oral Surg. Oral Med. Oral Pathol. Oral Radiol. Endod. 84, 676–682. https://doi.org/10.1016/S1079-2104(97)90372-3

Rey, L., May, J.C. (Eds.), 2011. Freeze drying/lyophilization of pharmaceutical and biological products, 3rd ed, Drugs and the pharmaceutical sciences. Informa Healthcare, New York ; London.

Rodriguez-Perez, A.I., Rodriguez-Tenreiro, C., Alvarez-Lorenzo, C., Taboada, P., Concheiro, A., Torres-Labandeira, J.J., 2006. Sertaconazole/hydroxypropyl-β-cyclodextrin complexation: Isothermal titration calorimetry and solubility approaches. J. Pharm. Sci. 95, 1751–1762. https://doi.org/10.1002/jps.20661

Rollyson, W.D., Stover, C.A., Brown, K.C., Perry, H.E., Stevenson, C.D., McNees, C.A., Ball, J.G., Valentovic, M.A., Dasgupta, P., 2014. Bioavailability of capsaicin and its implications for drug delivery. J. Controlled Release 196, 96–105. https://doi.org/10.1016/j.jconrel.2014.09.027

Schmidt, A.C., 2005. The Role of Molecular Structure in the Crystal Polymorphism of Local Anesthetic Drugs: Crystal Polymorphism of Local Anesthetic Drugs, Part X. Pharm. Res. 22, 2121–2133. https://doi.org/10.1007/s11095-005-8135-6

Schröder Iw., 1893. Über die Abhängigkeit der Löslichkeit eines festen Körpers von seiner Schmelztemperatur. Z. Für Phys. Chem. 11Schulman, 449. https://doi.org/10.1515/zpch-1893-1134

Schulman, J.M., Strichartz, G.R., 2011. Local anesthetic pharmacology, in: Principles of Pharmacology: The Pathophysiologic Basis of Drug Therapy. Wolters Kluwer Health, Philadelphia, pp. 147–162.

Seager, H., Taskis, C.B., Syrop, M., 1985. Structure of Products Prepared by Freeze-Drying Solutions Containing Organic Solvents. J. Parenter. Sci. Technol. 39, 161–179.

Shen, C., Yang, X., Wang, Y., Zhou, J., Chen, C., 2012. Complexation of capsaicin with β-cyclodextrins to improve pesticide formulations: effect on aqueous solubility, dissolution rate, stability and soil adsorption. J. Incl. Phenom. Macrocycl. Chem. 72, 263–274. https://doi.org/10.1007/s10847-011-9971-0

Sheokand, S., Modi, S.R., Bansal, A.K., 2014. Dynamic Vapor Sorption as a Tool for Characterization and Quantification of Amorphous Content in Predominantly Crystalline Materials. J. Pharm. Sci. 103, 3364–3376. https://doi.org/10.1002/jps.24160

Shimpi, S., Chauhan, B., Shimpi, P., 2005. Cyclodextrins: application in different routes of drug administration. Acta Pharm. 55, 139–156.

Shrestha, M., Chen, A., 2018. Modalities in managing postherpetic neuralgia. Korean J. Pain 31, 235. https://doi.org/10.3344/kjp.2018.31.4.235

Simova, S., Berger, S., 2005. Diffusion Measurements vs. Chemical Shift Titration for Determination of Association Constants on the Example of Camphor–

Cyclodextrin Complexes. J. Incl. Phenom. Macrocycl. Chem. 53, 163–170. https://doi.org/10.1007/s10847-005-2631-5

Smith, E.L., Abbott, A.P., Ryder, K.S., 2014. Deep Eutectic Solvents (DESs) and Their Applications. Chem. Rev. 114, 11060–11082. https://doi.org/10.1021/cr300162p

Soares, L.A., Leal, A.F.V.B., Fraceto, L.F., Maia, E.R., Resck, I.S., Kato, M.J., Sousa Gil, E., Sousa, A.R., Cunha, L.C., Rezende, K.R., 2009. Host–guest system of 4-nerolidylcatechol in 2-hydroxypropyl-β-cyclodextrin: preparation, characterization and molecular modeling. J. Incl. Phenom. Macrocycl. Chem. 64, 23–35. https://doi.org/10.1007/s10847-009-9532-y

Sommer, C., Cruccu, G., 2017. Topical Treatment of Peripheral Neuropathic Pain: Applying the Evidence. J. Pain Symptom Manage. 53, 614–629. https://doi.org/10.1016/j.jpainsymman.2016.09.015

Stella, V., 1999. Mechanisms of drug release from cyclodextrin complexes. Adv. Drug Deliv. Rev. 36, 3–16. https://doi.org/10.1016/S0169-409X(98)00052-0

Strickley, R.G., 2004. Solubilizing excipients in oral and injectable formulations. Pharm. Res. 21, 201–230.

Su, N., Liu, Y., Yang, X., Shi, Z., Huang, Y., 2014. Efficacy and safety of mepivacaine compared with lidocaine in local anaesthesia in dentistry: a meta-analysis of randomised controlled trials. Int. Dent. J. 64, 96–107. https://doi.org/10.1111/idj.12087

Suzuki, S., Gerner, P., Lirk, P., 2019. Local Anesthetics, in: Pharmacology and Physiology for Anesthesia. Elsevier, pp. 390–411. https://doi.org/10.1016/B978-0-323-48110-6.00020-X

Swarbrick, J., Boylan, J.C., 2000. Encyclopedia of Pharmaceutical Technology: Volume 20 - Supplement 3, Pharmaceutical Technology Encyclopedia. Taylor & Francis.

Szallasi, A., Blumberg, P.M., 1999. Vanilloid (Capsaicin) Receptors and Mechanisms. Pharmacological Reviews 51, 2, 159–212.

Tamjidi, F., Shahedi, M., Varshosaz, J., Nasirpour, A., 2013. Nanostructured lipid carriers (NLC): A potential delivery system for bioactive food molecules. Innov. Food Sci. Emerg. Technol. 19, 29–43. https://doi.org/10.1016/j.ifset.2013.03.002

Tang, X.T., Pikal, M.J., 2004. Design of freeze-drying processes for pharmaceuticals: practical advice. Pharm. Res. 21, 191–200.

Tavano, L., Alfano, P., Muzzalupo, R., de Cindio, B., 2011. Niosomes vs microemulsions: New carriers for topical delivery of Capsaicin. Colloids Surf. B Biointerfaces 87, 333–339. https://doi.org/10.1016/j.colsurfb.2011.05.041

Tiwari, G., Tiwari, R., Rai, A.K., others, 2010. Cyclodextrins in delivery systems: Applications. J. Pharm. Bioallied Sci. 2, 72–79.

Treede, R.-D., Jensen, T.S., Campbell, J.N., Cruccu, G., Dostrovsky, J.O., Griffin, J.W., Hansson, P., Hughes, R., Nurmikko, T., Serra, J., 2008. Neuropathic pain: Redefinition and a grading system for clinical and research purposes. Neurology 70, 1630–1635. https://doi.org/10.1212/01.wnl.0000282763.29778.59

Tsesis, I., 2014. Complications in Endodontic Surgery: Prevention, Identification and Management. Springer.

Tsuchiya, H., 2016. Dental Anesthesia in the Presence of Inflammation: Pharmacological Mechanisms for the Reduced Efficacy of Local Anesthetics. Int J Clin Anesthesiol 4, 1–16.

Turgut, C., Newby, B., Cutright, TeresaJ., 2004. Determination of optimal water solubility of capsaicin for its usage as a non-toxic antifoulant. Environ. Sci. Pollut. Res. 11, 7–10. https://doi.org/10.1065/espr2003.12.180

Ueno, T., Tsuchiya, H., Mizogami, M., Takakura, K., 2008. Local anesthetic failure associated with inflammation: verification of the acidosis mechanism and the hypothetic participation of inflammatory peroxynitrite. J. Inflamm. Res. 1, 41.

USP, 32. Capsaicin monograph. U. S. Pharmacop. Natl. Formul. Vol 1 Rockv. MD Capsain Monograh P 1776.

Van Laar, J.J., 1903. . Arch. neerl. 8, 264–284.

Wang, C.H., Wang, J.C., Soens, M.A., Gerner, P., Strichartz, G., 2014. Addition of Capsaicin to Local Anesthetics for Spinal Anesthesia in Rats Shortens Motor Deficits and Prolongs Anti-Nociception. Open J. Anesthesiol. 04, 123–130. https://doi.org/10.4236/ojanes.2014.46019

Wang, H., Gurau, G., Shamshina, J., Cojocaru, O.A., Janikowski, J., MacFarlane, D.R., Davis, J.H., Rogers, R.D., 2014. Simultaneous membrane transport of two active pharmaceutical ingredients by charge assisted hydrogen bond complex formation. Chem. Sci. 5, 3449–3456. https://doi.org/10.1039/C4SC01036A

Webster, L.R., Nunez, M., Tark, M.D., Dunteman, E.D., Lu, B., Tobias, J.K., Vanhove, G.F., 2011. Tolerability of NGX-4010, a capsaicin 8% dermal patch, following pretreatment with lidocaine 2.5%/prilocaine 2.5% cream in patients with post-herpetic neuralgia. BMC Anesthesiol. 11, 1–8. https://doi.org/10.1186/1471-2253-11-25

Wiest, J., Saedtler, M., Balk, A., Merget, B., Widmer, T., Bruhn, H., Raccuglia, M., Walid, E., Picard, F., Stopper, H., Dekant, W., Lühmann, T., Sotriffer, C., Galli, B., Holzgrabe, U., Meinel, L., 2017. Mapping the pharmaceutical design space by amorphous ionic liquid strategies. J. Controlled Release 268, 314–322. https://doi.org/10.1016/j.jconrel.2017.10.040

Williams III, R.O., Mahaguna, V., Sriwongjanya, M., 1998. Characterization of an inclusion complex of cholesterol and hydroxypropyl-β-cyclodextrin. Eur. J. Pharm. Biopharm. 46, 355–360.

Zhao, Y., Sun, C., Shi, F., Firempong, C.K., Yu, J., Xu, X., Zhang, W., 2016. Preparation, characterization, and pharmacokinetics study of capsaicin via hydroxypropyl-beta-cyclodextrin encapsulation. Pharm. Biol. 54, 130–138. https://doi.org/10.3109/13880209.2015.1021816

Zi, P., Yang, X., Kuang, H., Yang, Y., Yu, L., 2008. Effect of HPβCD on solubility and transdermal delivery of capsaicin through rat skin. Int. J. Pharm. 358, 151–158. https://doi.org/10.1016/j.ijpharm.2008.03.001

Zografi, G., 1988. States of Water Associated with Solids. Drug Dev. Ind. Pharm. 14, 1905–1926. https://doi.org/10.3109/03639048809151997

APPENDIX 1

1.0. Quantification of CAP by UV

CAP quantification by UV/Vis absorption spectrophotometry. The absorption spectra of capsaicin in the UV region, in water and ethanol was recorded. It is not possible to distinguish between pure CAP, dihydrocapsaicin and other capsainoids. Therefore, the main peak is attributed to CAP. The wavelength of maximum absorption of CAP was 278 nm and 280 nm in aqueous solution and ethanol, respectively.
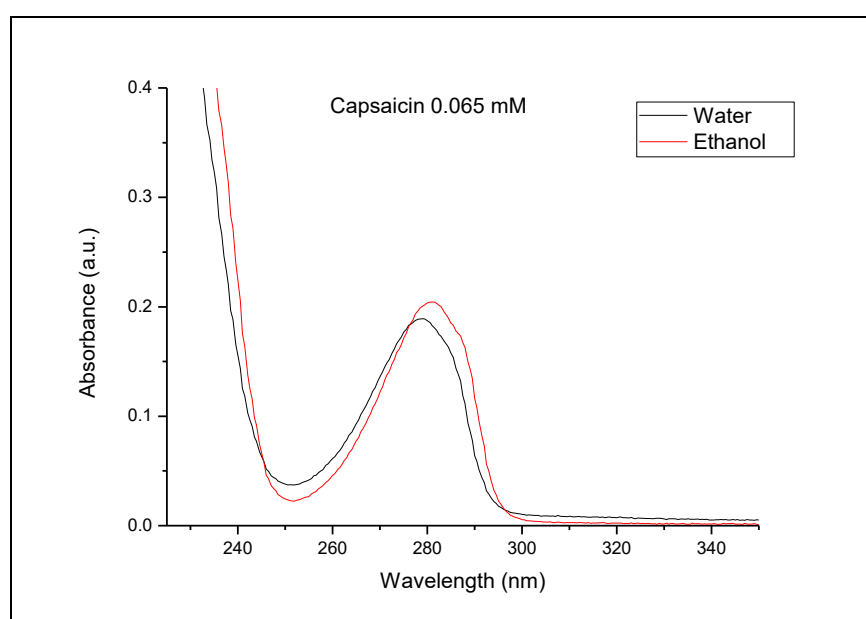
UV absorption spectrum of capsaicin (0.065 mM), in water and ethanol.

Representative concentration curves for capsaicin, in water and ethanol (50% v/v) are presented here. They were used to calculate molar absorptivity coefficient (ε) quantitative assay of CAP in solution. The calculated coefficient of molar absorptivity (ε) for capsaicin was 2760 ± 345 and 3004 ± 257, in water and ethanol (50% v/v), respectively.
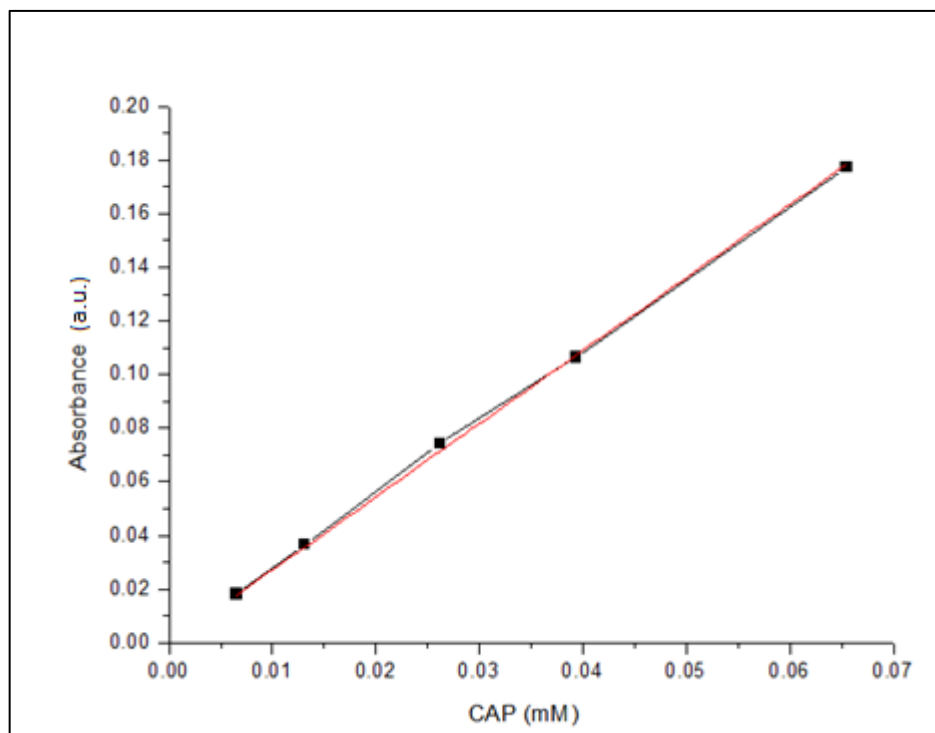
Representative analytical curve for UV absorption (λ = 278 nm) for capsaicin in water.
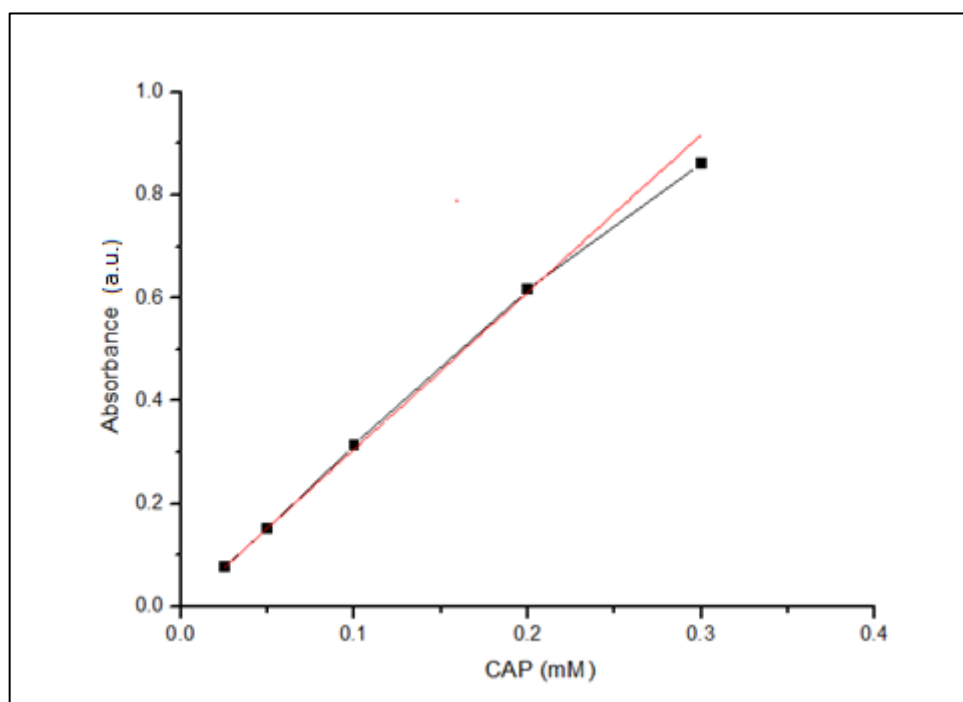
Representative analytical curve for UV absorption (λ = 280 nm) for capsaicin in ethanol.

The regression coefficients of all curves of CAP diluted in ethanol (50% v/v) were above 0.99. The linearity of the method was evaluated using analytical curves obtained on three consecutive days, each area of the points of the curve being determined in triplicate. From the analytical curves, we determined the linear regression equation and the correlation coefficients (R^2) presented in the table below. The values of r^2 were higher than 0.99, in the three days evaluated confirming the linearity of the method.

Equations of linear regression and correlation coefficients (r^2) obtained from the analytical curves of CAP in ethanol (50% v/v) constructed on three consecutive days (n = 3).

|	Day 1	Day 2	Day 3
Linear regression	y=3.0057x+0.0006	y=3.2611x+0.0007	y=2.7473x+0.0007
R^2	0.998	0.996	0.997

2.0. Quantification of CAP by HPLC

According to the American Pharmacopoeia (USP, 32), the raw material capsaicin is composed of 90-110% capsainoids, containing not less than 55% pure capsaicin, 20% dihydrocapsaicin and no more than 15% of other capsainoids. The parameters evaluated for standardization of the methodology of capsaicin quantification by HPLC were specificity, linearity, precision, limit of detection and quantification.

2.1. Specificity

In the quantification of capsaicin by HPLC, we used a 50% ethanol solution as solvent, due to the low solubility of capsaicin in water.

The chromatographic conditions (item 4.2.2.1.) used were considered appropriate and the capsaicin peak was recorded in the figure below, with retention time of 6.60 min and 8.26 min, for capsaicin and dihydrocapsaicin, respectively.
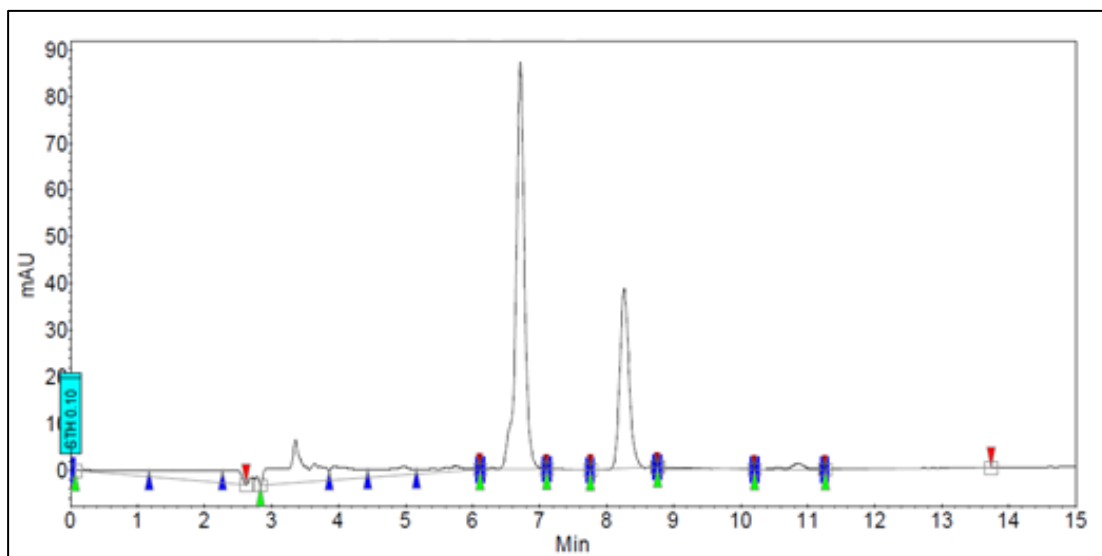
Chromatogram obtained of capsaicin in ethanolic solution (0,327 mM), C18 reverse phase, 25 x 4.6 mm, flow of 1.0 mL/min, 30ºC.

The same retention time for capsacin was found in the capsaicin primary reference standard solution.
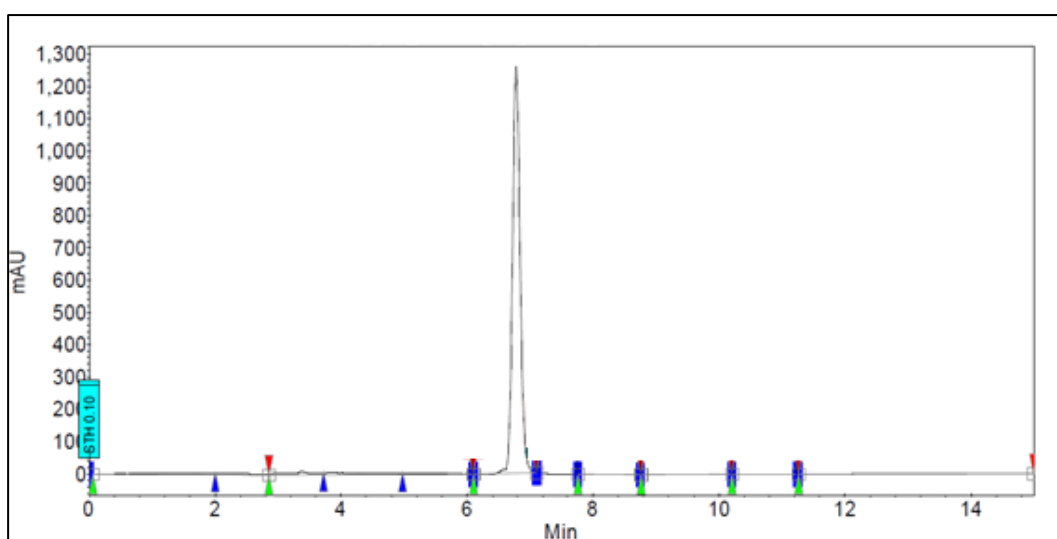
Chromatogram of the primary capsaicin standard solution with retention time of 6.6 minutes, C18 reverse phase, 25 x 4.6 mm, flow of 1.0 mL/min, 30ºC.

The method was shown to be specific since in the placebo chromatogram no interference was detected in the retention time corresponding to the chromatographic peak of capsaicin and dihydrocapsaicin. By way of example, the chromatogram obtained with 0.13 mM HP-β-CD.
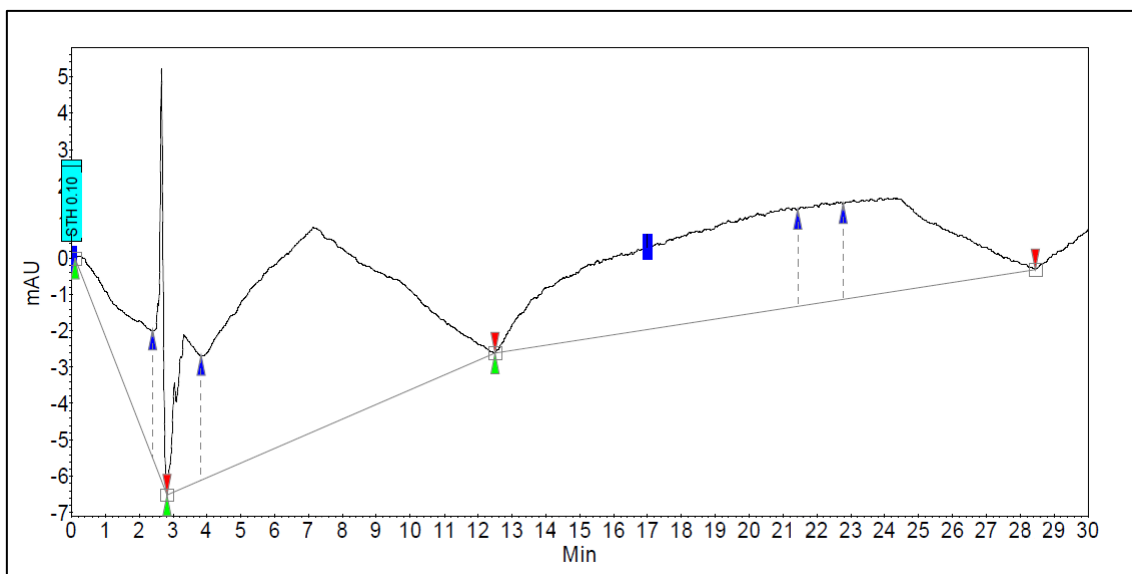
Chromatogram for injection of placebo solution of HP-β-CD (0.13 mM).

2.2. Linearity

The linearity of the method was evaluated using analytical curves obtained on three consecutive days, each area of the points of the curve being determined in triplicate. From the analytical curves, we determined the linear regression equation and the correlation coefficients (R^2) presented in the table below. The values of R^2 were higher than 0.99, in the three days evaluated, according to the recommendations of RDC n° 166, 2017, confirming the linearity of the method.

Equations of linear regression and correlation coefficients (r^2) obtained from the analytical curves (n = 3) constructed on three consecutive days

	Day 1	Day 2	Day 3
Linear regression	y=108655x+98	y=115251x+87	y=118115x+76
R^2	0.999	0.996	0.997

2.3. Precision

The precision parameter evaluated the proximity of the results obtained in a series of multiple sampling measures.

Accuracy is expressed by calculating the relative standard deviation of the concentrations determined in the method. All analyzes, Intra and Interdia have a DPR of less than 5%. Thus, the experimental results indicated adequate repeatability of the analytical method, in accordance with the requirements of RDC n°166, 2017.

Results of the Intraday and Interday precision test obtained from the relative standard deviation (DPR) of triplicates of different concentrations of CAP on 3 consecutive days.

[CAP*] (mM)	DPR Dia 1 (%) Intraday	DPR Dia 2 (%) Intraday	DPR Dia 3 (%) Intraday	DPR (%) Interday
0.006	0.50	1.03	0.30	4.32
0.075	0.30	0.91	1.07	4.20
0.125	0.26	0.78	1.06	1.74

*Theoretical concentration of CAP

2.4. Limit of detection and limit of quantification

From the linearity data it was possible to calculate the limit of detection (LD) and the limit of quantification (LQ) of capsaicin by the analytical method proposed, in HPLC. The lowest amount of CAP that can be quantified and detected (LQ and LD) in a given sample was 0.0010 mM and 0.0003 mM, respectively.

APPENDIX 2

Activities and academic productivity during doctorate

Published articles:

COUTO, VERONICA MUNIZ; PRIETO, MARIA J. ; IGARTÚA, DANIELA E.; FEAS, DANIELA A. ; RIBEIRO, LÍGIA N.M. ; SILVA, CAMILA M.G. ; CASTRO, SIMONE R. ; GUILHERME, VIVIANE A. ; DANTZGER, DARLENE D. ; MACHADO, DAISY ; ALONSO, SILVIA DEL V. ; DE PAULA, ENEIDA . Dibucaine in Ionic-Gradient Liposomes: Biophysical, Toxicological, and Activity Characterization. JOURNAL OF PHARMACEUTICAL SCIENCES, v. 107, p. 2411-2419, 2018. https://doi.org/10.1016/j.xphs.2018.05.010

RIBEIRO, LÍGIA N.M.; BREITKREIT, MARCIA C.; GUILHERME, VIVIANE A.; SILVA, GUSTAVO H.R.; **COUTO, VERONICA MUNIZ**; CASTRO, SIMONE R.; PAULA, BARBARA O.; MACHADO, DAISY; DE PAULA, ENEIDA. Natural lipids-based NLC containing lidocaine: from pre-formulation to in vivo studies. EUROPEAN JOURNAL OF PHARMACEUTICAL SCIENCES, v.106, p. 102-112, 2018. https://doi.org/10.1016/j.ejps.2017.05.060

RIBEIRO, LÍGIA N.M.; **COUTO, VERONICA MUNIZ**; FRACETO, LEONARDO FERNANDES; DE PAULA, ENEIDA. Use of nanoparticle concentration as a tool to understand the structural properties of colloids. SCIENTIFIC REPORTS, v. 8, p. 1-8, 2018. https://doi.org/10.1038/s41598-017-18573-7

SILVA, CAMILA M.G., FRACETO, LEONARDO F., FRANZ-MONTAN, MICHELLE, **COUTO, VERONICA MUNIZ**, CASADEI, BRUNA R.; CEREDA, CINTIA M. S.; DE PAULA, ENEIDA. Development of egg PC/cholesterol/α-tocopherol liposomes with ionic gradients to deliver ropivacaine. JOURNAL OF LIPOSOME RESEARCH, v. 26, p. 1-10, 2016. https://doi.org/10.3109/08982104.2015.1022555

RIBEIRO, LÍGIA N. M.; ALCÂNTARA, ANA C. S.; RODRIGUES DA SILVA, GUSTAVO H.; FRANZ-MONTAN, MICHELLE; NISTA, SILVIA V. G.; CASTRO, SIMONE R.; **COUTO, VERONICA MUNIZ**; GUILHERME, VIVIANE A.; DE PAULA, ENEIDA. Advances in Hybrid Polymer-Based Materials for Sustained Drug Release. INTERNATIONAL JOURNAL OF POLYMER SCIENCE, v. 2017, p. 1-16, 2017. https://doi.org/10.1155/2017/1231464

WOOD, IRENE; ALBANO, JUAN M. R.; FILHO, PEDRO L. O.; **COUTO, VERONICA MUNIZ**; DE FARIAS, MARCELO A.; PORTUGAL, RODRIGO V.; DE PAULA, ENEIDA; OLIVEIRA, CRISTIANO L. P.; PICKHOLZ, MONICA, A. sumatriptan coarse-grained model to explore different environments: interplay with experimental techniques. EUROPEAN BIOPHYSICS JOURNAL WITH BIOPHYSICS LETTERS, v. 47, p. 561-571, 2018. https://doi.org/10.1007/s00249-018-1278-2

ALBANO, JUAN M. R., RIBEIRO, LÍGIA N. M., **COUTO, VERONICA MUNIZ**, MESSIAS, MARIANA BARBOSA, RODRIGUES DA SILVA, GUSTAVO H., BREITKREIT, MARCIA CRISTINA, DE PAULA, ENEIDA, PICKHOLZ, MONICA. Rational design of polymer-lipid nanoparticles for docetaxel delivery. COLLOIDS AND SURFACES B: BIOINTERFACES, v. 175, p. 56-64, 2019. https://doi.org/10.1016/j.colsurfb.2018.11.077

OLIVEIRA, JULIANA DAMASCENO, RIBEIRO, LÍGIA NUNES DE MORAIS, RODRIGUES DA SILVA, GUSTAVO H., CASADEI, BRUNA RENATA, **COUTO, VERONICA MUNIZ**, MARTINEZ, ELIZABETH FERREIRA, DE PAULA, ENEIDA. Sustained Release from Ionic-Gradient Liposomes Significantly Decreases ETIDOCAINE Cytotoxicity. PHARMACEUTICAL RESEARCH, v. 35P, p. 1-10, 2018. https://doi.org/10.1007/s11095-018-2512-4

CASADEI, BRUNA RENATA; DOMINGUES, CLEYTON CREPALDI; CLOP, EDUARDO M.; **COUTO, VERÔNICA MUNIZ**; PERILLO, MARIA ANGELICA; DE PAULA, ENEIDA. Molecular features of nonionic detergents involved in the binding kinetics and solubilization efficiency, as studied in model (Langmuir films) and biological (Erythrocytes) membranes. COLLOIDS AND SURFACES B-BIOINTERFACES, v. 166, p. 152-160, 2018. https://doi.org/10.1016/j.colsurfb.2018.03.012

Published book chapter:

RIBEIRO, LÍGIA N. M.; ALCÂNTARA, ANA C. S.; FRANZ-MONTAN, MICHELLE; **COUTO, VERONICA MUNIZ;** NISTA, SILVIA V. G.; DE PAULA, ENEIDA. Nanostructured organic-organic bio-hybrid delivery systems. BIOMEDICAL APPLICATIONS OF NANOPARTICLES, Ed. Elsevier, Chapter 13, p.341-374, 2019. ISBN: 978-0-12-816506-5 Doi 10.1016/B978-0-12-816506-5.00011-5

Presentation in Scientific Meeting:

COUTO, V.M.; OLIVEIRA-NASCIMENTO, L.; DE PAULA, E. Characterization of capsaicin HP-B-ciclodextrin complex. II Congresso Regional da Sociedade Brasileira de Biofísica, Acarajú, Brazil, 2016.

COUTO, V.M., CASADEI, B.R., DA SILVA, G.H.R., RISKE, K.A., OLIVEIRA-NASCIMENTO, L., de Paula, E. Capsaicin and local anesthetics interaction with model membranes. IUPAB meeting, Edinburgh, Scotland, 2017.

COUTO, V. M., ZOTOVA, J., OLIVEIRA-NASCIMENTO, LAURA, TAJBER, LIDIA, DE PAULA, ENEIDA. Thermodynamic properties of local anaesthetic/capsaicin-based ionic liquids. Lisboa, Portugal, 2018.

Courses attended:

Planejamento e Otimização Experimental aplicados ao desenvolvimento farmacêutico, UNICAMP, Brazil, 2016

Freeze-drying training, Biopharma Group, Winchester, UK, 2018.

Academic Writing, Trinity College Dublin, Dublin, Ireland, 2018

Pulmonary drug delivery, Unicamp, Campinas, Brazil, 2019

ANNEX 1

UNICAMP

CEUA/UNICAMP

C E R T I F I C A D O

Certificamos que a proposta intitulada **ANESTÉSICO LOCAL COMBINADO COM O COMPLEXO DE INCLUSÃO CAPSAICINA:HIDROXIPROPIL-BETA-CICLODEXTRINA PARA AUMENTO SELETIVO DA POTÊNCIA ANESTÉSICA**, registrada com o nº **4402-1**, sob a responsabilidade de **Profa. Dra. Eneida de Paula e Verônica Muniz Couto**, que envolve a produção, manutenção ou utilização de animais pertencentes ao filo *Chordata*, subfilo *Vertebrata* (exceto o homem) para fins de pesquisa científica (ou ensino), encontra-se de acordo com os preceitos da **LEI Nº 11.794, DE 8 DE OUTUBRO DE 2008**, que estabelece procedimentos para o uso científico de animais, do **DECRETO Nº 6.899, DE 15 DE JULHO DE 2009**, e com as normas editadas pelo **Conselho Nacional de Controle da Experimentação Animal (CONCEA), tendo sido** aprovada pela **Comissão de Ética no Uso de Animais da Universidade Estadual de Campinas - CEUA/UNICAMP**, em **03 de novembro de 2016**.

Finalidade:	( ) Ensino (X) Pesquisa Científica
Vigência do projeto:	20/11/2016- 20/07/2017
Vigência da autorização para manipulação animal:	30/11/2016- 20/07/2017
Espécie / linhagem/ raça:	Camundongo heterogênico / Unib:SW (Swiss)
No. de animais:	98
Peso / Idade:	03 semanas / 10g
Sexo:	machos
Origem:	CEMIB/UNICAMP

A aprovação pela CEUA/UNICAMP não dispensa autorização prévia junto ao **IBAMA, SISBIO** ou **CIBio** e é **restrita** a protocolos desenvolvidos em biotérios e laboratórios da Universidade Estadual de Campinas.

Campinas, 30 de novembro de 2016.

Profa. Dra. Liana Maria Cardoso Verinaud
Presidente

Fátima Alonso
Secretária Executiva

IMPORTANTE: Pedimos atenção ao prazo para envio do relatório final de atividades referente a este protocolo: até 30 dias após o encerramento de sua vigência. O formulário encontra-se disponível na página da CEUA/UNICAMP, área do pesquisador responsável. A não apresentação de relatório no prazo estabelecido impedirá que novos protocolos sejam submetidos.

CEUA/Unicamp

Comissão de Ética no Uso de Animais
CEUA/Unicamp

CERTIFICADO

Certificamos que o projeto de pesquisa intitulado **ANESTÉSICO LOCAL COMBINADO COM O COMPLEXO DE INCLUSÃO CAPSAICINA:HIDROXIPROPIL-BETA-CICLODEXTRINA PARA AUMENTO SELETIVO DA POTÊNCIA ANESTÉSICA** (protocolo CEUA/UNICAMP nº **4402-1**), de responsabilidade da **Profa. Dra. Eneida de Paula** e **Verônica Muniz Couto**, teve a solicitação de prorrogação de término do projeto em **20/02/2019** aprovada pela CEUA/UNICAMP

Este documento é válido apenas se apresentado junto com o certificado emitido originalmente pela CEUA/UNICAMP em 30/11/2016.

Campinas, 20 de junho de 2017.

Profa. Dra. Liana M. C. Verinaud
Presidente
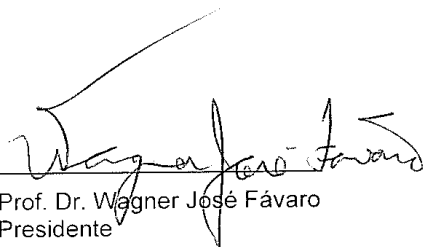
Fátima Alonso
Secretária Executiva

Comissão de Ética no Uso de Animais
CEUA/Unicamp

CERTIFICADO

Certificamos que o projeto de pesquisa intitulado **ANESTÉSICO LOCAL COMBINADO COM O COMPLEXO DE INCLUSÃO CAPSAICINA:HIDROXIPROPIL-BETA-CICLODEXTRINA PARA AUMENTO SELETIVO DA POTÊNCIA ANESTÉSICA** (protocolo CEUA/UNICAMP nº **4402-1**), de responsabilidade da **Profa. Dra. Eneida de Paula** e **Veronica Muniz Couto**, teve o título alterado para **ASSOCIAÇÃO DE CAPSAICINA COM ANESTÉSICOS LOCAIS PARA AUMENTO DA ANALGESIA**.

Este documento é válido apenas se apresentado junto com o certificado emitido originalmente pela CEUA/UNICAMP em 30/11/2016.

Campinas, 04 de abril de 2019.

Prof. Dr. Wagner José Fávaro
Presidente

Rosangela dos Santos
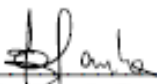Secretária Executiva

ANNEX 2

As cópias de artigos de minha autoria ou de minha co-autoria, já publicados ou submetidos para publicação em revistas científicas ou anais de congressos sujeitos a arbitragem, que constam da minha Dissertação/Tese de Mestrado/Doutorado, intitulada **ASSOCIATION OF CAPSAICIN WITH LOCAL ANESTHETICS TO INCREASE ANALGESIA (ASSOCIAÇÃO DE CAPSAICINA COM ANESTÉSICOS LOCAIS PARA AUMENTO DA ANALGESIA)**, não infringem os dispositivos da Lei n.° 9.610/98, nem o direito autoral de qualquer editora.

Campinas, 04 de julho de 2019

Assinatura : _____

Nome do(a) autor(a): **Verônica Muniz Couto**

RG n.° 43617786-9

Assinatura : _____

Nome do(a) orientador(a): **Eneida de Paula**

RG n.° 151215595